THE MISSISSIPPIAN LEADVILLE LIMESTONE EXPLORATION PLAY, UTAH AND COLORADO – EXPLORATION TECHNIQUES AND STUDIES FOR INDEPENDENTS

SEMI-ANNUAL TECHNICAL PROGRESS REPORT October 1, 2004 - March 31, 2005

by

Thomas C. Chidsey, Jr., Principal Investigator/Program Manager,
and Craig D. Morgan, Utah Geological Survey,
David E. Eby, Eby Petrography & Consulting, Inc.,
Joe Moore, Energy & Geoscience Institute,
and
Louis Taylor, Standard Geological Services, Inc.

August 2005

Contract No. DE-FC26-03NT15424

Virginia Weyland, Contract Manager
U.S. Department of Energy
National Petroleum Technology Office
Williams Center Tower One
1 West 3rd Street
Tulsa, OK 74103-3519

DISCLAIMER

This report was prepared as an account of work sponsored by an agency of the United States Government. Neither the United States Government nor any agency thereof, nor any of their employees, makes any warranty, expressed or implied, or assumes any legal liability or responsibility for the accuracy, completeness, or usefulness of any information, apparatus, product, or process disclosed, or represents that its use would not infringe privately owned rights. Reference herein to any specific commercial product, process, or service by trade name, trademark, manufacturer, or otherwise does not necessarily constitute or imply its endorsement, recommendation, or favoring by the United States Government or any agency thereof. The views and opinions of authors expressed herein do not necessarily state or reflect those of the United States Government or any agency thereof.

Although this product represents the work of professional scientists, the Utah Department of Natural Resources, Utah Geological Survey, makes no warranty, expressed or implied, regarding its suitability for a particular use. The Utah Department of Natural Resources, Utah Geological Survey, shall not be liable under any circumstances for any direct, indirect, special, incidental, or consequential damages with respect to claims by users of this product.

THE MISSISSIPPIAN LEADVILLE LIMESTONE EXPLORATION PLAY, UTAH AND COLORADO – EXPLORATION TECHNIQUES AND STUDIES FOR INDEPENDENTS

SEMI-ANNUAL TECHNICAL PROGRESS REPORT October 1, 2004 – March 31, 2005

by

Thomas C. Chidsey, Jr., Principal Investigator/Program Manager,
and Craig D. Morgan, Utah Geological Survey,
David E. Eby, Eby Petrography & Consulting, Inc.,
Joe Moore, Energy & Geoscience Institute,
and
Louis Taylor, Standard Geological Services, Inc.

Date of Report: August 2005

Contract No. DE-FC26-03NT15424

Virginia Weyland, Contract Manager
U.S. Department of Energy
National Petroleum Technology Office
Williams Center Tower One
1 West 3rd Street
Tulsa, OK 74103-3519

Submitting Organization: Utah Geological Survey
1594 West North Temple, Suite 3110
P.O. Box 146100
Salt Lake City, Utah 84114-6100
Ph.: (801) 537-3300/Fax: (801) 537-3400

ABSTRACT

The Mississippian Leadville Limestone is a shallow, open-marine, carbonate-shelf deposit. The Leadville has produced over 53 million barrels (8.4 million m^3) of oil from six fields in the Paradox fold and fault belt of the Paradox Basin, Utah and Colorado. The environmentally sensitive, 7500-square-mile (19,400 km^2) area that makes up the fold and fault belt is relatively unexplored. Only independent producers operate and continue to hunt for Leadville oil targets in the region. The overall goal of this study is to assist these independents by (1) developing and demonstrating techniques and exploration methods never tried on the Leadville, (2) targeting areas for exploration, and (3) conducting a detailed reservoir characterization study. The final results will hopefully reduce exploration costs and risks, especially in environmentally sensitive areas, and add new oil discoveries and reserves.

This report covers research and technology transfer activities for the first half of the second project year (October 1, 2004 through March 31, 2005), Budget Period I. This work consisted of diagenetic analysis of the Leadville Limestone reservoir at the Lisbon case-study field, Utah, which accounts for most of the Leadville oil production in the Paradox Basin. Analyses included scanning electron microscopy, epifluorescence, cathodoluminescence, and study of fluid inclusions from Leadville core samples and thin sections from Lisbon field.

Two major types of diagenetic dolomite are observed using these techniques: (1) tight "stratigraphic" dolomite consisting of very fine grained (<5 μm), interlocking crystals that faithfully preserve depositional fabrics; and (2) porous, coarser (>100-250 μm), rhombic and saddle crystals that discordantly replace limestone and earlier "stratigraphic" dolomite. Predating or concomitant with late dolomite formation are pervasive leaching episodes that produced vugs and extensive microporosity. Solution-enlarged fractures and autobreccias are also common. Pyrobitumen and sulfide minerals appear to coat most crystal faces of the rhombic and saddle dolomites. The fluid inclusion and mineral relationships suggest the following sequence of events: (1) dolomite precipitation, (2) anhydrite deposition, (3) anhydrite dissolution and quartz precipitation, (4) dolomite dissolution and late calcite precipitation, (5) trapping of a mobile oil phase, and (6) formation of bitumen. Fluid inclusions in calcite and dolomite display variable liquid to vapor ratios suggesting reequilibration at elevated temperatures (50^{o}C). Fluid salinities exceed 10 weight percent NaCl equivalent. Low ice-melting temperatures of quartz- and calcite-hosted inclusions suggest chemically complex Ca-Mg-bearing brines associated with evaporite deposits were responsible for mineral deposition.

The overall conclusion from this work indicates late dolomitization, saddle dolomite, and dolomite cement precipitation, as well as sulfides and brecciation, may have developed from hydrothermal events that can greatly improve reservoir quality. The result can be the formation of large, diagenetic-type, hydrocarbon traps. The reservoir characteristics, particularly diagenetic overprinting and history, can be applied regionally to other fields and exploration trends in the basin.

Technology transfer activities for the reporting period consisted of a technical presentation on Leadville characteristics and dolomitization, and publications. An abstract describing Leadville diagenesis with emphasis on dolomitization was submitted and accepted by the American Association of Petroleum Geologists, for presentation at the 2005 Annual Convention in Calgary, Canada. The project home page was updated on the Utah Geological Survey Web site.

CONTENTS

FIGURES

TABLE

EXECUTIVE SUMMARY

The Mississippian Leadville Limestone is a shallow, open marine, carbonate-shelf deposit. The Leadville has produced over 53 million barrels (8.4 million m^3) of oil from six fields in the Paradox fold and fault belt of the Paradox Basin, Utah and Colorado. These fields are currently operated by small, independent producers. The environmentally sensitive, 7500-square-mile (19,400 km^2) area that makes up the fold and fault belt is relatively unexplored. Only independent operators continue to hunt for Leadville oil targets in the region. The overall goal of this study is to assist these independents by (1) developing and demonstrating techniques and exploration methods never tried on the Leadville Limestone, (2) targeting areas for exploration, and (3) conducting a detailed reservoir characterization study. The final results will hopefully reduce exploration costs and risk especially in environmentally sensitive areas, and add new oil discoveries and reserves.

To achieve this goal and carry out the Leadville Limestone study, the Utah Geological Survey (UGS) and Eby Petrography & Consulting, Inc., have entered into a cooperative agreement with the U.S. Department of Energy (DOE), National Petroleum Technology Office, Tulsa, Oklahoma. The research is funded as part of the DOE Advanced and Key Oilfield Technologies for Independents (Area 2 – Exploration) Program. This report covers research and technology transfer activities for the first half of the second project year (October 1, 2004 through March 31, 2005), Budget Period I. This work consisted of diagenetic analysis of the Leadville Limestone reservoir at the Lisbon case-study field, Utah, which accounts for most of the Leadville oil production in the Paradox Basin. Analyses included scanning electron microscopy, epifluorescence, cathodoluminescence, and study of fluid inclusions from Leadville core samples and thin sections from Lisbon field. The overall conclusion from this work indicates late dolomitization, saddle dolomite, and dolomite cement precipitation, as well as sulfides and brecciation, may have developed from hydrothermal events that can greatly improve reservoir quality. The result can be the formation of large, diagenetic-type, hydrocarbon traps. The reservoir characteristics, particularly diagenetic overprinting and history, can be applied regionally to other fields and exploration trends in the basin.

Scanning electron microscopy demonstrates how Leadville reservoir quality at Lisbon is greatly enhanced by dolomitization and dissolution of shallow water limestone. There are two basic types of dolomite: (1) very fine, early dolomite, and (2) coarse, late dolomite. Early dolomitization preserves depositional fabrics and has limited porosity development, except for limited dissolution of fossils, and has very low permeabilities. Late dolomitization has two morphologies: rhombic dolomites and saddle dolomites. Most reservoir rocks within Lisbon field appear to be associated with the second, late type of dolomitization and associated leaching events. Pyrobitumen coats most intercrystalline dolomite as well as dissolution pores associated with the second type of dolomite. Fractures enhance the permeability in several intervals. Minor euhedral quartz is present in several samples. Anhydrite and sulfide mineral (s) are present in moderate abundance. The general diagenetic sequence for these samples, based on scanning electron microscopy analysis, is (1) dolomitization, (2) dissolution, (3) dolomite cementation, (4) fracturing, (5) quartz cementation, (6) calcite cementation, (7) clay precipitation, (8) anhydrite cementation, (9) pyrobitumen emplacement, and (10) sulfide precipitation.

Epifluorescence petrography makes it possible to clearly identify grain types and shapes, within both limestone and dolomite reservoir intervals. In particular, identification of

peloids, skeletal grain types, and coated grains are easy to see in rocks where these grains have been poorly preserved, partially leached, or completely dolomitized. Epifluorescence petrography clearly and rapidly images pore spaces that cannot otherwise be seen in standard viewing under transmitted polarized lighting. In many of the limestones and finely crystalline dolomites, the differences between muddy and calcarenitic fabrics can only be clearly appreciated with fluorescence lighting. Much of the Leadville porosity is very heterogeneous and poorly connected as viewed under epifluorescence. The epifluorescence examination helps in seeing the dissolution origin of most types of porosity. Transmitted polarized lighting does not image intercrystalline porosity in carbonate samples very well, even though blue-dyed epoxy can be impregnated into even very small pores. In addition, opaque bitumen pore linings prevent light from passing through some of the pores to the observer. Without the aid of the epifluorescence view, the amount of visible open pore space would be underestimated in the plane-light image. Where dolomitization has occurred, epifluorescence petrography often shows the crystal size, shape, and zonation far better than transmitted plane or polarized lighting. This information is often very useful when considering the origin and timing of dolomitization, as well as evaluating the quality of the pore system within the dolomite. Low-permeability carbonates from this study area show bright yellow fluorescence due to trapped live oil that is retained within tighter parts of the reservoir system. More permeable rocks show red fluorescence due to the epoxy fluorescence where oil has almost completely drained from the better quality portions of the reservoir.

Cathodoluminescence imaging of samples nicely complements the types of information derived from epifluorescence of carbonate thin sections. The amount of open porosity under cathodoluminescence is considerably greater than that visible under plane-light microscopy. Cathodoluminescence also displays original depositional textures and the outlines of original carbonate grains and distinctly images pore spaces. This information is often very useful when considering the origin and timing of dolomitization, as well as evaluating the quality of the pore system within the dolomite. Cathodoluminescence shows a wide range of crystal size and growth habits within the dull red luminescing, matrix-replacing dolomite. The vast majority of the dolomite within areas of fabric-selective dolomitization is a deep or intense red color. Between many of the grains, there is a lighter red luminescence where early cements have been dolomitized. Some of the coarser dolomite crystals appear to have an overgrowth of brighter red luminescent material. Examination of saddle dolomites under cathodoluminescence can provide more information about these late, elevated temperate (often hydrothermal) mineral phases. For instance, saddle dolomites show nice growth banding. These saddle dolomites display dull, red luminescence in their core areas and slightly bright, orange-red luminescence toward their rim areas.

The fluid inclusion and mineral relationships suggest the following sequence of events: (1) dolomite precipitation, (2) anhydrite deposition, (3) anhydrite dissolution and quartz precipitation, (4) dolomite dissolution and late calcite precipitation, (5) trapping of a mobile oil phase, and (6) formation of bitumen. Aqueous fluid inclusions in early calcite, which typically forms coarse-grained crystals, display a range of liquid-to-vapor ratios suggesting they have necked. Oil inclusions yielded homogenization temperatures ranging from 48 to 70^{o}C (118-158^{o}F). These temperatures represent the minimum temperature of oil formation, not of calcite deposition. The oil was generated in place by maturation of organic material. Both the oil inclusions and the common presence of two-phase, necked aqueous inclusions imply trapping at elevated temperatures. It is suggested trapping occurred when the original calcite recrystallized

during burial. Fluid inclusions in dolomite have re-equilibrated (stretched, necked, refilled) since trapping. The common presence of single-phase aqueous inclusions suggests that the fine-grained dolomite and cores of saddle dolomite were deposited at temperatures less than about 50°C (<~122 °F). Low ice-melting temperatures of quartz- and calcite-hosted inclusions suggest chemically complex Ca-Mg-bearing brines associated with evaporite deposits were responsible for mineral deposition. Oil deposited in healed fractures within late, pore-filling calcite has similar fluorescence to the primary inclusions, but lower homogenization temperatures of about 40°C (~104 °F). The lower temperatures of the secondary oil inclusions allow the possibility that the temperatures were decreasing, perhaps due to unroofing, prior to bitumen formation. It is possible live oil was preserved in the calcite and dolomite, but not in the main fractures, which now contain bitumen because the oil was not degassed.

Technology transfer activities for the reporting period consisted of a technical presentation, poster, and core display at the Rocky Mountain Association of Geologists *Hydrothermal Dolomite Symposium and Core Workshop*, November 15, 2004, in Golden, Colorado. The presentation included the general petroleum geology of the Leadville Limestone, and facies, petrography, and diagenesis, especially dolomite, of the Lisbon case-study field in Utah. The project home page was updated on the Utah Geological Survey Web site. Project team members published an abstract, non-technical newsletter article, and semi-annual report detailing project progress and results. An abstract describing Leadville diagenesis with emphasis on dolomitization was submitted and accepted by the American Association of Petroleum Geologists, for presentation at the 2005 Annual Convention in Calgary, Canada.

INTRODUCTION

Project Overview

The Mississippian Leadville Limestone has produced over 53 million barrels (bbls) (8.4 million m^3) of oil from six fields in the northern Paradox Basin region, referred to as the Paradox fold and fault belt, of Utah and Colorado. All of these fields are currently operated by small, independent producers. There have been no new discoveries since the early 1960s, and only independent producers continue to explore for Leadville oil targets in the region, 85 percent of which is under the stewardship of the federal government. This environmentally sensitive, 7500-square-mile (19,400 km^2) area is relatively unexplored with only about 100 exploratory wells that penetrated the Leadville (less than one well per township), and thus the potential for new discoveries remains great.

The overall goals of this study are to (1) develop and demonstrate techniques and exploration methods never tried on the Leadville Limestone, (2) target areas for exploration, (3) increase deliverability from new and old Leadville fields through detailed reservoir characterization, (4) reduce exploration costs and risk especially in environmentally sensitive areas, and (5) add new oil discoveries and reserves.

The Utah Geological Survey (UGS) and Eby Petrography & Consulting, Inc., have entered into a cooperative agreement with the U.S. Department of Energy (DOE) as part of its Advanced and Key Oilfield Technologies for Independents (Area 2 – Exploration) Program. The project will be conducted in two phases, each with specific objectives and separated by a continue-stop decision point based on results as of the end of Phase I. The objective of Phase 1 is to conduct a case study of the Leadville reservoir at Lisbon field (the largest Leadville producer), San Juan County, Utah, in order understand the reservoir characteristics and facies that can be applied regionally. The first objective of Phase 2 will be to conduct a low-cost field demonstration of new exploration technologies to identify potential Leadville oil migration directions (evaluating the middle Paleozoic hydrodynamic pressure regime), and surface geochemical anomalies (using microbial, soil, gas, iodine, and trace elements), especially in environmentally sensitive areas. The second objective will be to determine regional facies (evaluating cores, geophysical well logs, outcrop and modern analogs), identify potential oil-prone areas based on shows (using low-cost epifluorescence techniques), and target areas for Leadville exploration.

These objectives are designed to assist the independent producers and explorers who have limited financial and personnel resources. All project maps, studies, and results will be publicly available in digital (interactive, menu-driven products on compact disc) or hard-copy format and presented to the petroleum industry through a proven technology transfer plan. The technology transfer plan includes a Technical Advisory Board composed of industry representatives operating in the Paradox Basin and a Stake Holders Board composed of representatives of state and federal government agencies, and groups with a financial interest within the study area. Project results will also be disseminated via the UGS Web site, technical workshops and seminars, field trips, technical presentations at national and regional professional meetings, convention displays, and papers in various technical or trade journals, and UGS publications.

This report covers research and technology transfer activities for the first half of the second project year (October 1, 2004 through March 31, 2005), Budget Period I. This work

consisted of diagenetic analysis of the Leadville Limestone reservoir at the Lisbon case-study field, Utah, which accounts for most of the Leadville oil production in the Paradox Basin. Analyses included scanning electron microscopy, epifluorescence, cathodoluminescence, and study of fluid inclusions.

Project Benefits and Potential Application

Exploring for the Leadville Limestone is high risk, with less than a 10 percent chance of success based on the drilling history of the region. Prospect definition requires expensive, three-dimensional (3D) seismic acquisition, often in environmentally sensitive areas. These facts make exploring difficult for independents that have limited funds available to try new, unproven techniques that might increase the chance of successfully discovering oil. We believe that one or more of the project activities will reduce the risk taken by an independent producer in looking for Leadville oil, not only in exploring but in trying new techniques. For example, the independent would not likely attempt surface geochemical surveys without first knowing they have been proven successful in the region. If we can prove geochemical surveys are an effective technique in environmentally sensitive areas, the independent will save both time and money exploring for Leadville oil.

Another problem in exploring for oil in the Leadville Limestone is the lack of published or publicly available geologic and reservoir information, such as regional facies maps, complete reservoir characterization studies, surface geochemical surveys, regional hydrodynamic pressure regime maps, and oil show data and migration interpretations. Acquiring this information or producing these studies would save cash and manpower resources which independents simply do not possess or normally have available only for drilling. The technology, maps, and studies generated from this project will help independents to identify or eliminate areas and exploration targets prior to spending significant financial resources on seismic data acquisition and environmental litigation, and therefore increase the chance of successfully finding new accumulations of Leadville oil.

These benefits may also apply to other high-risk, sparsely drilled basins or regions where there are potential shallow-marine carbonate reservoirs equivalent to the Mississippian Leadville Limestone. These areas include the Utah-Wyoming-Montana thrust belt (Madison Limestone), the Kaiparowits Basin in southern Utah (Redwall Limestone), the Basin and Range Province of Nevada and western Utah (various Mississippian and other Paleozoic units), and the Eagle Basin of Colorado (various Mississippian and other Paleozoic units).

Many mature basins have productive carbonate reservoirs of shallow-marine shelf origin. These mature basins include the Eastern Shelf of the Midland Basin, West Texas (Pennsylvanian-age reservoirs in the Strawn, Canyon, and Cisco Formations); the Permian Basin, West Texas and southeast New Mexico (Permian age Abo and other formations along the northwest shelf of the Permian Basin); and the Illinois Basin (various Silurian units). A successful demonstration in the Paradox Basin makes it very likely that the same techniques could be applied in other basins as well. In general, the average field size in these other mature basins is larger than fields in the Paradox Basin. Even though there are differences in depositional facies and structural styles between the Paradox Basin and other basins, the fundamental use of the techniques and methods is a critical commonality.

PARADOX BASIN - OVERVIEW

The Paradox Basin is located mainly in southeastern Utah and southwestern Colorado, with a small portion in northeastern Arizona and northwestern New Mexico (figure 1). The Paradox Basin is an elongate, northwest-southeast-trending, evaporitic basin that predominately developed during the Pennsylvanian. The basin can generally be divided into three areas: the Paradox fold and fault belt in the north, the Blanding sub-basin in the south-southwest, and the Aneth platform in southeasternmost Utah (figure 1). The Mississippian Leadville Limestone is one of two major oil and gas reservoirs in the Paradox Basin, the other being the Pennsylvanian Paradox Formation (figure 2). Most Leadville production is from the Paradox fold and fault belt (figure 3).

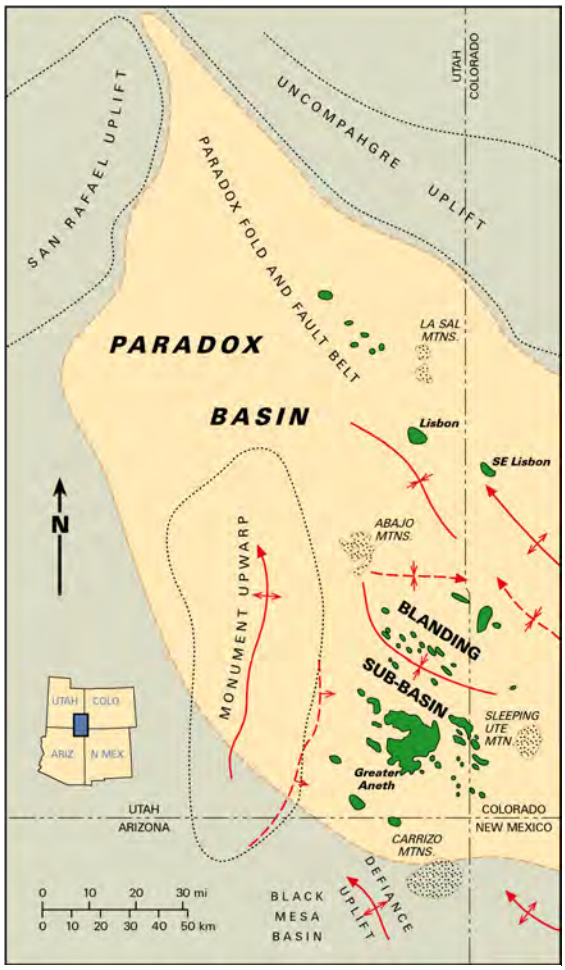

Figure 1. Oil and gas fields in the Paradox Basin of Utah and Colorado.

The most obvious structural features in the basin are the spectacular anticlines that extend for miles in the northwesterly trending fold and fault belt. The events that caused these and many other structural features to form began in the Proterozoic, when movement initiated on high-angle basement faults and fractures 1700 to 1600 Ma (Stevenson and Baars, 1987). During Cambrian through Mississippian time, this region, as well as most of eastern Utah, was the site of typical, thin, marine deposition on the craton while thick deposits accumulated in the miogeocline to the west (Hintze, 1993). However, major changes occurred beginning in the Pennsylvanian. A series of basins and fault-bounded uplifts developed from Utah to Oklahoma as a result of the collision of South America, Africa, and southeastern North America (Kluth and Coney, 1981; Kluth, 1986), or from a smaller scale collision of a microcontinent with south-central North America (Harry and Mickus, 1998). One result of this tectonic event was the uplift of the Ancestral Rockies in the western United States. The Uncompahgre Highlands in eastern Utah and western Colorado initially formed as the westernmost range of the Ancestral Rockies during this ancient mountain-building period. The southwestern flank of the Uncompahgre Highlands (uplift) is bounded by a large, basement-involved, high-angle, reverse fault identified from seismic surveys and exploration drilling. As the highlands rose, an accompanying depression, or foreland basin, formed to the southwest – the Paradox Basin. Rapid subsidence, particularly during the Pennsylvanian and continuing into the Permian, accommodated large volumes of evaporitic and marine sediments that intertongue with non-marine arkosic material shed from the highland area to the northeast (Hintze, 1993).

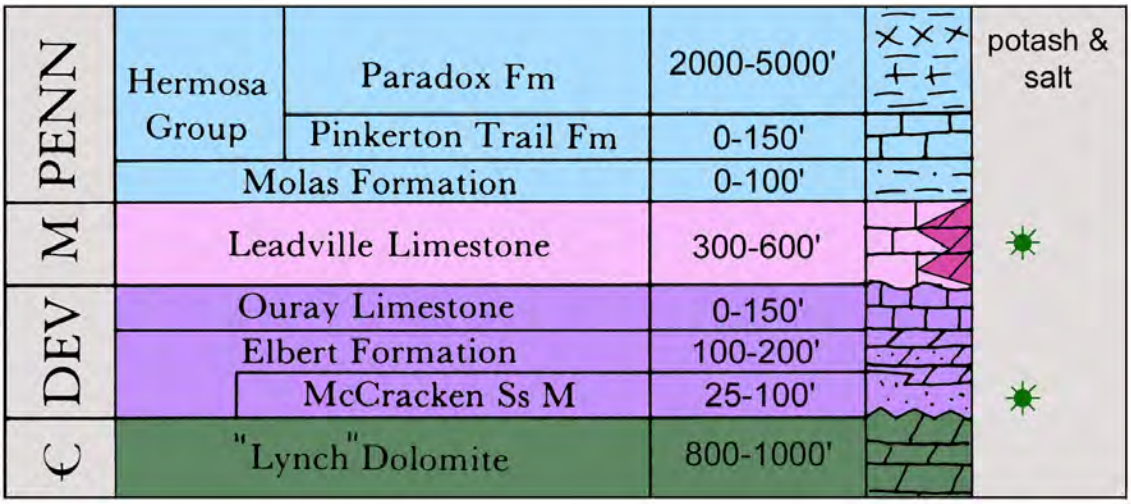

Figure 2. Stratigraphic column of a portion of the Paleozoic section determined from subsurface well data in the Paradox fold and fault belt, Grand and San Juan Counties, Utah (modified from Hintze, 1993).

The Paradox Basin is surrounded by other uplifts and basins, which formed during the Late Cretaceous-early Tertiary Laramide orogeny (figure 1). The Paradox fold and fault belt was created during the Tertiary and Quaternary by a combination of (1) reactivation of basement normal faults, (2) salt flowage, dissolution and collapse, and (3) regional uplift (Doelling, 2000).

Most oil and gas produced from the Leadville Limestone is found in basement-involved, northwest-trending structural traps with closure on both anticlines and faults (figure 4). Lisbon, Big Indian, Little Valley, and Lisbon Southeast fields (figure 3) are sharply folded anticlines that close against the Lisbon fault zone. Salt Wash and Big Flat fields (figure 3), northwest of the Lisbon area, are unfaulted, east-west- and north-south-trending anticlines, respectively.

RESERVOIR CHARACTERIZATION OF THE LEADVILLE LIMESTONE, LISBON CASE-STUDY FIELD, SAN JUAN COUNTY, UTAH – RESULTS AND DISCUSSION

Introduction and Field Synopsis

Lisbon field, San Juan County, Utah (figure 3) accounts for most of the Leadville oil production in the Paradox Basin. A wealth of Lisbon core, petrographic, and other data is available to the UGS. The reservoir characteristics, particularly diagenetic overprinting and history, and Leadville facies can be applied regionally to other fields and exploration trends in the Paradox Basin. Therefore, we selected Lisbon as the major case-study field for the Leadville Limestone project.

The Lisbon trap is an elongate, asymmetric, northwest-trending anticline, with nearly 2000 feet (600 m) of structural closure and bounded on the northeast flank by a major, basement-involved normal fault with over 2500 feet (760 m) of displacement (Smith and

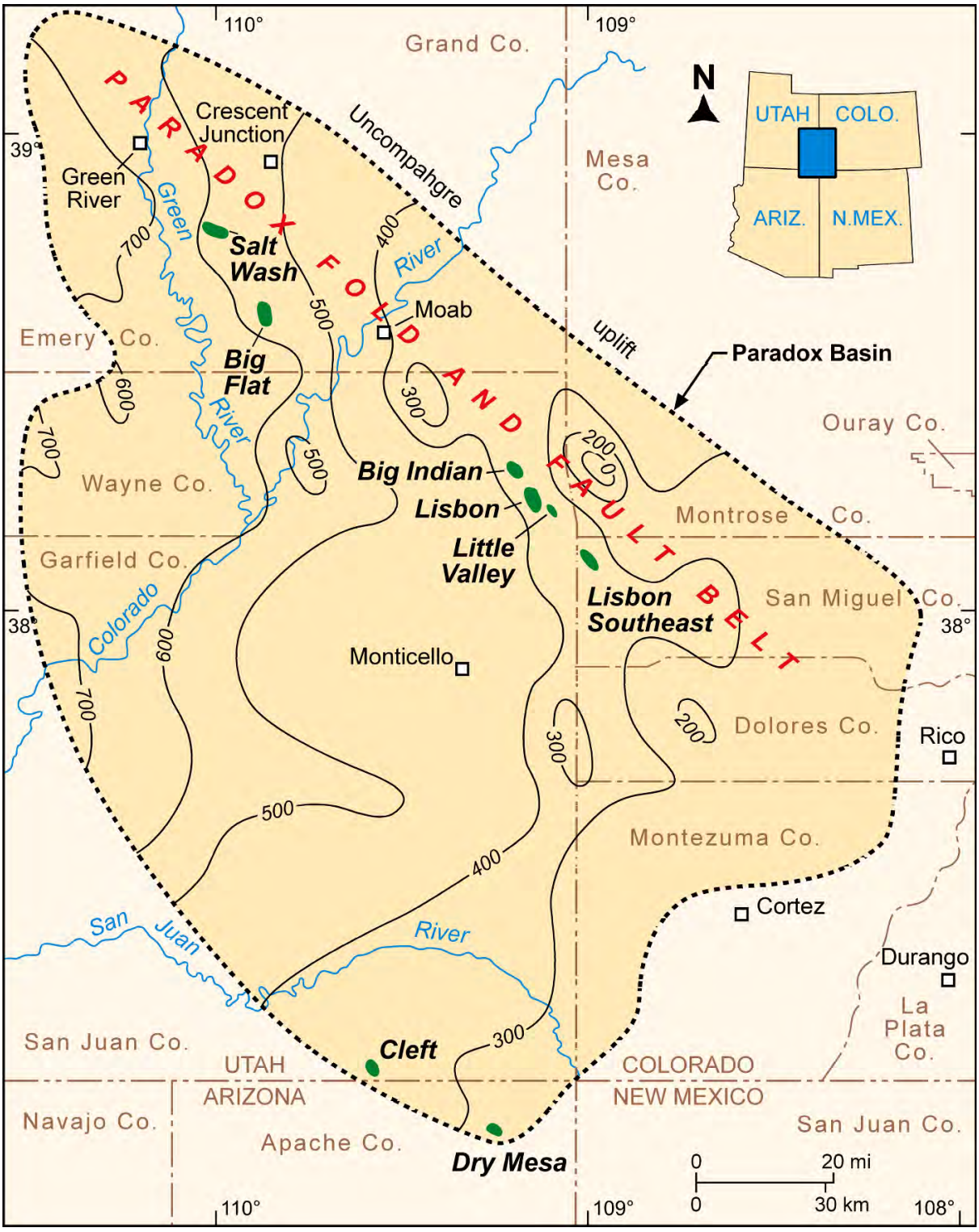

Figure 3. Location of fields that produce oil (green) from the Mississippian Leadville Limestone, Utah and Colorado. Thickness of the Leadville is shown; contour interval is 100 feet (modified from Parker and Roberts, 1963).

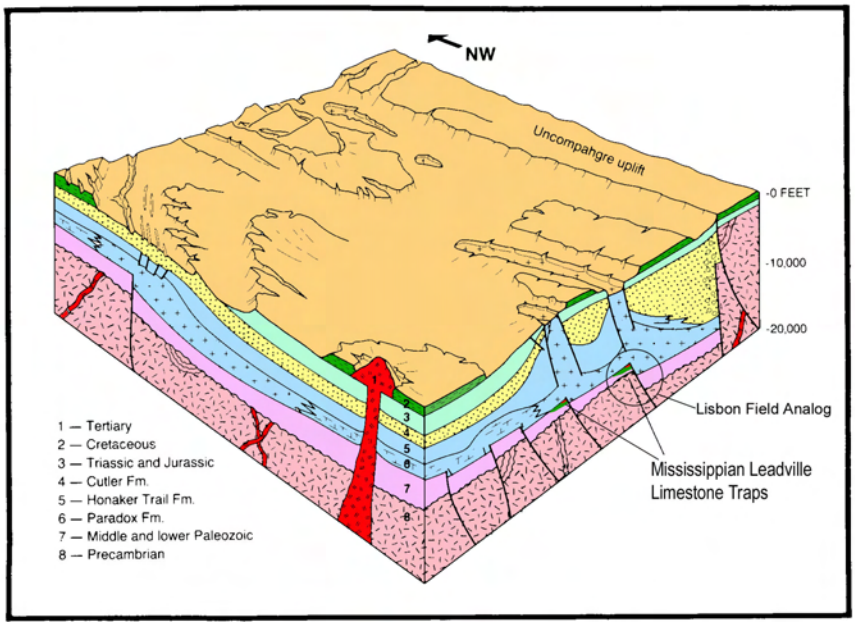

Figure 4. Schematic block diagram of the Paradox Basin displaying basement-involved structural trapping mechanisms for the Leadville Limestone fields (modified from Petroleum Information, 1984; original drawing by J.A. Fallin).

Prather, 1981) (figure 5). Several minor, northeast-trending normal faults dissect the Leadville reservoir into segments. Producing units contain dolomitized crinoidal/skeletal grainstone, packstone, and wackestone fabrics. Diagenesis includes fracturing, autobrecciation, karst development, hydrothermal dolomite, and bitumen plugging. The net reservoir thickness is 225 feet (69 m) over a 5120-acre (2100 ha) area (Clark, 1978; Smouse, 1993). Reservoir quality is greatly improved by natural fracture systems associated with the Paradox fold and fault belt. Porosity averages 6 percent in intercrystalline and moldic networks enhanced by fractures; permeability averages 22 millidarcies (mD). The drive mechanism is an expanding gas cap and gravity drainage; water saturation is 39 percent (Clark, 1978; Smouse, 1993). The bottom-hole temperature ranges from 153 to 189ºF (53-73ºC).

Lisbon field was discovered in 1960 with the completion of the Pure Oil Company No. 1 NW Lisbon USA well, NE1/4NW1/4 section 10, T. 30 S., R. 24 E., Salt Lake Base Line and Meridian (SLBL&M) (figure 5), with an initial flowing potential (IFP) of 179 bbls of oil per day (BOPD) (28 m^3) and 4376 thousand cubic feet of gas per day (MCFGPD) (124 MCMPD). The original reservoir field pressure was 2982 pounds per square inch (psi) (20,560 kPa) (Clark, 1978). There are currently 22 producing (or shut-in wells), 11 abandoned producers, five injection wells (four gas injection wells and one water/gas injection well), and four dry holes in the field. Cumulative production as of April 1, 2005, was 51,120,967 bbls of oil (8,128,234 m^3), 777 billion cubic feet of gas (BCFG) (22.0 BCMG) (cycled gas), and 49,889,526 bbls of water (7,932,434 m^3) (Utah Division of Oil, Gas and Mining, 2005). Gas that was re-injected into the crest of the structure to control pressure decline is now being produced.

Three factors create reservoir heterogeneity within productive zones: (1) variations in carbonate fabrics and facies, (2) diagenesis (including karstification), and (3) fracturing. The extent of these factors and how they are combined affect the degree to which they create barriers to fluid flow.

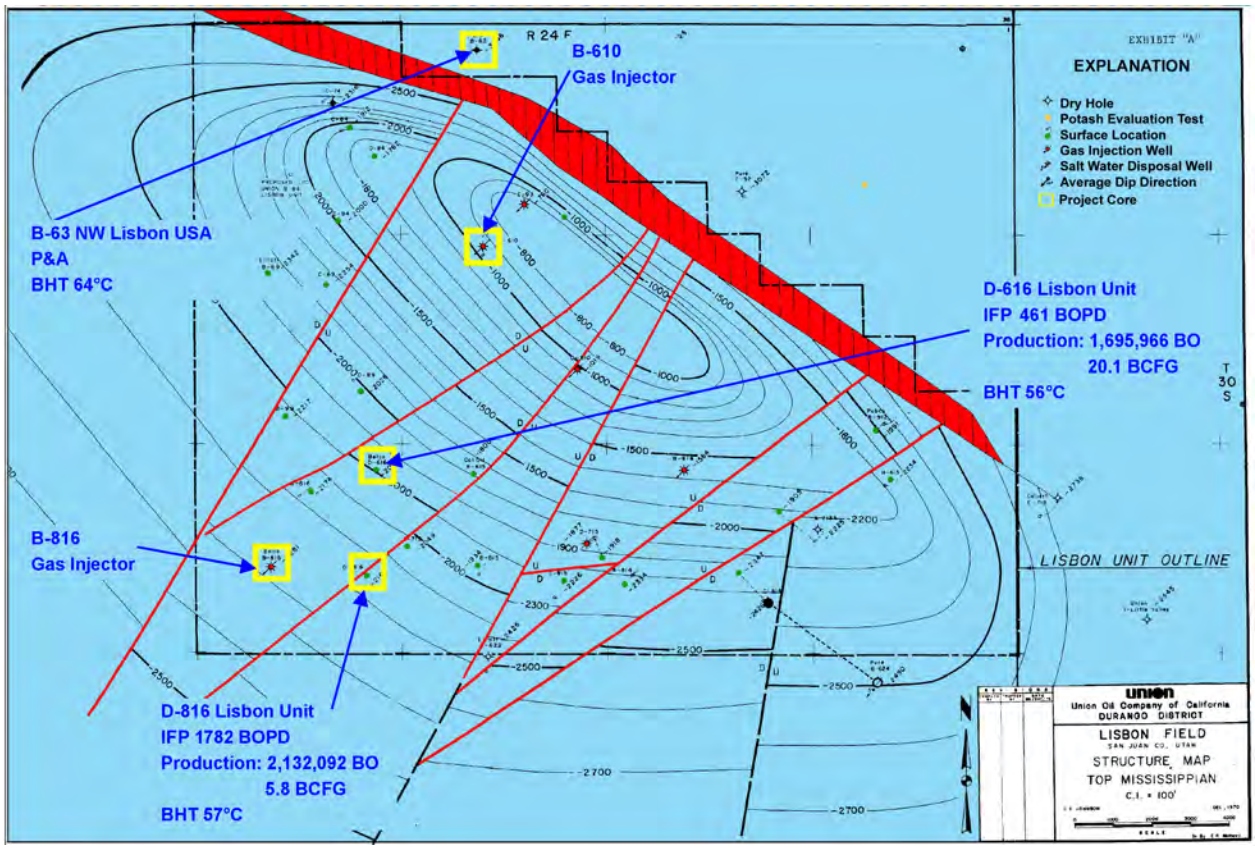

Figure 5. Top of structure of the Leadville Limestone, Lisbon field, San Juan County, Utah (modified from C.F. Johnson, Union Oil Company of California files, 1970; courtesy of Tom Brown, Inc.). Also displayed are wells from which cores were described and sampled in this study.

Diagenetic Analysis - Overview

The diagenetic fabrics and porosity types found in the various hydrocarbon-bearing rocks of Lisbon field can be indicators of reservoir flow capacity, storage capacity, and untested potential. Diagenetic characterization focused on reservoir heterogeneity, quality, and compartmentalization within the field. All depositional, diagenetic, and porosity information will be combined with the production history in order to analyze the potential for the Leadville regionally. In order to determine the diagenetic histories of the various Leadville rock fabrics, including both reservoir and non-reservoir, representative samples were selected from the conventional cores for petrographic description and geochemical analysis. Carbonate fabrics were determined according to Dunham's (1962) and Embry and Klovan's (1971) classification schemes. Pores and pore systems were described using Choquette and Pray's (1970) classification (figure 6).

An ideal diagenetic sequence based on our analysis of Leadville thin sections from Lisbon field is presented in figure 7. Leadville reservoir quality at Lisbon is greatly enhanced by dolomitization and dissolution of limestone. There are two basic types of dolomite: very fine, early dolomite and coarse, late dolomite. The early dolomitization and leaching of skeletal grains resulted in low-porosity and/or low-permeablility rocks. Most reservoir rocks within

Lisbon field appear to be associated with the second, late type of dolomitization and associated leaching events. Other diagenetic products include pyrobitumen, syntaxial cement, sulfide minerals, anhydrite cement and replacement, and late macrocalcite. Fracturing and brecciation caused by hydrofracturing are widespread within Lisbon field. Sediment-filled cavities, related to karstification of the exposed Leadville, are present in the upper third of the formation. Late dolomitization, sulfides, and brecciation may have developed from hydrothermal events that can greatly improve reservoir quality.

The geochemical and petrographic techniques that were employed consisted of (1) scanning electron microscope (SEM) analysis of various dolomites to determine reservoir quality of the dolomites as a function of diagenetic history, (2) epifluorescence (EF), (3) cathodoluminescence (CL) petrography for the sequence of diagenesis, and (4) fluid inclusion (FI) evaluation to determine the temperatures of secondary dolomite formation and the salinity of the original brines. Additional geochemical analysis will include (1) stable carbon and oxygen isotope analysis of diagenetic components such as cementing minerals and different generations of dolomites, and (2) strontium isotope analysis for tracing the origin of fluids responsible for different diagenetic events.

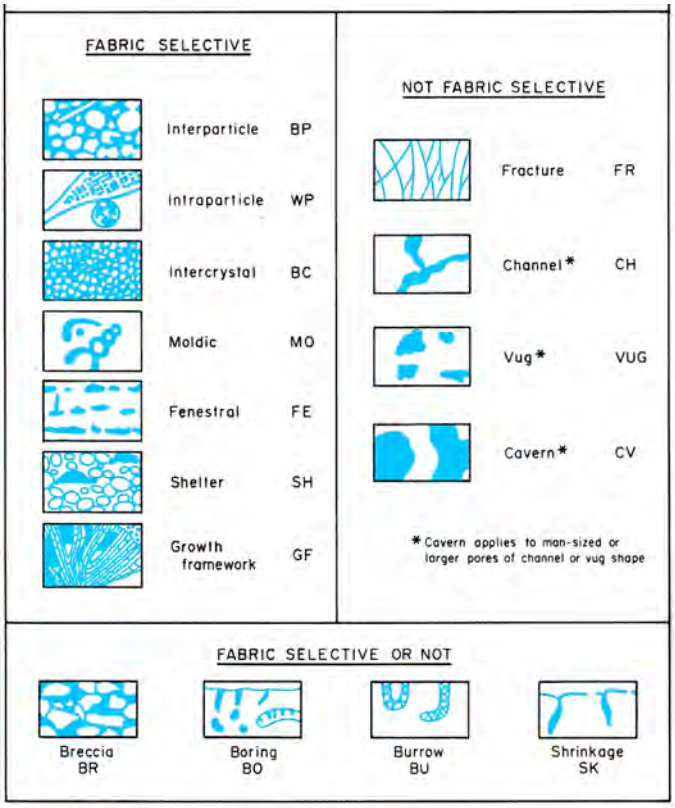

Figure 6. Classification of pores and pore systems in carbonate rocks (Choquette and Pray, 1970).

Scanning Electron Microscopy

Introduction

The diagenetic fabrics and porosity types found in the various hydrocarbon-bearing rocks in the Leadville Limestone of Lisbon field can be indicators of reservoir flow capacity and storage capacity. In order to determine the diagenetic histories of the Leadville reservoir, representative samples were selected from the conventional cores which were used for thin sections. Carbonate fabrics were determined according to Dunham's (1962) and Embry and Klovan's (1971) classification schemes. A scanning electron microscope (SEM) was used to photograph: (1) typical preserved primary and secondary pore types and pore throats, (2) cements, (3) sedimentary structures, (4) fractures, and (5) pore plugging anhydrite, halite, and bitumen. Diagenetic characterization focussed on reservoir heterogeneity, quality, and compartmentalization within the field. Of special interest is the identification of possible

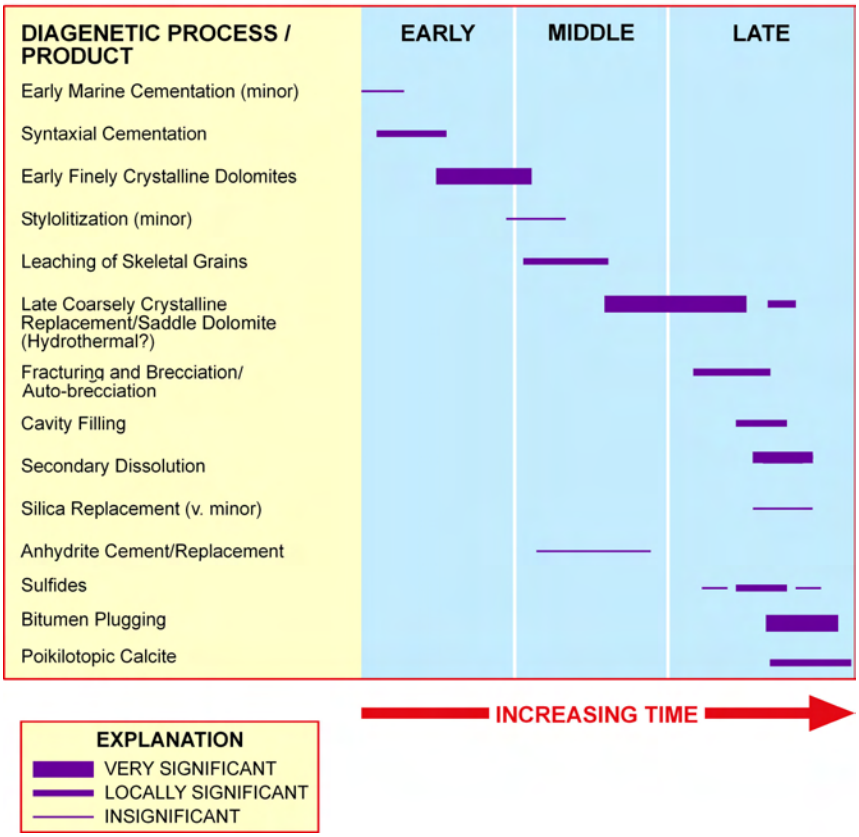

Figure 7. Ideal diagenetic sequence through time based on thin section analysis, Leadville Limestone, Lisbon field.

hydrothermal dolomite and the determination of the most effective pore systems for oil drainage versus storage. Scanning electron microscope analyses were conducted on 12 thin section blanks from the core samples that displayed particular characteristics of interest (table 1). Porosity types and associated abbreviations included in this report are from Choquette and Pray (1970) (figure 6).

Porosity Types

All samples exhibit microporosity in the form of intercrystalline (BC) porosity (figure 8). Dissolution has contributed to porosity in most samples as well. Dissolution has created moldic (MO), vuggy (VUG), and channel (CH) porosity. Dissolution pores are most often in the mesopore size range (62.5 microns to 4.0 mm.).

Permeability is related to the size and number of pore throats, and, particularly, to the continuity of pore throats. In general, permeability is good in the samples studied, but is limited slightly by mineral cements and pyrobitumen (figure 9).

Fractures enhance the permeability in several intervals (figure 10). Scanning electron microscopic examination identified fractures in the 8423- and 8442-foot (2567- and 2573-m) intervals of the Lisbon No. D-816 well, and the 8356- and 8682-foot (2547- and 2646-m) intervals of the Lisbon No. D-616 well. In addition to the fractures reported here, petrographic analysis revealed fractures in the 8308- and 8619-foot (2532- and 2627-m) intervals of the Lisbon No. D-816 well, and the 7886-foot (2404-m) interval of the Lisbon No. B-610 well.

Table 1. Summary of characteristics observed with scanning electron microscopy in samples from the Lisbon No. D-816, Lisbon No. D-616, and Lisbon No. B-610 wells, Lisbon field, San Juan County, Utah.

Well	Lisbon D-816					Lisbon D-616					Lisbon B-610	
DEPTH (ft)	8423'	8426'	8433'	8442'	8486'	8308'	8356'	8559'	8619'	8682'	7886'	7897'
POROSITY												
Intergranular (Micro) (BC)	X	X	X	X	X	X	X	X	X	X	X	X
Dissolution (MO)	X	X	X	X	X		X		X		X	X
Dissolution (VUG)		X	X	X	X				X		X	X
Dissolution (CH)											X	
Fractures	X			X		X	X		X	X	X	
CEMENTS												
Anhydrite		X	X							X		
Calcite					X	X	X				X	
Quartz					X	X	X		X			
Dolomite	X	X	X	X	X	X	X	X	X	X	X	X
Illitic Clay	X					?				X		X
Pyrobitumen	X	X	X	X	X				X			
Sulfides	X		X	X	X				X		X	X
DIAGENESIS												
Dolomitization	X	X	X	X	X	X	X		X	X	X	X
Dissolution	X	X	X	X	X	X	X		X	X	X	X
Calcite Cementation					X	X	X					
Quartz Cementation					X	X	X		X			
Illitic clay Deposition	X					X			X	X	X	X
Anhydrite Cementation		X	X							X		
Pyrobitumen Emplacement	X	X	X	X	X				X			
Fracturing	X			X		X	X		X	X	X	
Data from SEM, EDS, and optical microscopy by Standard Geological Services, Inc. and petrography by Eby Petrography & Consulting.												

Undoubtedly, fractures enhance the permeability in the 8423- and 7886-foot (2567- and 2404-m) samples given their respective measured values of 46 mD and 114 mD. The 83 mD measured permeability of the 7897-foot (2407-m) interval and the 15 mD of the 8426-foot (2568-m) interval suggest that fractures are present in these intervals as well. They were not observed during analysis, however.

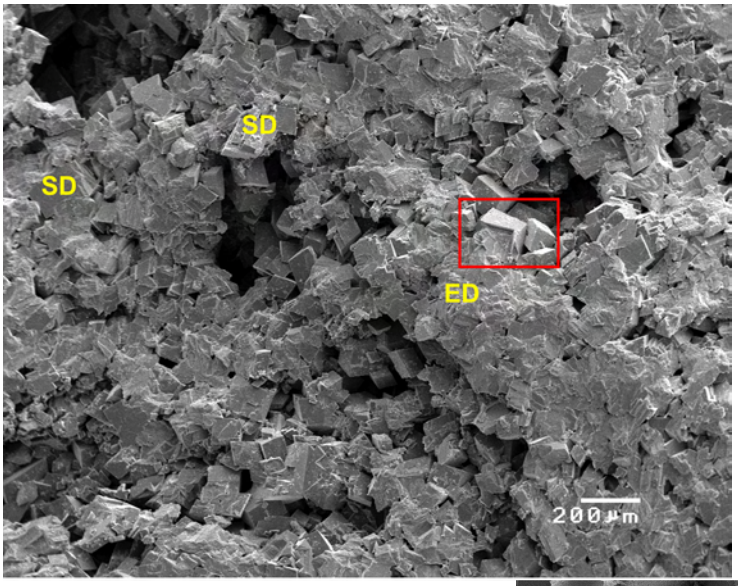

Figure 8. Scanning electron microscope photomicrograph of a core plug from 8433 feet, Lisbon No. D-816 well, showing typical Leadville dolomites at Lisbon field. Note the very fine, tight early dolomites (ED) that have been replaced with late, rhombic and saddle (SD) dolomites. There is a significant porosity increase associated with the late dolomite replacement. Scale bar represents 200 microns (0.2 mm). Porosity = 2 percent; permeability < 0.1 mD based on core-plug analysis.

Figure 9. Scanning electron microscope photomicrograph of a core plug from 7886 feet, Lisbon No. B-610 well, showing probable pyrobitumen (P) coating the rhombic dolomite crystal in the center. Pyrobitumen coats many other dolomite crystals as well. Scale bar represents 10 microns (0.01 mm). Porosity = 13.8 percent; permeability = 114 mD based on core-plug analysis.

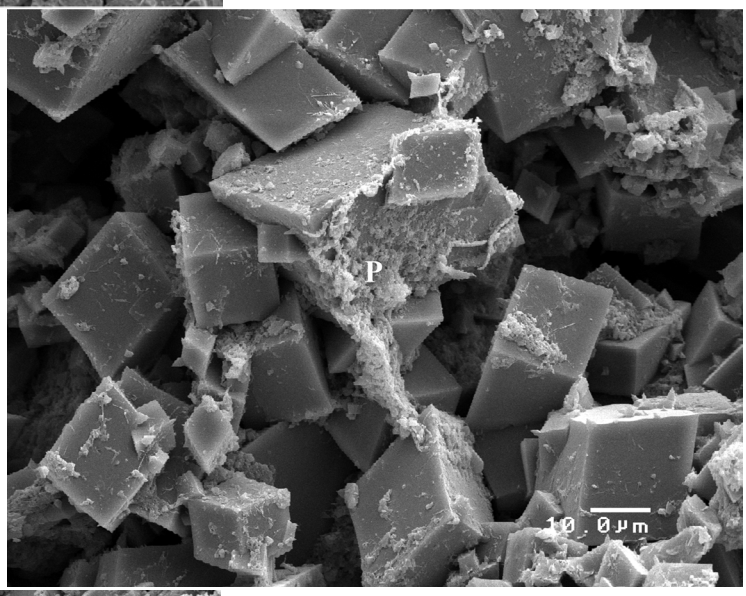

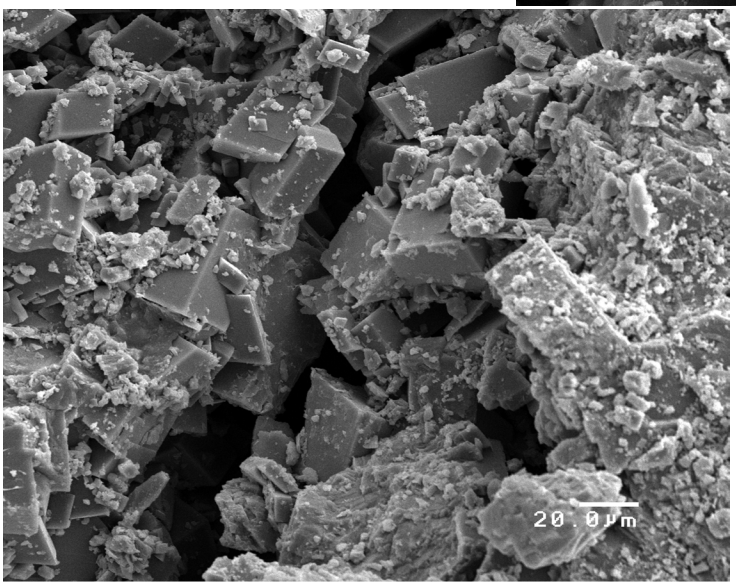

Figure 10. Scanning electron microscope photomicrograph of a core plug from 8423 feet, Lisbon No. D-816 well, showing enlargement a fracture partially filled with secondary dolomite. Scale bar represents 20 microns (0.02 mm). Porosity = 10.5 percent; permeability = 47 mD based on core-plug analysis.

Lithology, Diagenesis, and Cements

All samples are dolomite except for the limestone matrix present in the 8308-foot (2532-m) sample of the Lisbon No. D-616 well. That sample, however, contains dolomite as fill material. Secondary materials present include dolomite, calcite, clays, and pyrobitumen. Their presence is discussed below and also included in table 1.

Dolomite is the dominant cement (figure 8) in all samples except the 8426-foot (2568-m) sample from the Lisbon No. D-816 well, where anhydrite is the abundant cement. The two basic types of dolomite are well displayed by SEM (figure 8): the low-porosity and/or low-permeablility, very fine, early dolomite and higher porosity and/or high permeablility, coarse, late dolomite (figure 11).

Pores in the 8426-foot (2568-m) sample from the Lisbon No. D-816 well are partially filled with anhydrite (figure 12). Anhydrite is also reported from petrographic analays of the 8433-foot (2570-m) interval of this well and the 8682-foot (2646-m) sample of the Lisbon No. D-616 well. Scanning electron microscopic analysis indicates that anhydrite is abundant in the 8426-foot (2568-m) sample; it is most likely much less abundant in the other intervals.

Minor euhedral quartz is present in several samples (figure 13). Rare illitic clays, possibly illite/smectite mixed-layer clays, are also present. Sulfide mineral(s) containing an unknown cation are present in moderate abundance (figure 14). Calcite cement, although rare, was observed in a few samples. The minor constituents of quartz, clays, calcite, and sulfides contribute little to the overall lithology and are relatively insignificant with respect to reservoir quality. The quartz, clay, and calcite cements are rare, and the more abundant sulfide mineral (s) consist of extremely small crystals about 2 microns or smaller.

An approximate diagenetic sequence based on SEM is listed below (not all diagenetic events were identified in every sample). The various diagenetic events are included in table 1.

1. Dolomitization
2. Dissolution
3. Dolomite cementation
4. Fracturing
5. Quartz cementation
6. Calcite cementation
7. Clay precipitation
8. Anhydrite cementation
9. Pyrobitumen emplacement
10. Sulfide precipitation

Epifluorescence

Introduction

Epifluorescence microscopy is a technique that has been used successfully in recent years to provide additional information on diagenesis, pores, and organic matter (including “live” hydrocarbons) within sedimentary rocks. It is a rapid, non-destructive procedure that can be done using a high-quality petrographic (polarizing) microscope equipped with reflected light capabilities. The basic principles and equipment for EF were largely developed in the 1960s

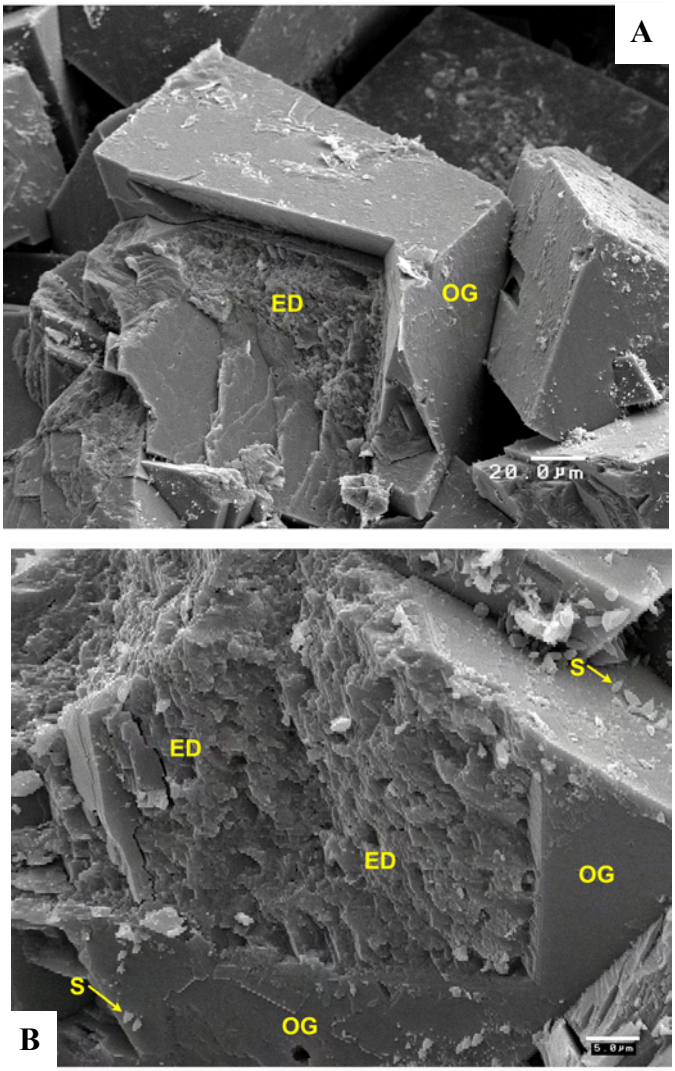

Figure 11. Scanning electron microscope photomicrograph of a core plug from 8433 feet shown in figure 8 (see red box), Lisbon No. D-816 well. A – Closeup shows the composition of typical replacement rhombic dolomites. The core of each rhombic crystal is composed of a dense remnant of fine, early dolomite (ED), which is surrounded by a euhedral dolomite overgrowth (OG). The rhombic dolomite faces are often covered with a thin film of pyrobitumen. Scale bar represents 20 microns (0.02 mm). B – High magnification across a section of poorly crystalline, early dolomite core (ED) and dense overgrowth (OG) that forms the dolomite into coarser rhombs. The very small, angular decorations on the crystal surfaces may very well be small sulfide precipitates (S). Scale bar represents 5 microns (0.005 mm). Porosity = 2 percent; permeability < 0.1 mD based on core-plug analysis.

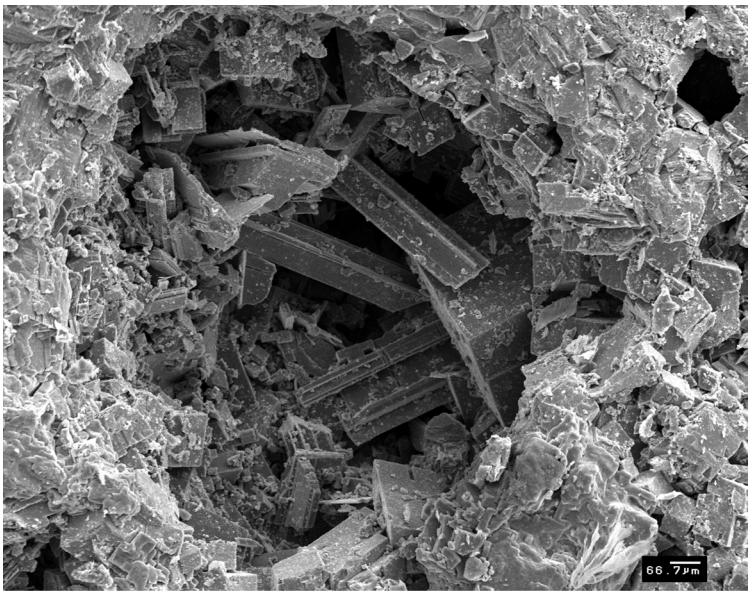

Figure 12. Scanning electron microscope photomicrograph of a core plug from 8426 feet, Lisbon No. D-816 well, showing anhydrite cement lathes partially filling a small dissolution vug. Scale bar represents 66.7 microns (0.067 mm). Porosity = 11.1 percent; permeability = 15 mD based on core-plug analysis.

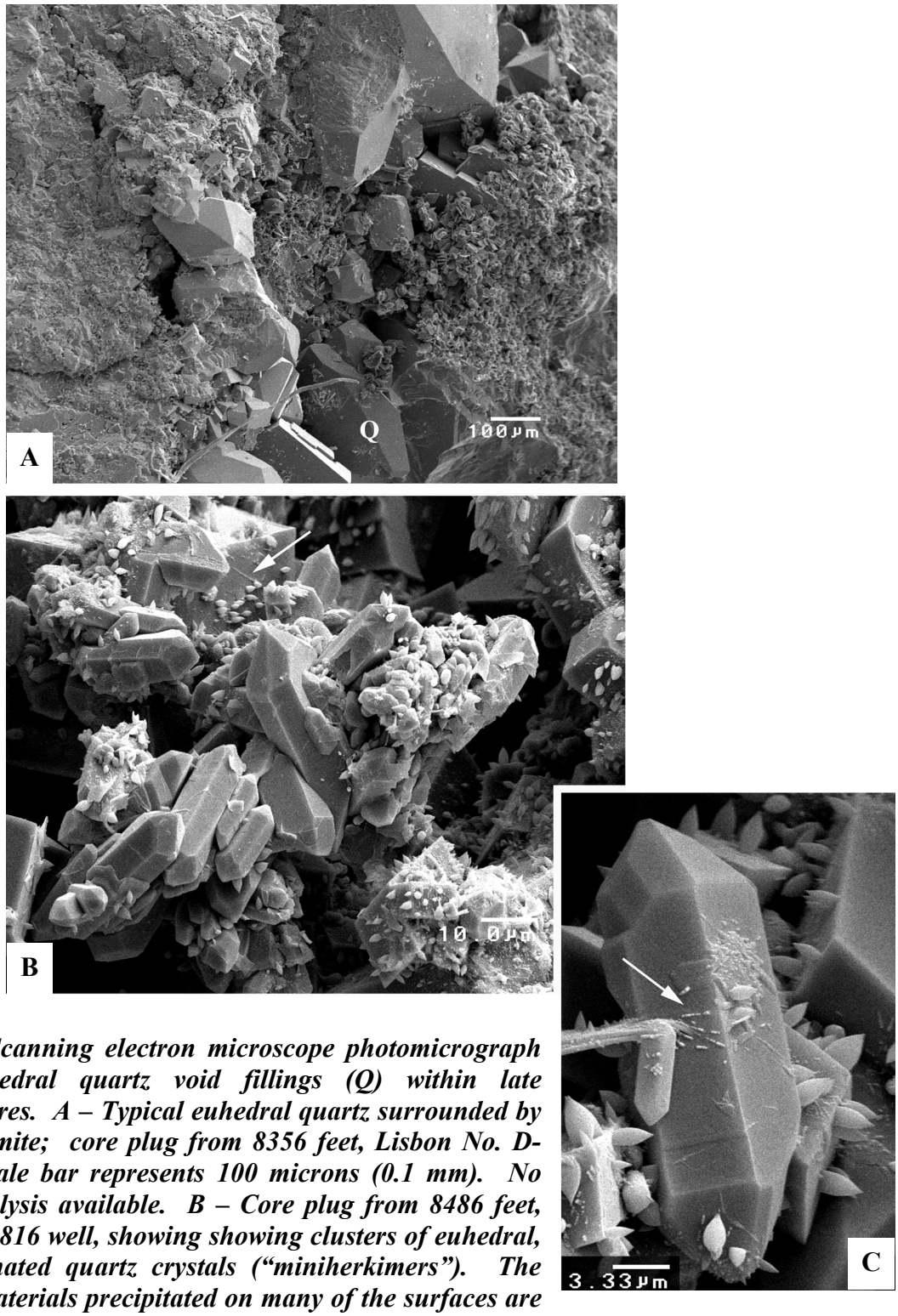

Figure 13. Scanning electron microscope photomicrograph showing euhedral quartz void fillings (Q) within late dissolution pores. A – Typical euhedral quartz surrounded by rhombic dolomite; core plug from 8356 feet, Lisbon No. D-616 well. Scale bar represents 100 microns (0.1 mm). No core-plug analysis available. B – Core plug from 8486 feet, Lisbon No. B-816 well, showing showing clusters of euhedral, doubly terminated quartz crystals ("miniherkimers"). The small spiky materials precipitated on many of the surfaces are either pyrobitumen or sulfide minerals. Scale bar represents 10 microns (0.01 mm). Porosity = 5.9 percent; permeability = 0.2 mD based on core-plug analysis. C - Closeup of a typical doubly terminated quartz crystal from same core sample in B. The linear features (arrow) and the spiky materials on many of the crystal surfaces are composed of either pyrobitumen or sulfide minerals.

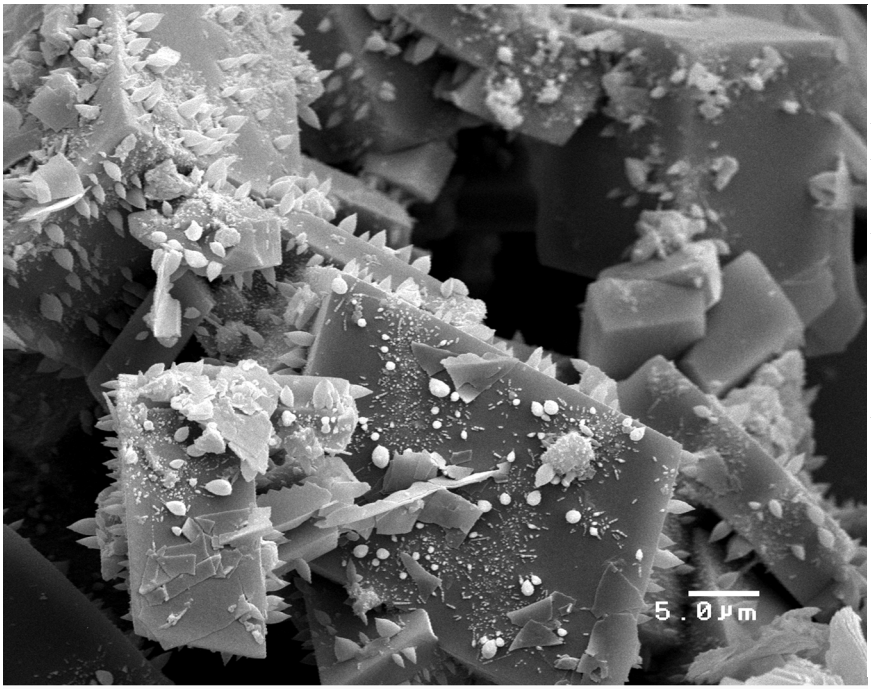

Figure 14. Scanning electron microscope photomicrograph of a core plug from 8442 feet, Lisbon No. D-816 well, showing possible sulfide minerals on large dolomite rhombs. Scale bar represents 5 microns (0.005 mm). Porosity = 8.6 percent; permeability = 1.0 mD based on core-plug analysis.

and 1970s for applications in coal petrology and palynology (see reviews by van Gijzel, 1967; Teichmuller and Wolf, 1977). All applications depend upon the emission of light (by a material capable of producing fluorescence) that continues only during absorption of the excitation-generating light beam (Rost, 1992; Scholle and Ulmer-Scholle, 2003).

Epifluorescence techniques have been used within industry and research for three objectives. Firstly, EF microscopy has been used extensively for enhancing petrographic observations, including the recognition of depositional and diagenetic fabrics within recrystallized limestone and massive dolomite (see, for instance, Dravis and Yurowicz, 1985; Cercone and Pedone, 1987; Dravis, 1991; LaFlamme, 1992). Secondly, the study of pore structures, microfractures, and microporosity within both carbonates and sandstones has been greatly facilitated by impregnating these voids with epoxy spiked with fluorescing dyes (Yanguas and Dravis, 1985; Gies, 1987; Cather and others, 1989a, 1989b; Soeder, 1990; and Dravis, 1991). Thirdly, the evaluation of "oil shows" (Eby and Hager, 1986; Kirby and Tinker, 1992) and determination of the gravity or type cements and minerals has been facilitated by EF microscopy (Burruss, 1981, 1991; Burruss and others, 1986; Guihaumou and others, 1990; LaVoie and others, 2001). Only the first two objectives were pursued in this study.

Previous Work

There is no known published use of EF microscopy on the Leadville Limestone of the Paradox Basin. However, the published work cited above, applications to carbonate reservoirs listed in Eby and Hager (1986) for a study done within a Permian Basin carbonate field, and case studies documented by Dravis (1988, 1992) provided incentives to apply EF petrography to Leadville reservoir rocks within the Lisbon case-study field.

Methodology

Epifluorescence petrography for this project used incident (reflected) blue-light fluorescence microscopy employing the general procedures outlined by Dravis and Yurewicz (1985), including the use of the modified "white card" technique outlined by Folk (1987) and Dravis (1991). Ultraviolet (UV) fluorescence did not effectively add any textural or pore structure information that could not otherwise be seen under blue-light excitation, even though some workers utilize UV fluorescence for evaluating fluid inclusions and compositional zoning within dolomite crystals (see Scholle and Ulmer-Scholle, 2003). Fluorescence data and observations collected for this study utilized a Jena (now part of Carl Zeiss) research-grade combination polarizing-reflected light microscope equipped with a high-pressure mercury vapor lamp for EF excitation, a Zeiss IIIRS epifluorescence nosepiece, and a 35-mm camera system. Magnification ranges for examination and photo-documentation were between ~130 and 320x. The EF optical configuration used is similar to that shown in figure 15.

The light pathways and mechanics of the EF used in this study have been generally described by Soeder (1990). As described by Burruss (1991), "these excitation wavelengths are reflected to the microscope objective and sample by a dichroic beamsplitter which has a dielectric coating that reflects a specific short wavelength range. Fluorescence emission and

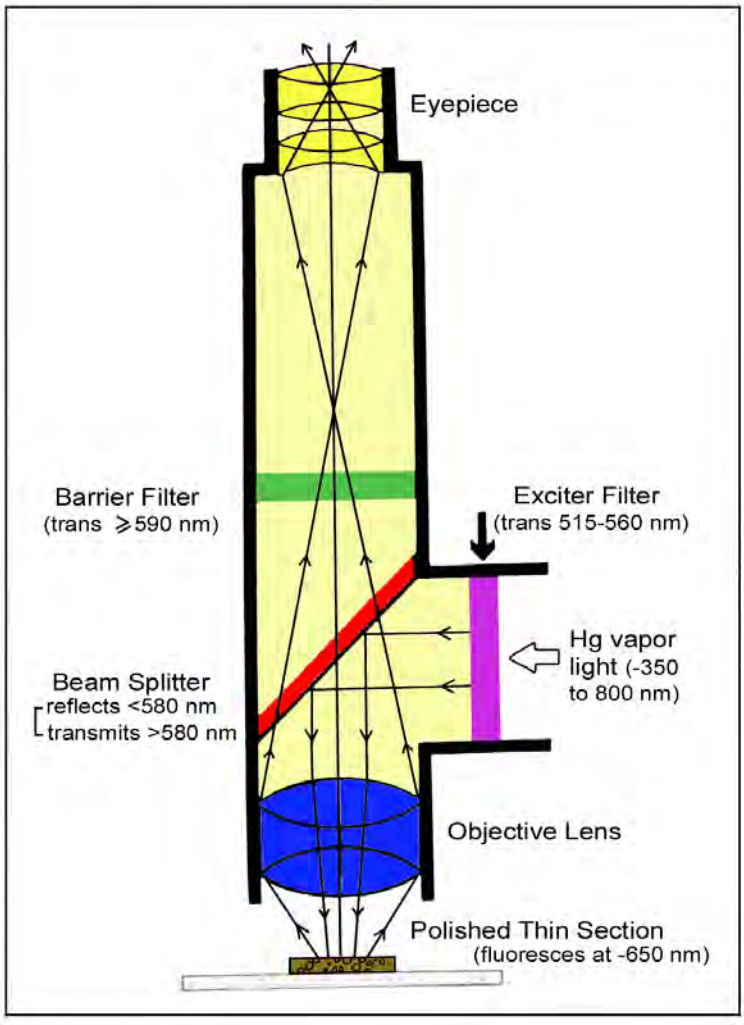

Figure 15. Generalized microscope optical configuration for observing fluorescence under incident light (modified from Soeder, 1990).

reflected short wavelength excitation light is collected by the objective. The dichroic beamsplitter transmits the long wavelength fluorescence emission, but reflects the short wavelengths back toward the light source. The fluorescence emission passes through a barrier filter which removes any remaining short wavelength excitation light." Blue light (~420-490 nm exciter filter/520 nm barrier filter) was used to excite the cuttings and core-chip samples. We have found broad-band, blue-light EF to be the most helpful in observational work on dolomite, although some workers report applications using UV light (330-380 nm exciter filter/420 nm barrier filter) or narrow-band, blue-violet light (400-440 nm exciter filter/480 nm barrier filter). Finally, the greater depth of investigation into a sample by the reflected fluorescence technique than by transmitted polarized light or other forms of reflected light make it possible to resolve grain boundary and compositional features that are normally not appreciated in cutting or thin-section petrography.

Sample preparation is inexpensive and rapid, involving standard thin section preparation techniques. Thin sections were prepared from representative Leadvlle fabrics. These thin sections were vacuum- and pressure-impregnated with blue-dyed epoxy (see Gardner, 1980) that was spiked with a fluorescing compound. Microscopy used only uncovered polished surfaces. Examination for each thin section area of interest included photo-documentation under EF and plane-polarized light at the same magnification. Photomicrography of the compositional, textural, and pore structure attributes was done using high-speed film (ISO 800 and 1600) with some bracketing of exposures as camera metering systems do not always reliably read these high-contrast images in the yellow and green light spectrum. Since the image brightness is directly proportional to magnification, the best images are obtained at relatively high magnifications (such as greater than 100x). Low-power fluorescence is often too dim to effectively record on film. These techniques are applicable to thin sections from both core and cuttings samples.

Epifluorescence Petrography of Leadville Limestone Thin Sections

Blue-light, EF microscopy was completed on 15 core samples for a variety of rock textures and diagenetic phases of Leadville limestone and dolomite within Lisbon field. These samples were selected to be representative of compositional, diagenetic, and pore types encountered within the five cored wells (see figure 5 for core locations). A detailed description and interpretation of the fluorescence petrography of each sample follows along with photomicrographs (as figures 16 through 20) to show representative views under both blue-light EF and plane-polarized light. Short descriptive captions for these photomicrographs are included with each photo pair.

Lisbon No. D-816 well: Blue-light, EF microscopy nicely shows pore spaces and structures that are not readily seen under transmitted, plane-polarized lighting and the range of crystal sizes or shapes within bitumen-rich areas (figure 16). Samples from this well are fairly massive dolomite which is generally non-fluorescence but has a slight hint of fluorescence showing vague relict grains. Some samples display complex zoning, alternating from dull to bright fluorescence within rhombs. Blue light, EF also shows the clear difference between dull replacement dolomite and much lighter replacement dolomite cement. Rare saddle dolomite cements in molds appear to show crystal zonation.

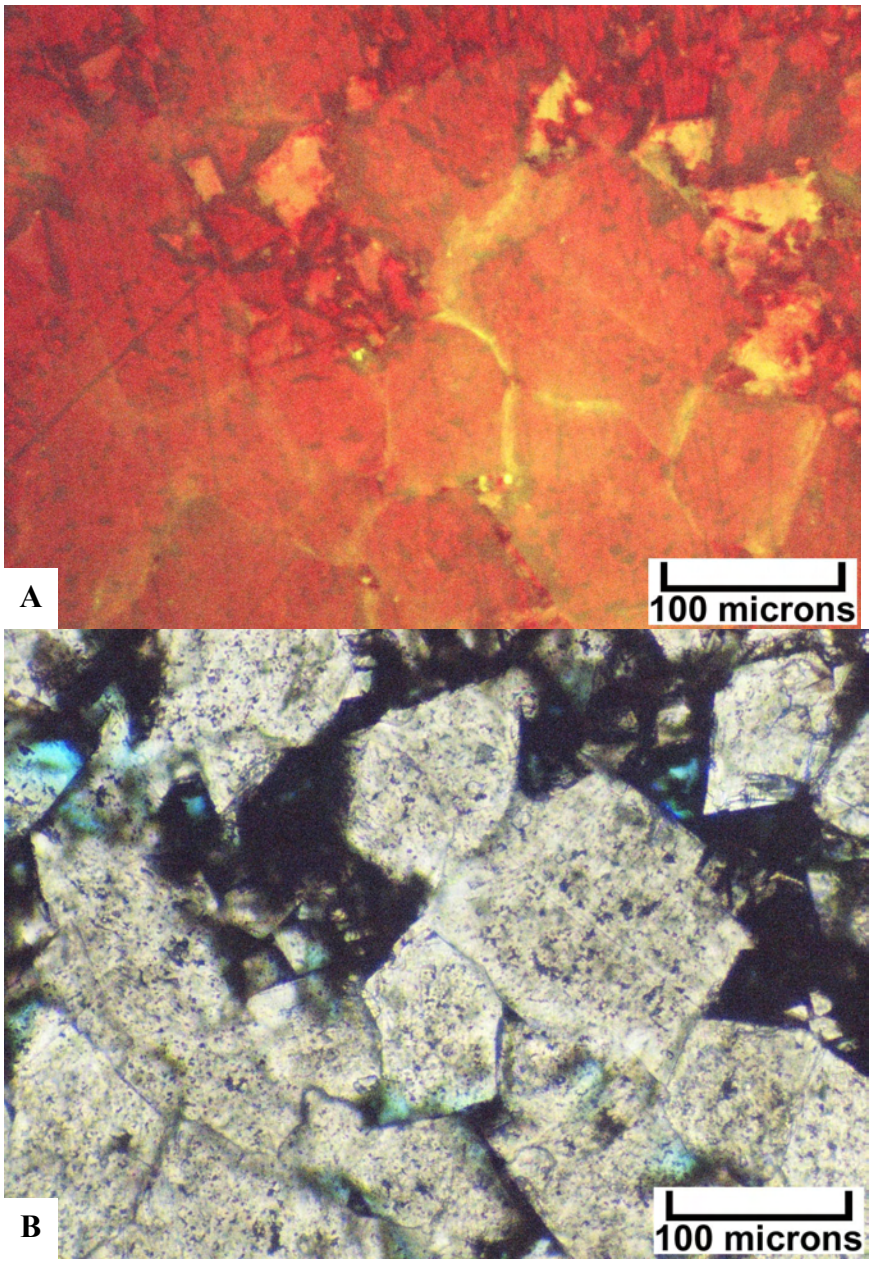

Figure 16. Photomicrographs from Lisbon No. D-816 well at 8435.8 feet. A – Epifluorescence under moderate magnification, showing a representative area showing fluorescence zonation within coarse dolomite crystals. The reddish areas are pores with abundant bitumen linings and plugging (see figure 16B). Fluorescence petrography makes it possible to clearly see the dolomite crystals versus the pore space. In places, very small rhombic outlines of dolomite crystals can be resolved. Many of these pores appear to be completely surrounded by an interlocking network of dolomite crystals. B - The same field of view as above is shown under plane light at the same magnification. Note that the black (and opaque) areas composed of bitumen mask the crystal boundaries of the dolomite as well as individual pore outlines. The white and gray areas are remnants of the dolomite matrix that are not masked by the bitumen. Only a small amount of pore space (blue-dyed areas) can be seen in this view compared to the fluorescence photomicrograph above.

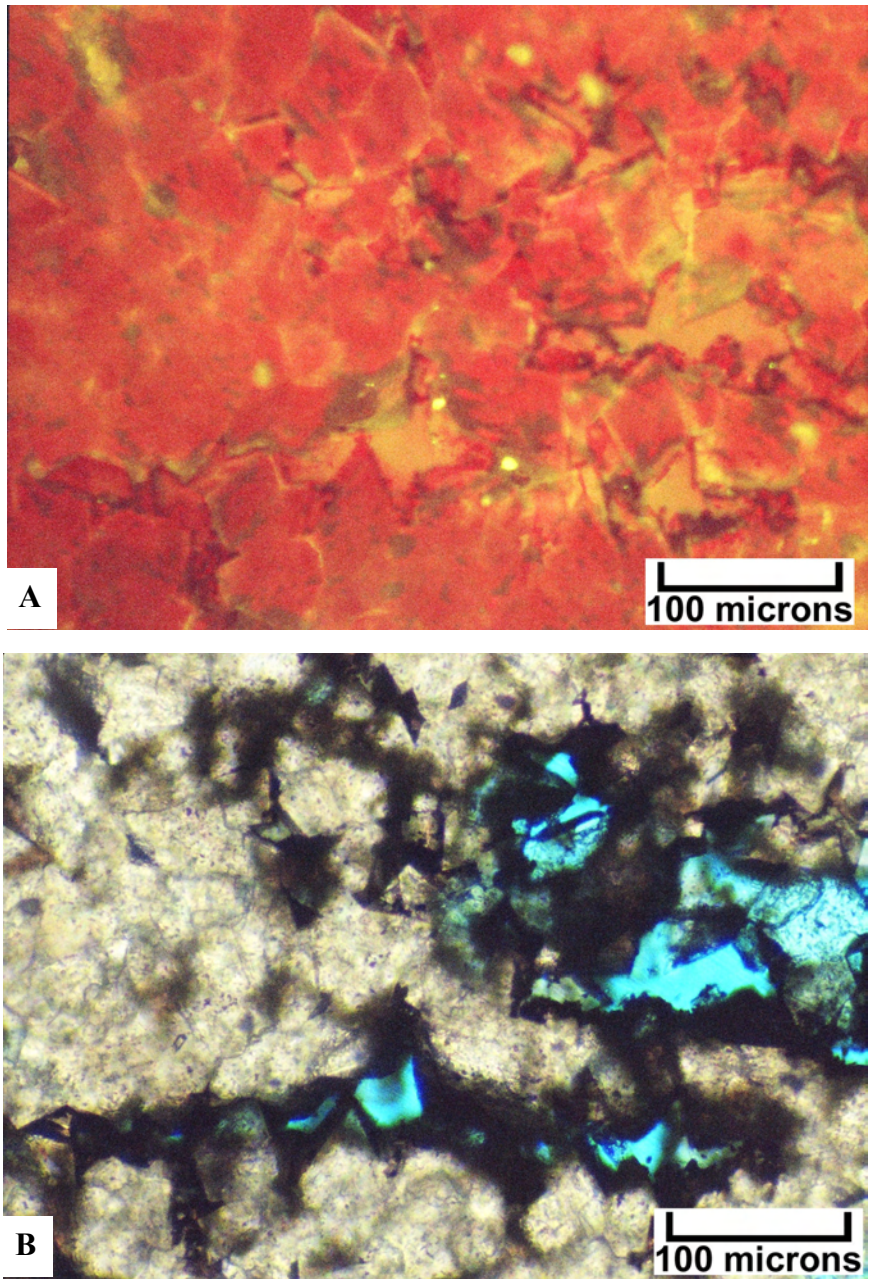

Figure 17. Photomicrographs from Lisbon No. D-616 well at 8435.8 feet. A – Epifluorescence under moderate magnification, showing fine- to medium-sized crystals of replacement dolomite. The rhombs display dead cores and fluorescent rims. B - The same field of view as above is shown under plane light at the same magnification. Again, note that the black (and opaque) areas composed of bitumen mask the crystal boundaries of the dolomite as well as individual pore outlines.

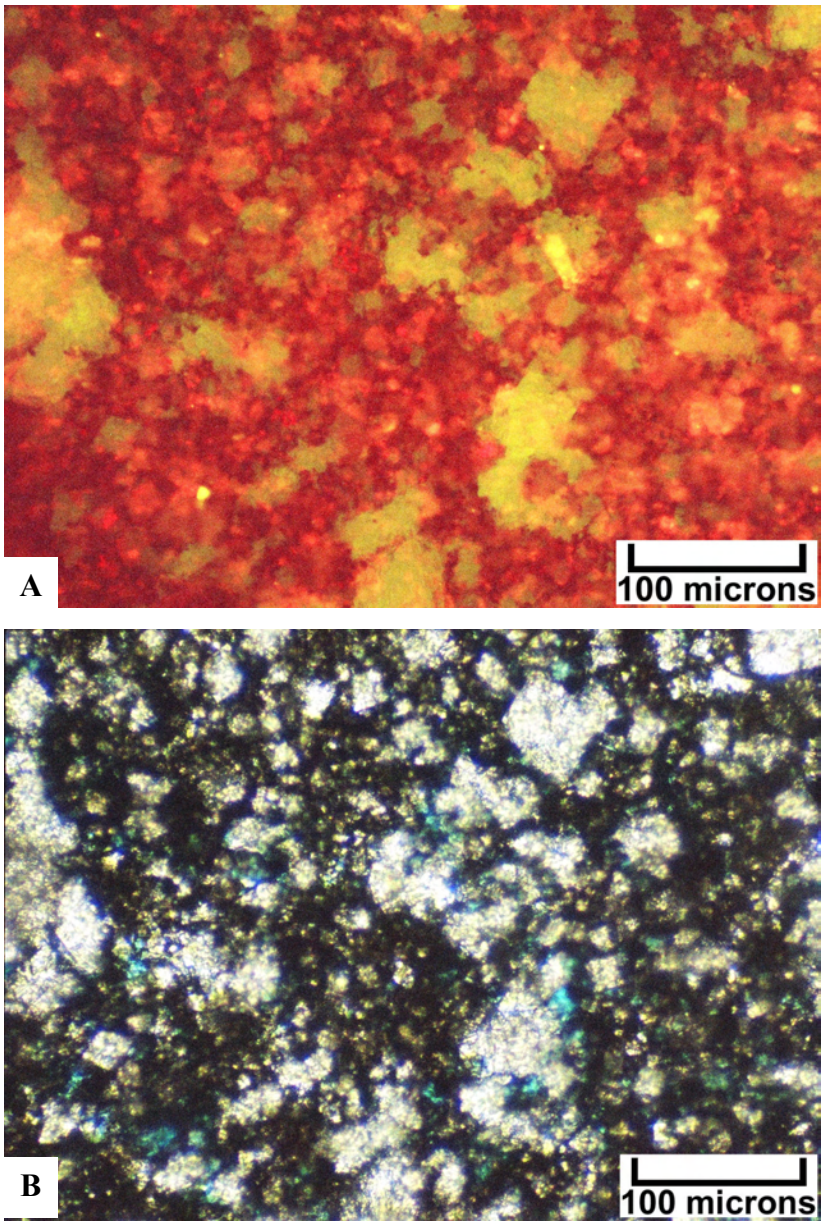

Figure 18. Photomicrographs from Lisbon No. B-610 well at 7897 feet. A – Epifluorescence under moderate magnification, showing individual, yellow-fluorescing dolomite rhombs "floating" in a of non-fluorescing dolomite matrix. B - The same field of view as above is shown under plane light at the same magnification.

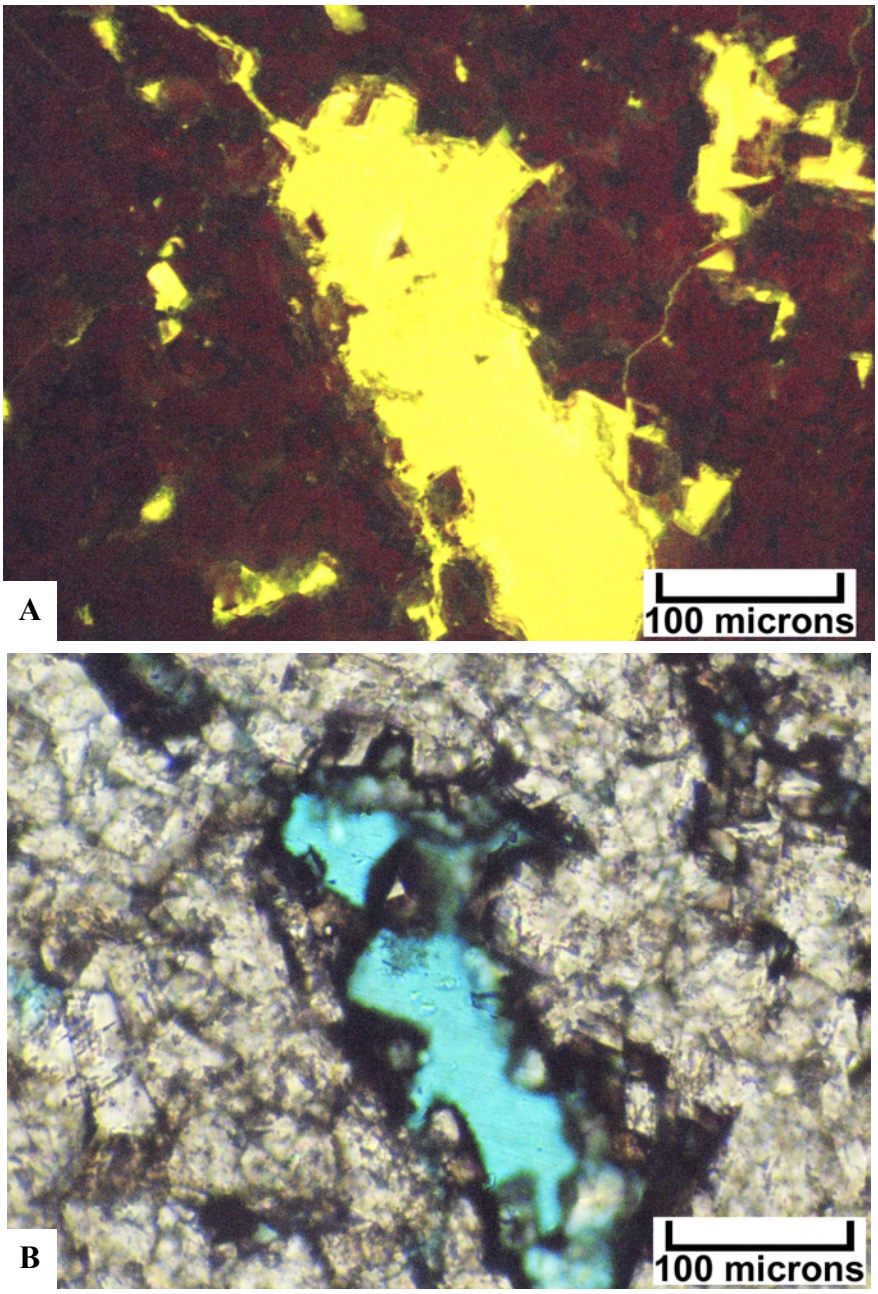

Figure 19. Photomicrographs from Lisbon No. B-816 well at 8486 feet. A – Epifluorescence under moderate magnification, showing zoned, rhombic replacement dolomite with dead cores and highly fluorescent rims. B - The same field of view as above is shown under plane light at the same magnification. Note the large solution pore (blue area).

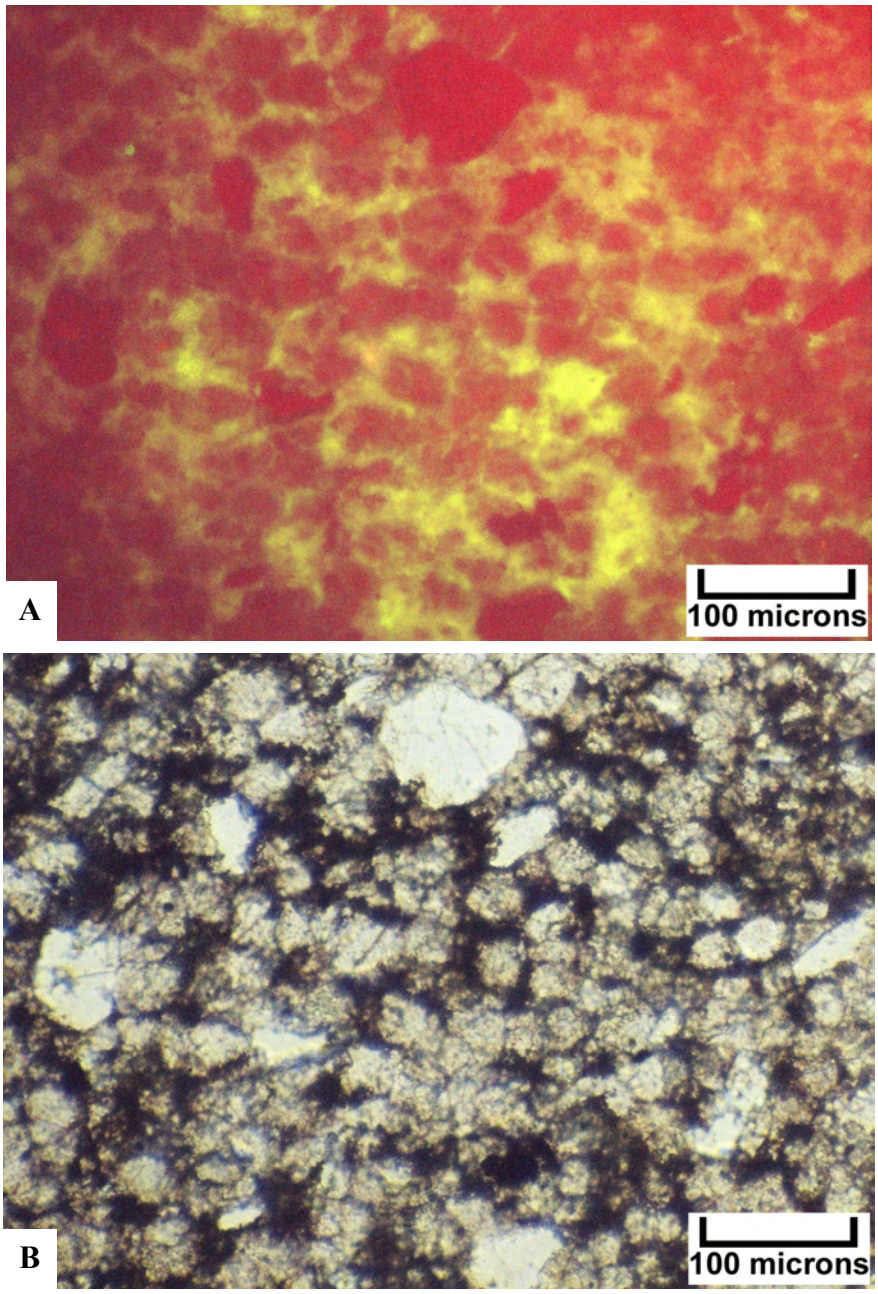

Figure 20. Photomicrographs from Northwest Lisbon No. B-63 well at 9935.6 feet. A – Epifluorescence under moderate magnification, showing dolomitized detrital fill within a karst cavity. B - The same field of view as above is shown under plane light at the same magnification. Note the large quartz grains, and angular limestone and dolomite clasts. These clasts do not fluoresce.

Microfractures cutting through tight dolomite matrix are visible only with blue-light EF. Some pores (isolated molds) are lined with bright, yellow oil film fluorescence possibly from oil staining while others show no oil staining.

Lisbon No. D-616 well: Blue-light, EF microscopy shows replacement dolomite that is fine to medium crystalline with planar to curved crystal faces, weakly yellow fluorescent with possible fluid inclusions (figure 17); limestone does not fluoresce. Saddle dolomite cements growing into some of the moldic pores display moderately dull blue fluorescence. Blue-light, EF displays replacement rhombic dolomite outlines with high intercrystalline porosity despite the appearance of significant bitumen plugging.

Blue-light, EF microscopy also shows syngenetic dolomite, laminated cryptoalgal (?) mudstone with soft pellets and abundant wispy seam, low-amplitude stylolites moderate yellow fluorescence is observed throughout the samples. Ghosts of original skeltetal/pelletal grains show moderate yellow fluorescence transitioning into coarse replacement dolomite displaying modest intercrystalline porosity. The replacement rhombs have generally dead cores and moderate yellow fluorescence overgrowths.

Lisbon No. B-610 well: Ultraviolet-light, EF microscopy shows two regions within the sample. Region 1 consists of white, syngenetic dolomite with no visible porosity and blue-purple moderate fluorescence. The UV fluorescence nicely shows a variety of corrosion and dissolution fabrics, which sometimes mimic original grain boundaries. Region 2 consists of black, non-fluorescent, finely crystalline dolomite, as well as "floating" large dolomite rhombs that appear to have precipitated out of the finely crystalline ground mass (figure 18).

Blue-light EF also displays syngenetic dolomite, both unaltered and corroded, with moderate yellow fluorescence. Within the black dolomite region, the larger floating dolomite rhombs have a dull green fluorescence.

Lisbon No. B-816 well: Blue-light, EF microscopy shows replacement dolomite with highly yellow fluorescent rims (figure 19). Saddle dolomite cement has moderate yellow-green fluorescence. Late calcite cements are generally non-fluorescent.

Lisbon NW USA No. B-63 well: Blue-light, EF microscopy shows massive, very finely crystalline, non-porous syngenetic dolomite displaying a mottled dull to medium yellow fluorescence with occasional ghosts of original grain types (can see grain outlines with fluorescence). Dolomitized grains include detrital carbonate (pellets) and siliciclastic (quartz silts and clays) components of the karst cavity infilling (figure 20); clay minerals between grains display a pale reddish fluorescence. Outside of the cavity, the host rock is almost pure limestone composed of fossils and coated grains – all calcitic with little visible fluorescence.

Late calcite (poikilotopic) also displays no fluorescence. This late calcite occurs as cements within former isolated molds, fracture fillings, and some replacement of syngenetic dolomitic matrix.

Cathodoluminescence

Introduction

Cathodoluminescence is the emission of light resulting from the bombardment of materials using a cathode ray (Allan and Wiggins, 1993). This petrographic technique can be an invaluable tool in petrographic studies of carbonate rocks. This technique can provide important information about the complex modification of rock fabrics and porosity within the Leadville Limestone of the Paradox Basin. Diagenesis played a major role in the development of reservoir heterogeneity in Lisbon field as well as throughout the all of the Leadville fields. Diagenetic processes started during deposition and continued throughout burial history (figure 7). A complete discussion on the diagenetic history based upon visual core examination and thin-section petrography was documented previously by Chidsey and others (2005).

Cathodoluminescence has been used in recent years to provide insights into the chemical differences between preserved remnants of depositional components resulting from various diagenetic events in carbonate rocks as recognized from core examination and thin section petrography. In particular, CL provides visual information on the spatial distribution of certain trace elements, especially manganese (Mn2+) and iron (Fe2+) in calcites and dolomites (Machel and Burton, 1991; Scholle and Ulmer-Scholle, 2003). The visible CL responses are red to orange in color, and their intensity is usually described as non-luminescent, dully luminescent, and brightly luminescent. As a general rule, incorporation of Mn2+ into the calcite lattice stimulates luminescence and the incorporation of Fe2+ quenches or reduces luminescence (Fairchild, 1983; Allan and Wiggins, 1993; Scholle and Ulmer-Scholle, 2003). Qualitative interpretation of CL usually assigns nonluminescent responses to oxidizing settings in which the reduced forms of both Mn and Fe are unavailable for incorporation into the lattices of carbonate mineral precipitates. Oxidized forms of Mn and Fe are not incorporated into calcite or dolomite crystals. Therefore, there is nothing in these crystals to excite luminescence. Bright luminescence is related to carbonate precipitates with high Mn/Fe trace element ratios, typically as a result of reducing environments during early (near-surface) to intermediate stages of burial diagenesis. Dull luminescence seems to happen where the Mn/Fe trace element ratios are present in carbonate precipitates. Thus, dull luminescence is usually thought to be the result of intermediate to late stages of burial diagenesis. It appears that elements other than Mn and Fe do not have any appreciable effect in enhancing or reducing luminescence (Budd and others, 2000).

Particularly useful references on the uses and limitations of CL interpretations in ancient carbonate studies include Sipple and Glover (1965), Frank and others (1982, 1996), Marshall (1988), Hemming and others (1989), Barker and Kopp (1991), Gregg and Karakus (1991), Machel (2000), Lavoie and others (2001), Coniglio and others (2003), and Lavoie and Morin (2004).

Methodology

The analysis done in this study was completed using uncovered, polished thin sections, although rock chips and unpolished thin sections could be used. The equipment needed for CL can be installed on almost any polarizing microscope (see Marshall, 1988; Miller, 1988). A

Cambridge Image Technology Ltd. luminoscope (model CLmk3A/4) mounted on an Olympus petrographic microscope (figure 21; see also Marshall, 1988) belonging to the Colorado School of Mines Department of Geological Engineering was used for this analysis (figure 22). Operating conditions were generally at 10-16kV accelerating potential, 0.5-0.7 mA of beam current and a beam focused at ~2 cm. All the work involved visual observations and some photographic documentation. Photomicrographs were recorded on a digital camera. No attempt was made to measure intensities or spectral information on the CL responses (for example Marshall, 1991; Filippelli and Delaney, 1992) to the Leadville carbonate samples. Image analysis and regional mapping of cement zones (that is "cement stratigraphy") have been done by some workers on carbonate cements (for example Meyers, 1974, 1978; Dorobek and others, 1987; Cander and others, 1988; Dansereau and Bourque, 2001), but these applications are beyond the scope of diagenesis documentation attempted in this project.

Cathodoluminescence Petrography of Leadville Limestone Thin Sections

Cathodoluminescence examination was completed on four thin-section samples from the Leadville limestone and dolomite within Lisbon field. These thin-section samples were selected to be representative of mineralogical (for example dolomite, calcite, anhydrite, and quartz), compositional, diagenetic, and pore types encountered within typical cores from the field (see figure 5 for core locations). The following remarks summarize our findings.

Lisbon No. D-816 well, 8442-8443 feet: Cathodoluminescence shows a wide range of crystal size and growth habits within the dull red luminescing, matrix-replacing dolomite (figure 23). The vast majority of the dolomite within areas of fabric selective dolomitization is a deep or intense red color. Between many of the grains, there is a lighter red luminescence where early cements have been dolomitization. Some of the coarser dolomite crystals appear to have an overgrowth of brighter red luminescent material. The range in dolomite rhomb sizes may reflect rapid precipitation. The amount of open porosity under CL is considerably greater than that visible under plane light microscopy. Cathodoluminescence also displays original depositional textures and the outlines of original carbonate grains. Between other grains, there are interparticle pores that are still open. In a few areas, these early pores have been solution-enlarged and lined with a later generation of coarse, rhombic dolomite.

Lisbon No. D-816 well, 8433 feet: Cathodoluminescence imaging was very useful in identifying various generations of dolomite. Two types of CL response is visible within these moderately coarse dolomite crystals. Bright red luminescence can be seen within the interiors of most of the replacement dolomite (figure 24). However, many of the crystals exhibit non-luminescent overgrowths of variable thickness. In addition, some crystals exhibit mostly non-luminescent material. These particular crystals may be largely dolomite cements. Finally, some dolomite crystals exhibit a thin rind of red-luminescing dolomite overlying the non-luminescent overgrowth stage. It is possible that the red luminescing dolomite is the product of the replacement of a previous limestone or earlier dolomite matrix while the non-luminescing crystal additions may be overgrowth cements growing into open pores. Dissolution and corrosion of some crystals is evident between the second (non-luminescent) and the final luminescent rim.

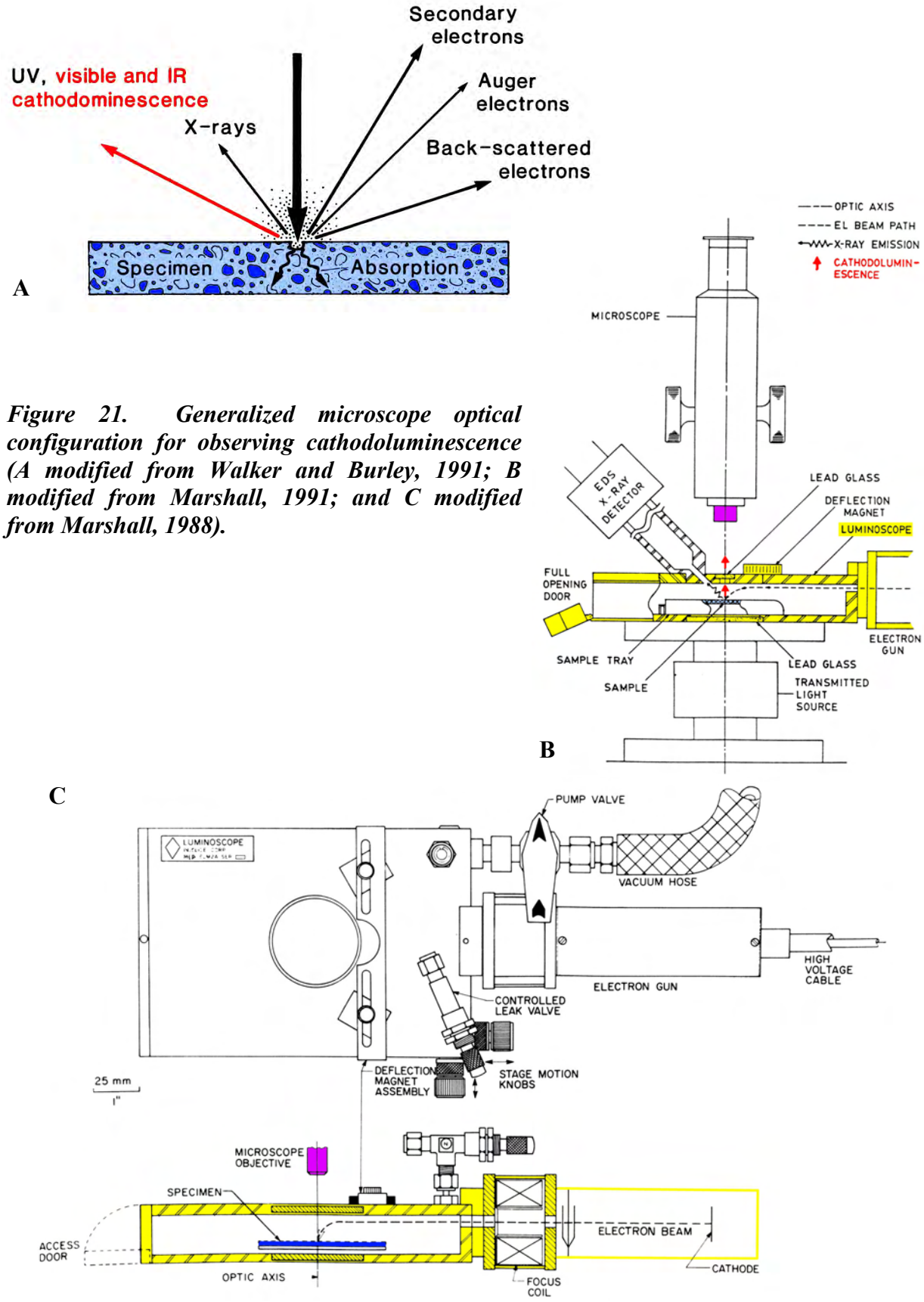

Figure 21. Generalized microscope optical configuration for observing cathodoluminescence (A modified from Walker and Burley, 1991; B modified from Marshall, 1991; and C modified from Marshall, 1988).

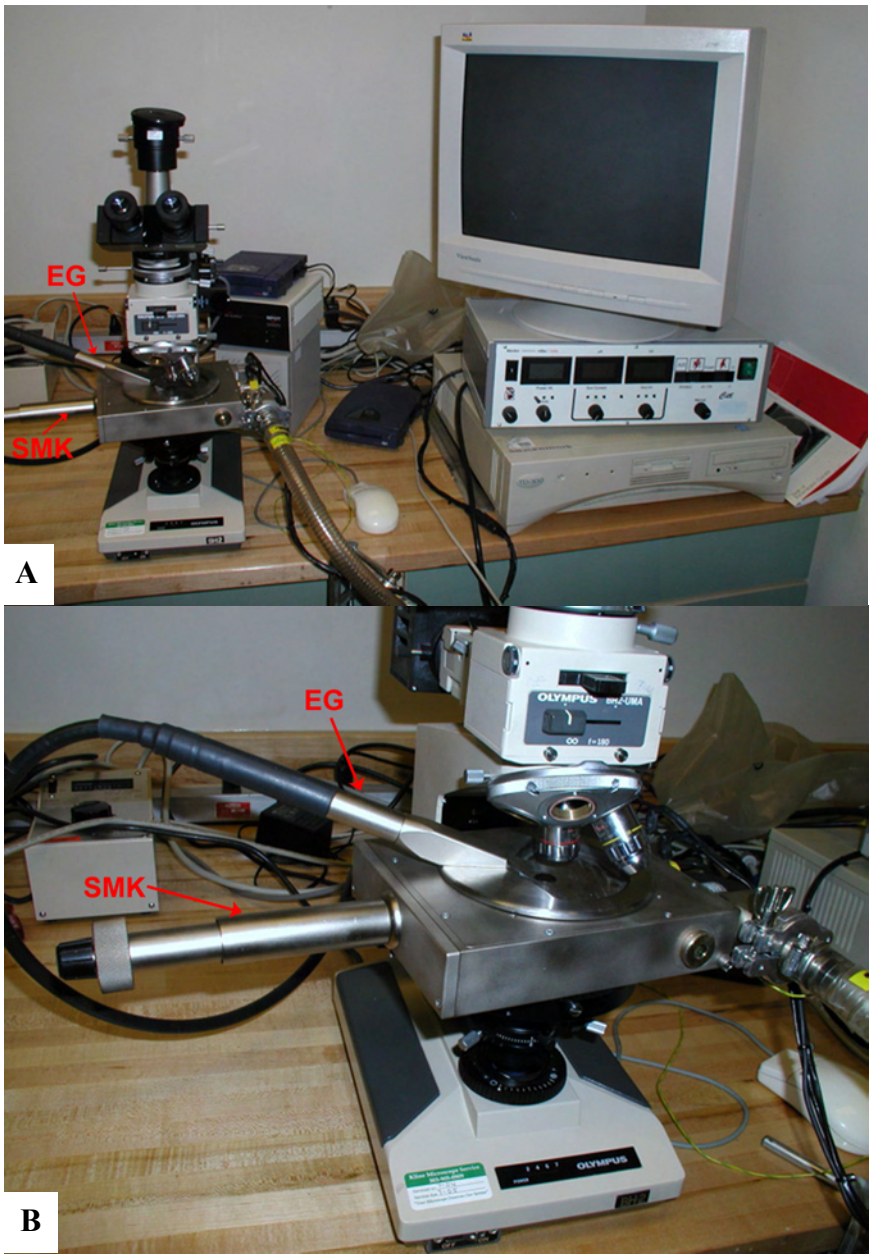

Figure 22. Colorado School of Mines cathodoluminescence setup used for the Leadville samples from Lisbon field. A - Cambridge Image Technology Ltd. CLmk3A/4 cathodouminescence instrument is mounted on an Olympus BH2 petrographic microscope. The electron gun (EG) can be seen in the inclined position to the left of the sample chamber. The stage motion knob (SMK) is the silver cylinder to the left of the sample chamber. The hose to the vacuum pump can be seen to the right of the chamber. The front panel controls (beneath the video monitor) include (from left to right) the diagnostic selector, vacuum and diagnostic metering, gun current metering, Gun kV metering, and main power switch. The video monitor and CPU were used for handling and displaying the CL images captured by a digital camera. B - Closeup of the Cathodoluminescence instrument sample chamber (SC), electron gun (EG) and stage motion knob (SMK) mounted on an Olympus BH2 petrographic microscope.

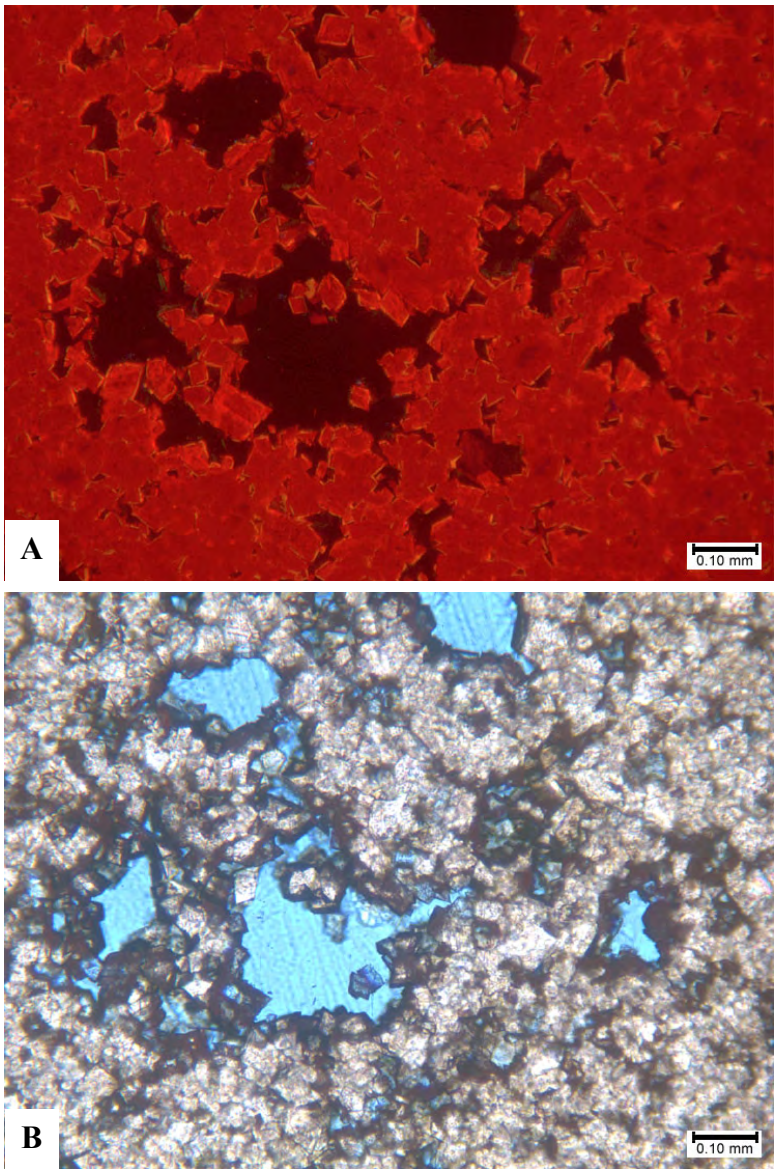

Figure 23. Photomicrographs from Lisbon No. D-816 well at 8442-8443 feet. A - Cathodoluminescence shows sharp outlines between the dolomite crystals and adjoining pore spaces. Note that the porosity (seen in black) in this sample seems to be a combination of intercrystalline space and solution-enlarged molds. The vast majority of the dolomite seen here consists of bright red luminescing dolomite with only occasional thin rinds of dull luminescing overgrowth. There are also rare non-luminescing dolomite cement crystals within some of the smaller pore spaces (see, for instance, the cement occluding a small pore in the lower center of this image). Finally, note that "ghosts" of former grains such as "hard" peloids can be seen in the luminescing pattern of the dolomites in the upper right corner of this view. B - The same field of view under plane light. The outlines of the dolomite crystals are not nearly as distinct and crisp here as in the previous CL view. In fact, it is difficult to pick out the crystal outlines or faces in this type of lighting. Black pyrobitumen makes is difficult to see the smaller, but important, intercrystalline pores. The larger solution-enlarged molds in blue are easy to see, but their interconnection through the smaller intercrystalline space is better seen under CL imaging.

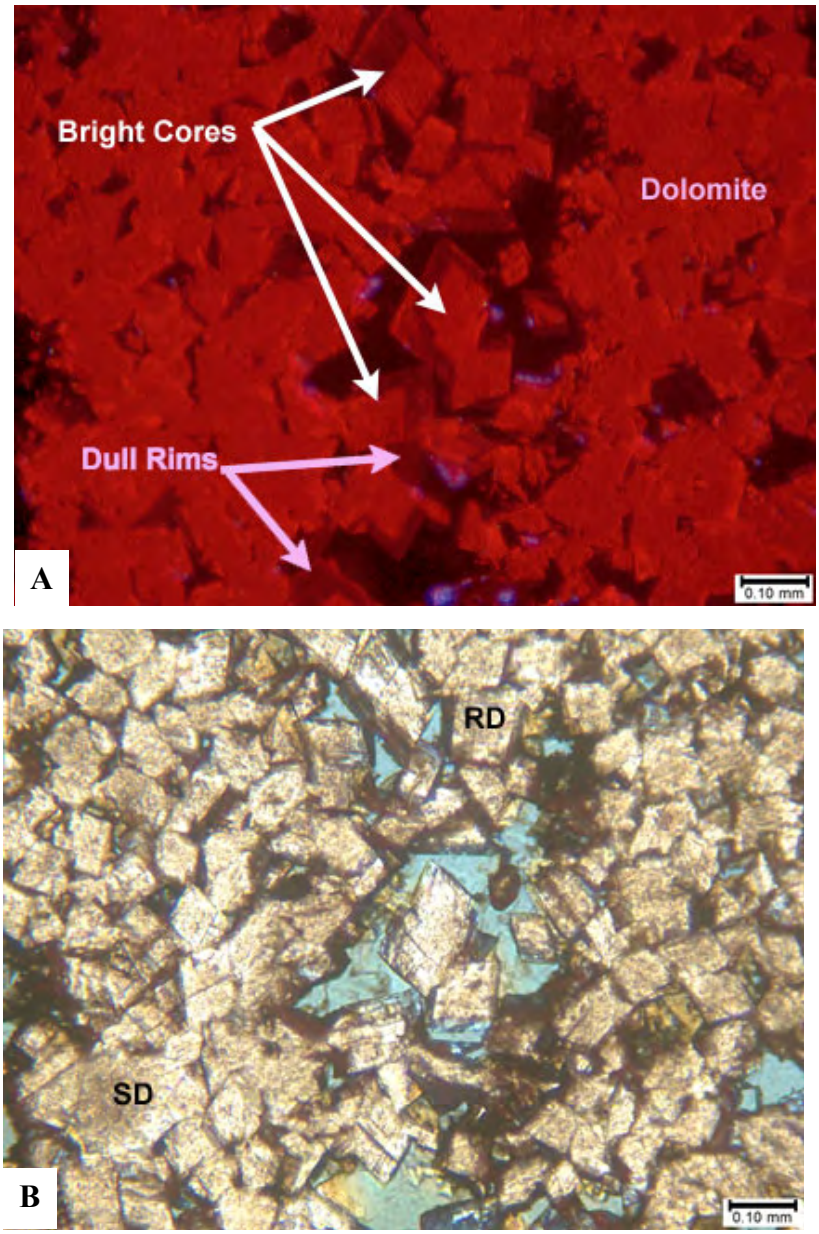

Figure 24. Photomicrographs from Lisbon No. D-816 well at 8433 feet. A - This CL image shows beautiful luminescence zonation of many of the dolomite crystals, especially in a band from the top center to the bottom center of the image. Note the bright red luminescing dolomite cores surrounded by rim zones of non-fluorescent overgrowth. The back areas on this image are currently open pore spaces. B - The same field of view under plane light showing replacement dolomite (RD) and saddle dolomite (SD). The dolomite crystals shown here are well formed with planar crystal faces and generally rhombic outlines. Note that some crystal terminations may display curved (or saddle) outlines. Plane light does not make it possible to distinguish the crystal composition zonation imaged in the CL photomicrograph. The black areas within this field of view are due to pyrobitumen coatings on many of the dolomite crystal surfaces. The blues areas between many of the replacement dolomite crystals are open pores.

Lisbon No. B-816 well, 8486 feet: Cathodoluminescence imaging was very useful in identifying the presence of saddle dolomites (Radke and Mathis, 1980) within microporous dolomites (figure 25). Large dolomite crystals (1.0 to 2.0 mm in diameter) with distinctly curved crystal faces occur as both replacements of finer, earlier dolomites, and as pore-filling cements. These saddle dolomites display dull, red luminescence in their core areas and slightly bright, orange-red luminescence toward their rim areas. In addition, CL makes it possible to see the growth bands in these coarse dolomite crystals due to slight luminescence differences between each growth zone.

In general, the presence of saddle dolomites within a carbonate sample is indicative of the growth of strained, slightly iron-rich, dolomite replacements and cements under elevated temperatures during burial conditions (Radke and Mathis, 1980). Thus, saddle dolomite, as well as the other coarse dolomite crystals with reddish luminescence, are probably late, burial or hydrothermal dolomites. Additional published descriptive work on saddle dolomites using CL may be found in LaVoie and Morin (2004).

Lisbon No. D-616 well, 8308 feet: Sediment-filled cavities are relatively common throughout the upper third of the Leadville Limestone in Lisbon field. These cavities or cracks were formed by karstification of the exposed Leadville. Infilling of the cavities by detrital carbonate and siliciclastic sediments occurred before the deposition of the Pennsylvanian Molas Formation. Cathodoluminescence imaging shows that the contact between the transported material and the limestone country rock can be sharp, irregular, and corroded with small associated mud-filled fractures (figure 26). The transported material consists of poorly sorted detrital quartz grains (silt size), chert fragments, carbonate clasts, clay, and occassional clasts of mud balls (desiccated and cracked). The carbonate muds infilling the karst cavities are largely dolomitized (a later diagenetic process), very finely crystalline, and non-porous.

Fluid-Inclusion Systematics of Lisbon Field Samples

Introduction

During crystal growth, imperfections may trap fluids present in the environment at that time. Later mineral precipitation and deformation, such as the development fractures, can create additional crystal imperfections that may also trap fluids (figure 27). These fluid inclusions are defined as fluid-filled vacuoles, typically 5 to 20 microns in size. They provide pressure, volume, and temperature information about the conditions when the crystal precipitated (Paul Carey and John Parnell, University of Aberdeen, written communication, 2005). The fluids in the inclusion may be connate water, oil, or a sample of the mineralizing fluid. The following properties are assumed not to have changed since an inclusion formed: (1) the composition of the trapped fluid, (2) the density of the trapped fluid, and (3) the volume of the inclusion (Paul Carey and John Parnell, University of Aberdeen, written communication, 2005). The study of fluid inclusions can help determine (1) the temperature of mineral precipitation, (2) the composition and origin of mineralizing fluids, (3) later history of temperature, pressure, and fluid composition, (4) petroleum migration history, (5) relative timing of porosity occlusion, and (6) deformation event conditions (Paul Carey and John Parnell, University of Aberdeen, written communication, 2005).

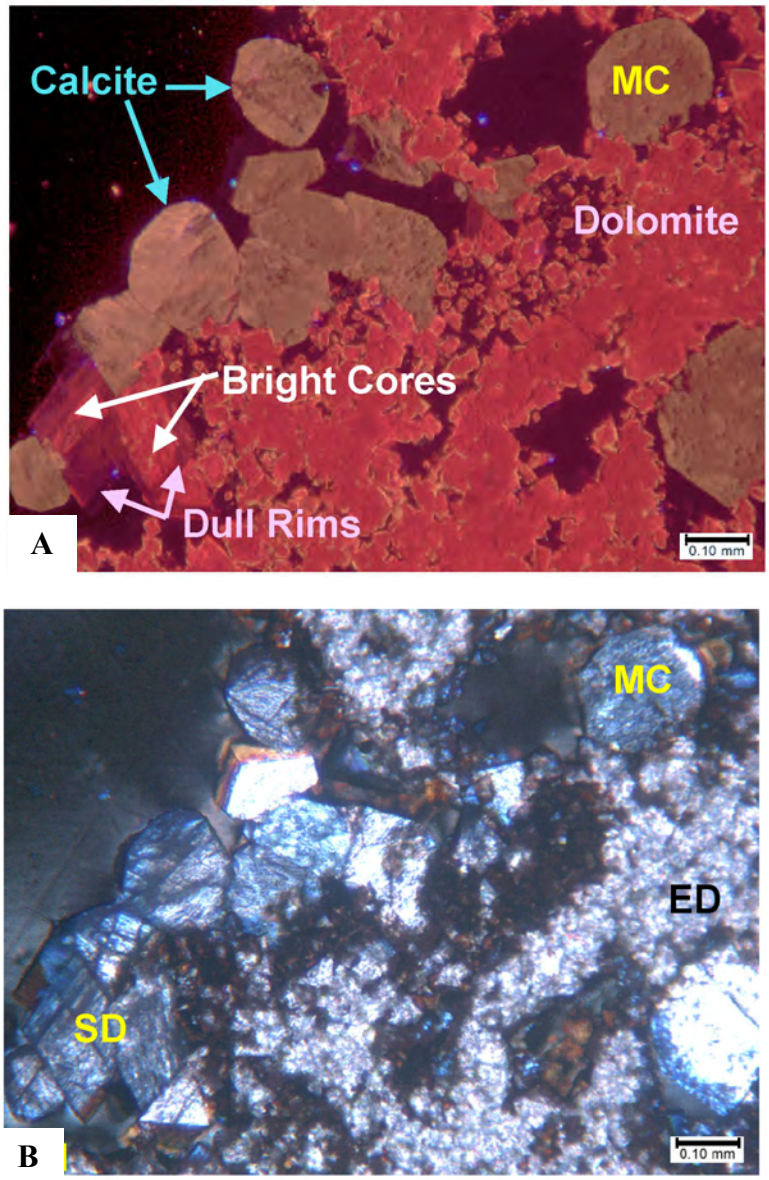

Figure 25. Photomicrographs from Lisbon No. B-816 well at 8486 feet. A - This area of high matrix porosity (in black) shows early replacement dolomite (ED) that displays intense red luminescence. Some of these replacement crystals display very thin orange overgrowths. However, some of the largest dolomite rhombs (saddle dolomite [SD]) in this field of view display a coarser crystal zonation in which the bright red luminescent core is overgrown with thick, dull luminescent rims (see the lower left corner of this photomicrograph). Finally, note the large, late calcite spar crystals (macrocalcite [MC]) with orange luminescence within the large pores from lower left to upper right as well as in the lower right portion of this view. B - The same field of view under crossed nicols. Note that some of the large dolomite crystals in the lower left portion of this image display sweeping extinction and possibly curved crystal faces that are consistent with probable saddle dolomites. The replacement dolomites throughout most of this field of view are too small or too inclusion-rich to distinguish extinction patterns. The late calcite spar cements generally display straight extinction.

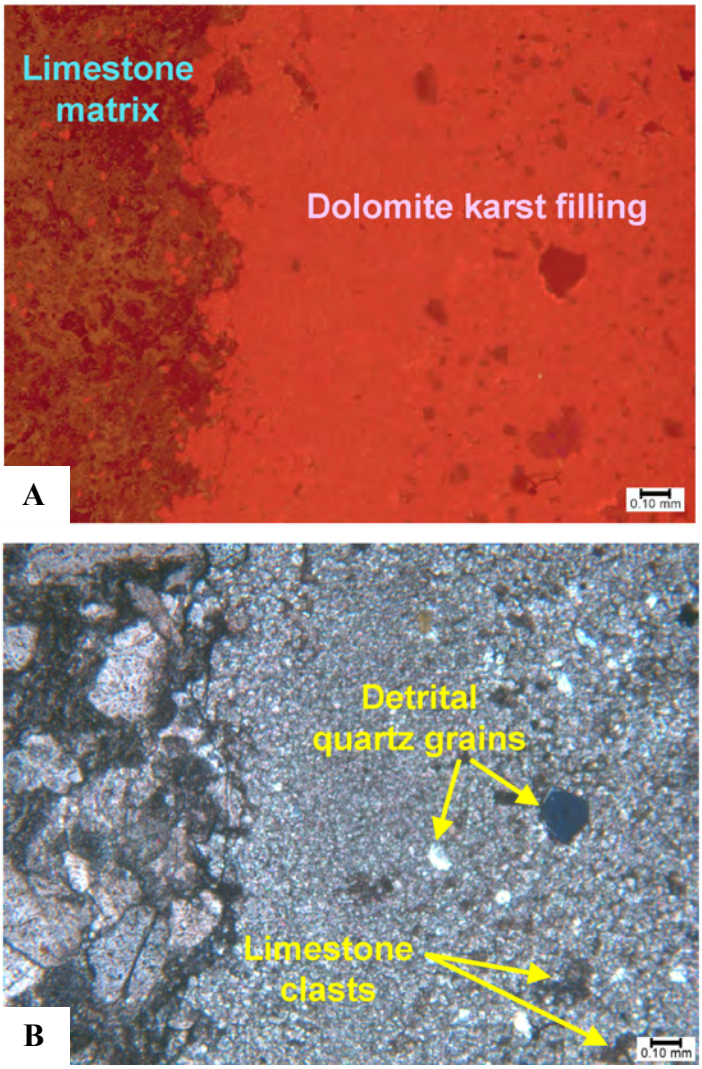

Figure 26. Photomicrographs from Lisbon No. D-616 well at 8308 feet. A - This low-magnification image nicely shows a sharp contact that runs from top to bottom toward the left side of the photomicrograph. The bright red field is composed mostly of dolomite, while the field with the orangish cast (to the left) is almost entirely limestone. The dolomite area is composed of carbonate grains and sediments that have filled a karst-related crack or cavity. The poorly sorted, angular grains that are seen "floating" within the dolomite field are a combination of detrital siliciclastic (mostly quartz) grains and lithified limestone clasts. The limestone field along the left side of the photomicrograph is composed of non-luminescent skeletal (crinoid-rich) sediments with orangish cements. Neither the dolomite with siliclastic sediments nor the limestone display any visible matrix porosity. The contact between the dolomite and limestone fields is irregular but sharp. Finally, there are few scattered replacement dolomite rhombs (also with red luminescence) within the well-cemented limestone. B - The same field of view under crossed nicols. Note that the siliciclastic grains within the microcrystalline dolomite field display plane extinction positions with colors ranging from white to yellow to dark grain. The polygonal grain in the right center contains overgrowths that form a prismatic quartz form in crossed section. In the limestone field to the left, many of the fossils are surrounded by straight extinction syntaxial cements.

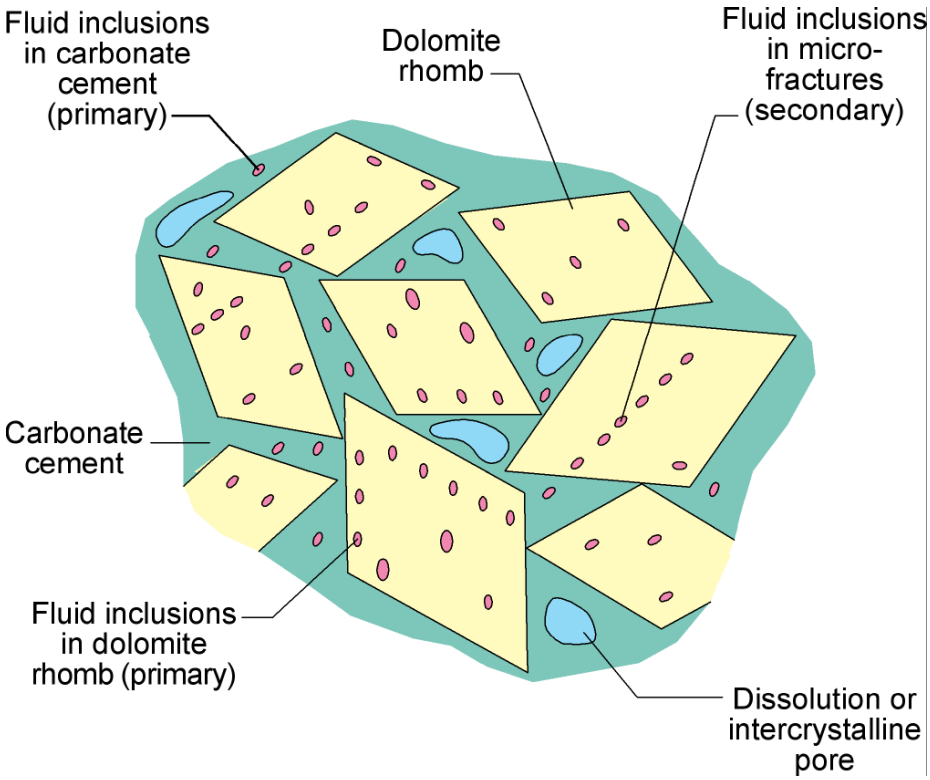

Figure 27. Schematic diagram of basic fluid inclusion types.

Fluid inclusions trapped in calcite, quartz, and dolomite were studied from three wells: Lisbon NW USA No. B-63, Lisbon No. D-616, and Lisbon No. D-816 (figure 5). The inclusions were categorized on the basis of origin, number of phases present, and composition. All inclusions were classified as either primary or secondary. Primary inclusions are trapped at the time of mineral growth; secondary inclusions are trapped along healed fractures. Primary inclusions typically define growth zones, although in quartz, large isolated inclusions are typical. All of the inclusions observed contained either one or two fluid phases at room temperature. Inclusions containing brine and vapor are the most common, but single-phase aqueous inclusions, gas-rich inclusions, and inclusions consisting of oil and vapor are present. Single-phase aqueous inclusions are indicative of trapping at temperatures less than 50°C (~122ºF) (Goldstein and Reynolds, 1994).

Fluid-Inclusion Measurements

Heating and freezing measurements were made on doubly polished thick sections and hand picked crystals using a Linkham THSMG 600 freezing and heating stage calibrated with synthetic fluid inclusions. The precision of the measurements is estimated to be ± 0.1°C at 0.0°C and ± 3°C at 374°C (37ºF at 705ºF). Homogenization and ice-melting temperatures were measured. Homogenization temperatures are minimum trapping temperatures. Ice-melting temperatures provide a measure of the fluid salinity. The salinities of the two-phase aqueous inclusions with ice-melting temperatures between 0 and -21.2°C (32 and -6.2ºF) were converted to weight percent NaCl equivalent using the equation of Bodnar (1993). Salinities of inclusions with lower ice-melting temperatures displayed eutectic (first melting) temperatures of <-45°C (-

49ºF), indicating the presence of divalent ions (most likely Ca and Mg). These inclusions had ice-melting temperatures as low as about -27°C (~ -17ºF). The equation of Bodnar (1993) cannot be used to calculate the salinities of these fluids. As a first approximation, assuming that only Ca, Na, and water are present in the inclusions, the salinities would be in the range of 25 to 30 weight percent NaCl-$CaCl_2$ equivalent (Yanatieva, 1946). Such high-salinity brines imply interactions with evaporite deposits.

Caveats and Practical Aspects of Fluid-Inclusion Studies

Several factors can affect the utility and validity of fluid-inclusion measurements and these factors can play a significant role in sedimentary environments. Two general tenets of fluid-inclusion research are that: (1) the volume of the cavity has not changed since generation of the vapor bubble, and (2) the bulk composition of the inclusion has remained constant. However, both the volume and compositions of the inclusions can be modified by necking, stretching, refilling, and leakage. As a general rule of thumb, a population of fluid inclusions that formed contemporaneously (termed a fluid inclusion assemblage by Goldstein and Reynolds, 1994) will yield homogenization temperatures within 15 to 20°C (59-68ºF).

All fluid inclusions neck or anneal after trapping as the temperatures decrease. This process typically leads to the splitting of a large inclusion into a number of smaller inclusions. Necking occurring after generation of the vapor bubble is recognized by the petrographic association of inclusions with variable liquid to vapor ratios. Many of the inclusions in calcite and dolomite have variable liquid to vapor ratios. Qualitatively, the presence of all inclusions with vapor bubbles, but variable ratios, suggests necking occurred at elevated temperatures greater than at least 50°C (122ºF). Although the homogenization temperatures of necked inclusions are not meaningful, because they can be both greater and lower than the true homogenization temperature, the minimum homogenization temperatures can provide a qualitative measure of the minimum temperatures that have affected the rocks. The salinities of necked inclusions, however, are not greatly affected by necking and can be measured and used. Oil inclusions are less prone to necking than aqueous inclusions, although some secondary inclusions in the latest calcite clearly displayed evidence of necking.

Stretching is the inelastic expansion of the fluid inclusion leading to an increase in its volume. This can lead to the generation or growth of a vapor bubble, which in turn yields an anomalously high temperature of homogenization. The degree of stretching is highly variable even within a single crystal. Its effect is dependent on original fluid inclusion size, shape, location in a crystal, degree of overheating, pressure, and fluid composition. Often a significant percentage of the inclusions will retain their original characteristics. For example, single-phase inclusions, if originally present, will persist after stretching. Stretched inclusions do not yield meaningful homogenization temperatures. The salinities of stretched inclusions, however, can be utilized.

Refilling of fluids may be common but is difficult to recognize. Both the homogenization temperatures and compositions can be utilized. Refilling of fluids can be recognized by comparing the fluid inclusion characteristics of minerals whose relative ages are known.

Leakage of fluids, particularly the liquid phase, from fluid inclusions is also common. Leaked inclusions are typically vapor-rich. Leakage can often be recognized because it will often affect only a small percentage of the total fluid inclusion population.

Fluid Inclusions in Early Calcite

Early calcite represents original fossil material (figure 28). It is characteristically coarsely crystalline and decorated with abundant aqueous liquid-rich inclusions with variable liquid to vapor ratios (figure 29). Less commonly, oil inclusions are present (figures 30 and 31). The vast majority of both the aqueous and oil inclusions are randomly distributed throughout the calcite crystals and appear to be primary in origin. Secondary inclusions defining healed fractures are uncommon.

Figure 28. Early calcite from the Lisbon No. D-616 well at 8356 feet. The mottled appearance of the calcite is due to abundant fluid inclusions. Width of image is 3.3 mm.

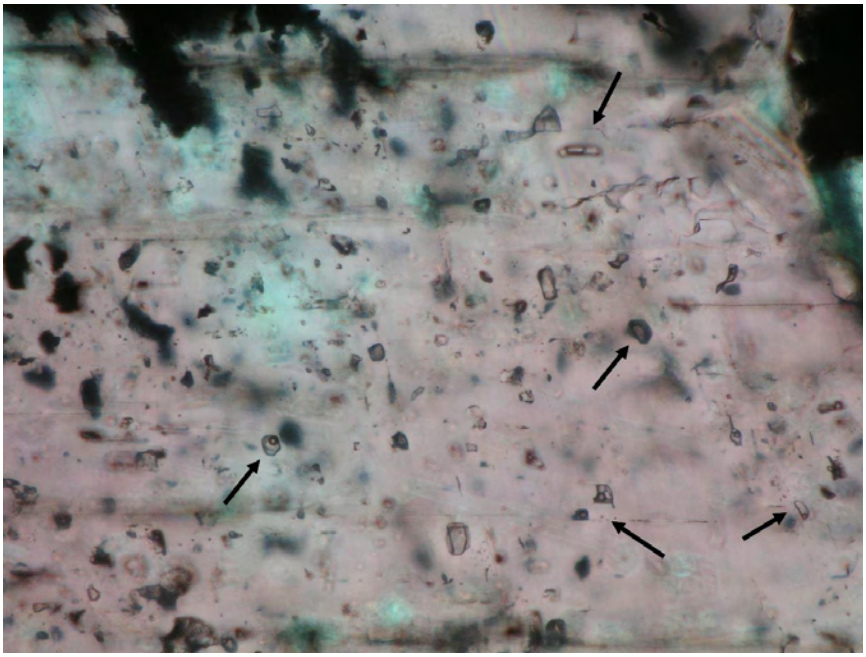

Figure 29. Fluid inclusions in early calcite from the Lisbon No. D-616 well at 8356 feet. Arrows point to inclusions with different liquid to vapor ratios, resulting from necking after trapping. Width of image is 0.7 mm.

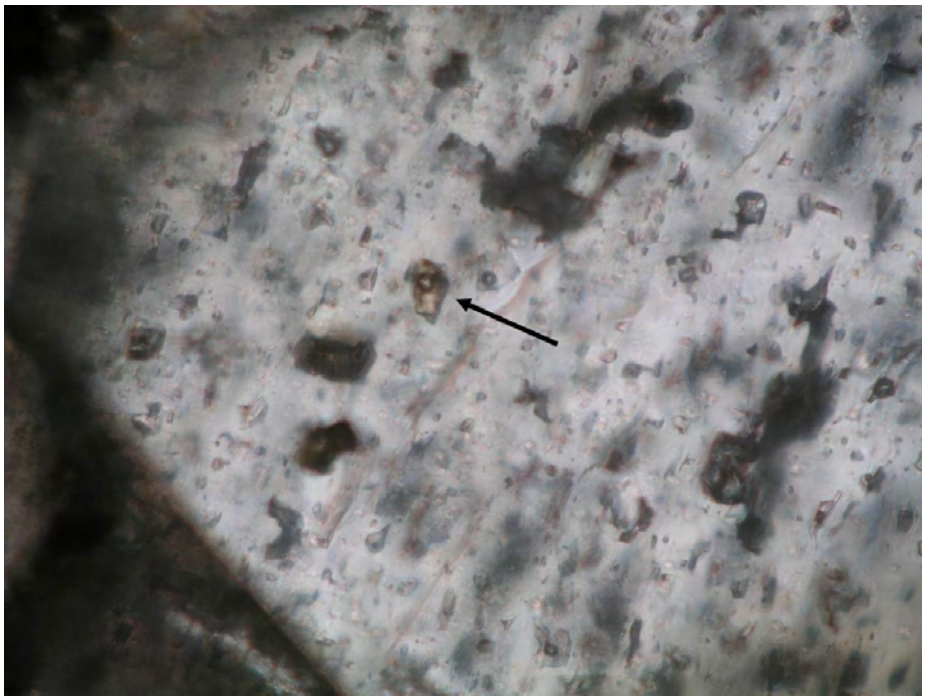

Figure 30. Brown primary oil inclusion (arrow) in calcite from the Lisbon No. D-616 well at 8356 feet. Clear inclusions are aqueous. Width of image is 0.3 mm.

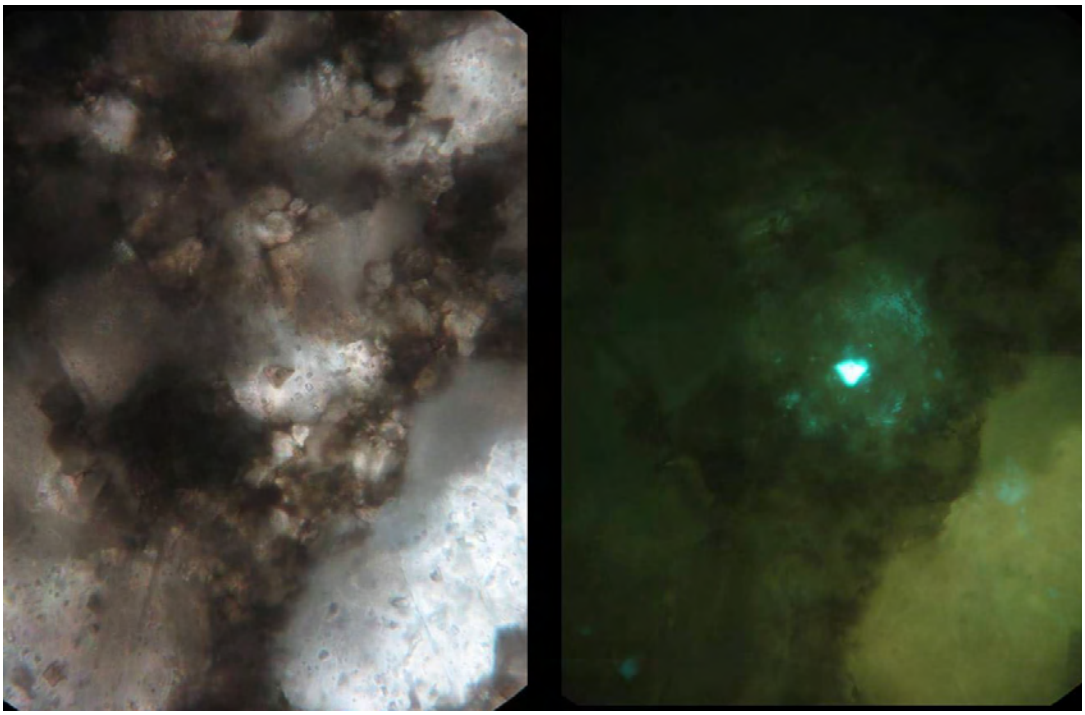

Figure 31. Primary oil inclusion in calcite from the Lisbon No. D-616 well at 8356 feet. Right-hand image taken under fluorescent light shows that the oil is live. Height of image is 0.3 mm.

The characteristically variable liquid to vapor ratios of the aqueous inclusions are interpreted as resulting from necking. Reconnaissance homogenization temperature measurements on spatially associated inclusions have temperatures greater than 20°C (>68°F) and are consistent with this interpretation. These homogenization temperatures are not considered meaningful and are not reported here. However, the occurrence of all two-phase inclusions, in contrast to the presence of numerous single-phase, liquid inclusions in dolomite suggests the inclusions in calcite were trapped at elevated temperatures.

Ice-melting temperatures were measured on the aqueous inclusions in two samples from Lisbon No. D-616 well (figure 32). These temperatures ranged from -19.5 to -25.5°C (-3.1 to -13.9°F) indicating that the fluids were highly saline.

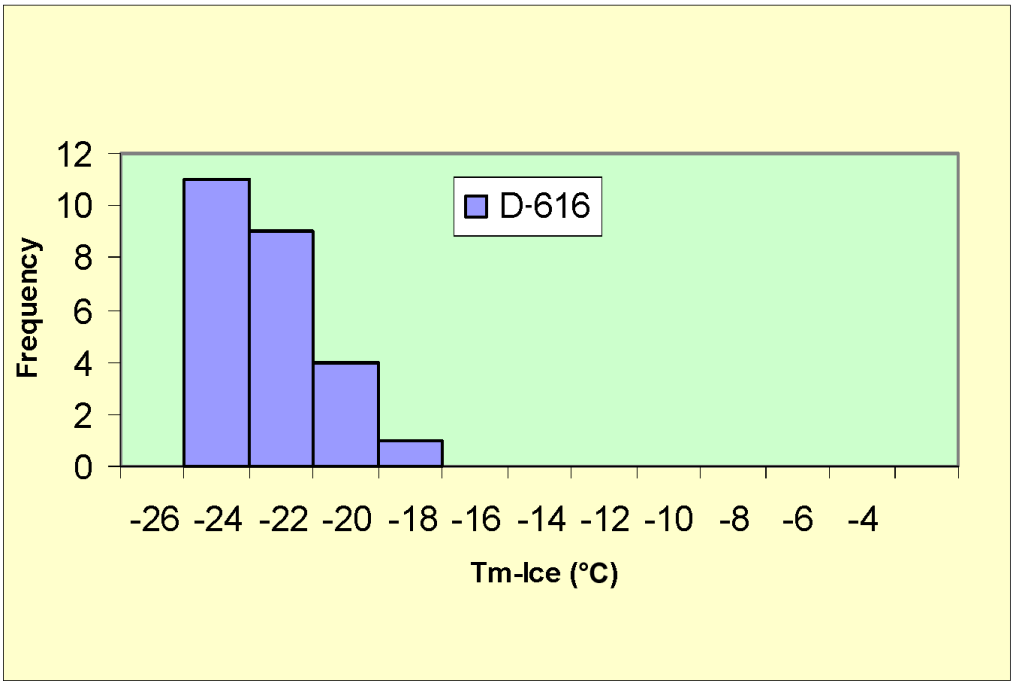

Figure 32. Ice-melting temperatures of fluid inclusions in early calcite from the Lisbon No. D-616 well at 8356 feet and 8372 feet.

Early calcite containing primary oil inclusions was found in Lisbon No. D-616 well at a depth of 8356 feet (2547 m) (figures 30 and 31). The color of the oil under fluorescent light suggests it has an API gravity of 35 to 45° (Goldstein and Reynolds, 1994). Twelve primary oil inclusions were measured in a single calcite crystal. All but two yielded homogenization temperatures ranging from 48 to 68°C (118-154°F). The oil is interpreted as having formed in place from trapped organic material. The homogenization temperatures are minimum trapping temperatures.

Although the aqueous and oil inclusions appear primary in origin, they clearly could not have been present at the time the fossils were deposited. Furthermore, the phase relationships indicate the aqueous inclusions cannot be regarded as original inclusions that have stretched. The most likely explanation for the distribution and character of these calcite-hosted inclusions is that the original calcite has recrystallized and that the fluids were trapped during recrystallization. Oil inclusions in saddle dolomite suggest a similar history.

Fluid Inclusions in Dolomite

Dolomite fills voids and replaces early calcite. Early dolomite is typically fine grained; later saddle dolomite is coarser grained. Small fluid inclusions, most of which are less than a few micrometers in length, are common in dolomite (figure 33). These inclusions define growth zones, and consequently are interpreted as being primary in origin. Coarse-grained saddle dolomite frequently contains cloudy cores and clear rims.

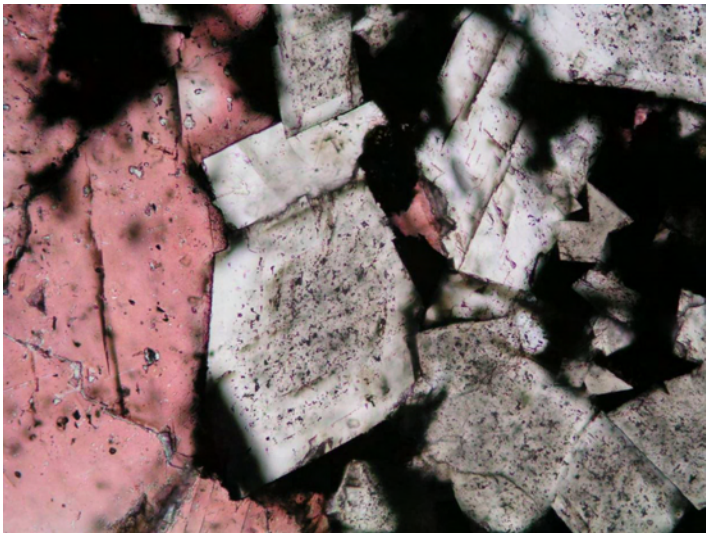

Figure 33. Dolomite (colorless) and calcite (red) from the Lisbon NW USA No. B-63 well at 10,004 feet. The cloudy appearance of the dolomite is due to abundant fluid inclusions. Saddle dolomites (center of photo) typically have cloudy cores and clear rims. Width of image is 0.7 mm.

Only aqueous inclusions were observed in the early fine-grained dolomite. Later saddle dolomite contains both aqueous and oil inclusions. Although many of the aqueous inclusions appear to contain only a single liquid phase, aqueous inclusions with variable liquid to vapor ratios are not uncommon. Reconnaissance measurements indicate that the two-phase (liquid plus vapor) inclusions commonly have homogenization temperatures ranging from 70 to 135°C (158-275ºF), although inclusions having homogenization temperatures several tens of degrees higher are locally abundant. Fluid inclusions trapped during mineral growth at temperatures greater than 70°C (>158ºF) will typically contain a vapor bubble. The common absence of a vapor bubble in many of the primary inclusions is inconsistent with dolomite formation at elevated temperatures and suggests that (1) the dolomite formed at temperatures of less than about 50°C (~122ºF), (2) the fluid inclusions have re-equilibrated (necked, stretched, or refilled), and (3) the homogenization temperatures of the two-phase inclusions are meaningless.

Ice-melting temperatures of inclusions trapped in fine-grained dolomite from depths of 8372 feet (2552 m) in Lisbon No. D-616 well and 8444 feet (2574 m) in Lisbon No. D-816 well and from the clear rims of saddle dolomite from a depth of 9939 feet (3029 m) in Lisbon NW USA No. B-63 well are shown in figure 34.

Oil inclusions occur in saddle dolomite from a depth of 9939 feet (3029 m) in Lisbon NW USA No. B-63 well (figure 35). The inclusions appear primary, occurring in light colored portions of the crystal. Figure 36 shows that the early, dark colored growth zones are truncated by the lighter colored dolomite, suggesting that the dolomite recrystallized during burial. These relationships indicate that the oil was trapped during recrystallization. Homogenization temperatures of the oil inclusions, which range from 60 to 70°C (º140-158ºF) (figure 37), provide a minimum temperature for this recrystallization.

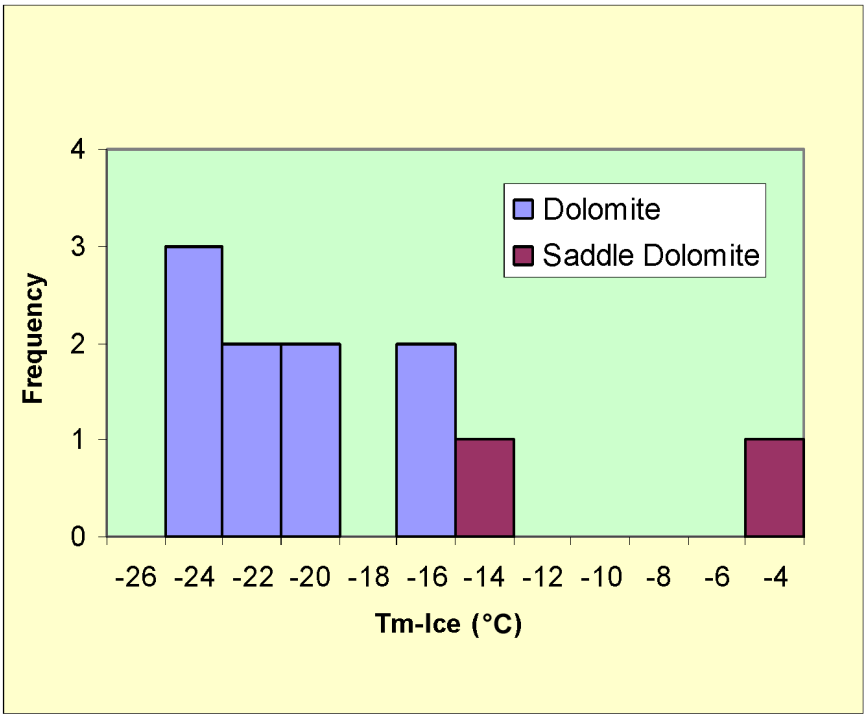

Figure 34. Ice-melting temperatures of dolomite-hosted fluid inclusions. Samples from depths of 8372 feet in the Lisbon No. D-616 well, 8444 feet in the Lisbon No. D-816 well, and from the clear rims of saddle dolomite from a depth of 9939 feet in the Lisbon NW USA No. B-63 well.

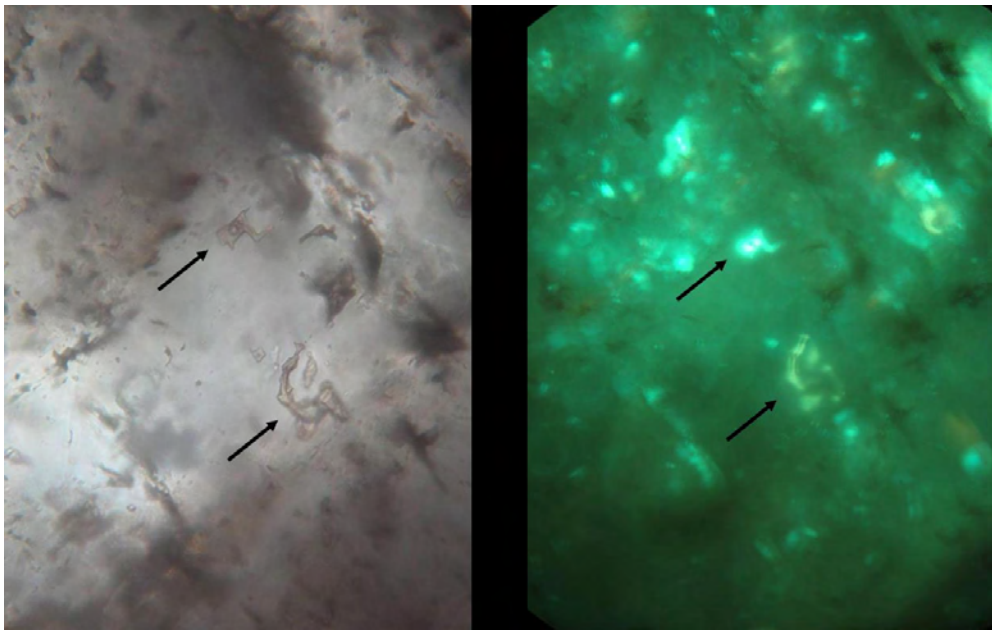

Figure 35. Oil inclusions in saddle dolomite from the Lisbon NW USA No. B-63 well at 9939 feet. Arrows point to two of the inclusions; others are apparent in the right-hand image taken under fluorescent light. Height of images is 0.3 mm.

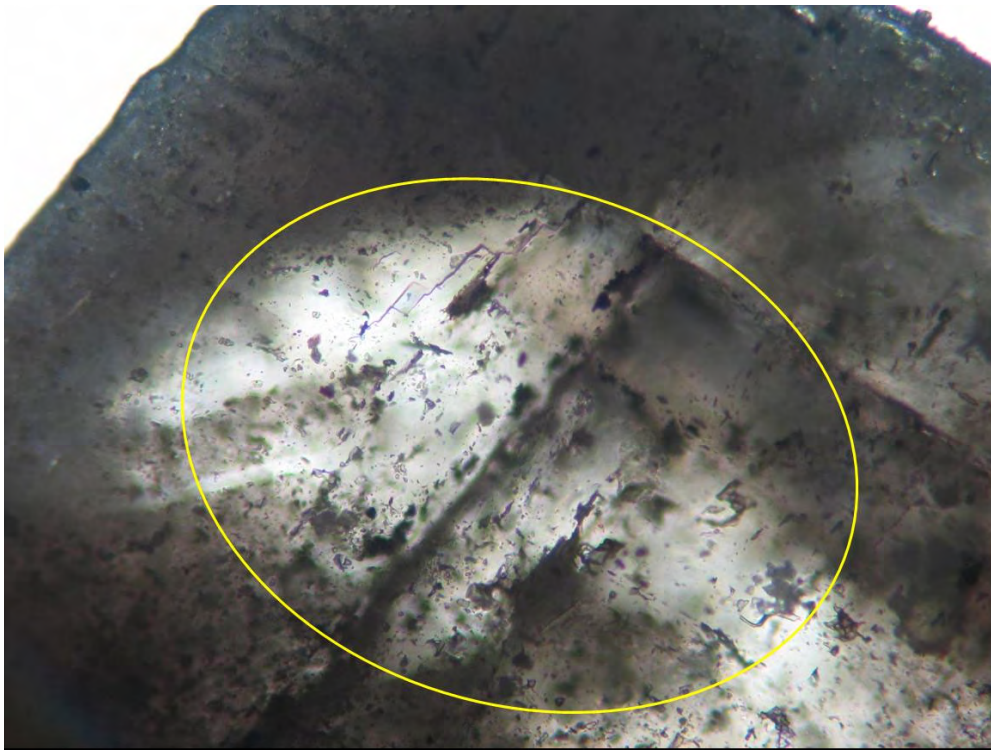

Figure 36. Low-magnification image of saddle dolomite shown in figure 35. Dark growth zones are truncated near the left side of the oval. Oil inclusions in figure 35 occur in the light colored dolomite on right side of oval. Width of image is 0.7 mm.

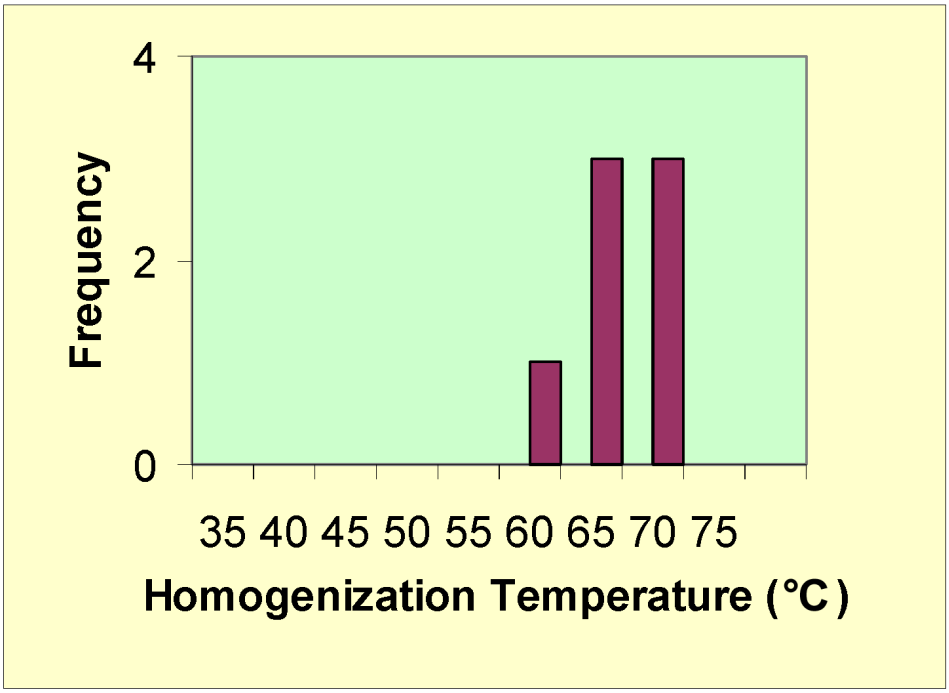

Figure 37. Homogenization temperatures of oil inclusions trapped in saddle dolomite from the Lisbon NW USA No. B-63 well at 9939 feet.

Fluid Inclusions in Quartz

Quartz occurs as fine- to medium-grained crystals that postdate dolomite. Figure 38 shows small quartz crystals filling cavities in dolomite. Larger euhedral quartz crystals encapsulate dolomite and anhydrite (figures 39 and 40). The anhydrite inclusions are frequently oriented and rounded, indicating they are remnants of large, partially dissolved crystals. Anhydrite has retrograde solubility (deposits as water is heated) whereas quartz has prograde solubility (deposits as fluids cool). These relationships suggest that the anhydrite formed from refluxing brines, while the later laterally or ascending cooling fluids that deposited quartz were undersaturated in anhydrite, leading to its dissolution.

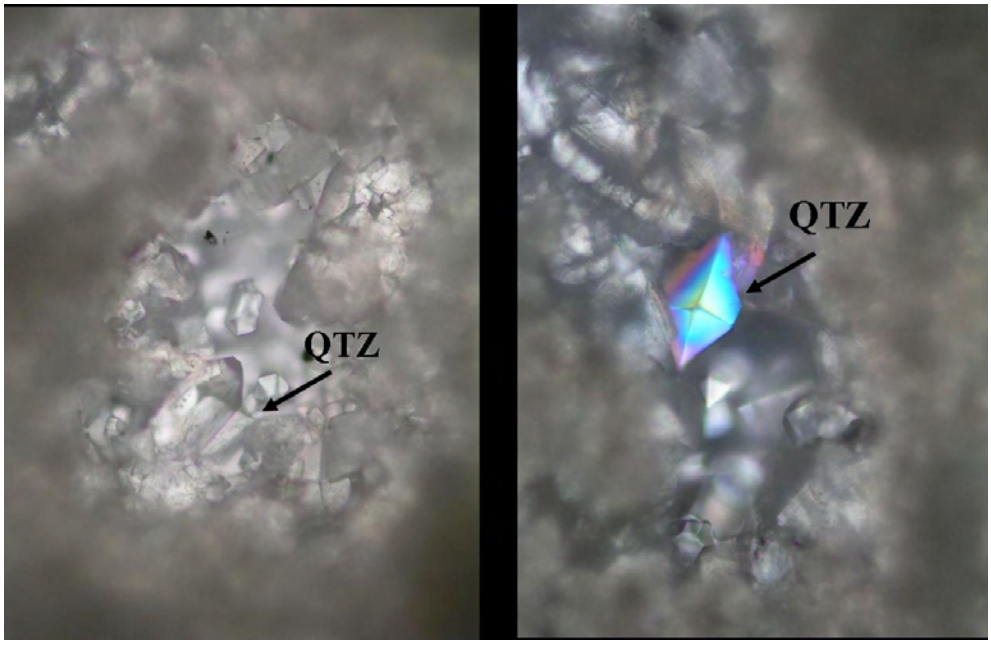

Figure 38. Quartz crystals partially filling a cavity in dolomite from the Lisbon NW USA No. B-63 well at 9981 feet. The right-hand image was taken under partially crossed nicols. Height of images 0.7 mm.

The quartz crystals from a depth of 8356 feet (2547 m) in the Lisbon No. D-616 well commonly contain numerous two-phase aqueous inclusions; rarely, gas-rich and single-phase, liquid-rich inclusions are present. Figures 41 and 42 show quartz crystals containing primary liquid-rich inclusions. In figure 41, primary inclusions define a growth zone within the interior of the crystal. Large isolated primary inclusions, up to 50 micrometers across occur in the quartz crystals shown in figure 42. Coexisting liquid- and vapor-rich inclusions were observed in the crystal shown in figure 43. Because of the small size of the gas-rich inclusions, it was not possible to estimate their compositions from phase changes during freezing and heating. However, in this environment, the gas is probably methane-rich. No primary oil inclusions were observed in the quartz crystals.

Secondary aqueous inclusions that define healed fractures are common in some of the quartz crystals. The majority of these inclusions contain liquid and vapor at room temperature; rarely single-phase aqueous inclusions are present. As noted above, these single-phase inclusions could represent the local incursion of low-temperature (less than about 50°C [<~ 122°F]) waters.

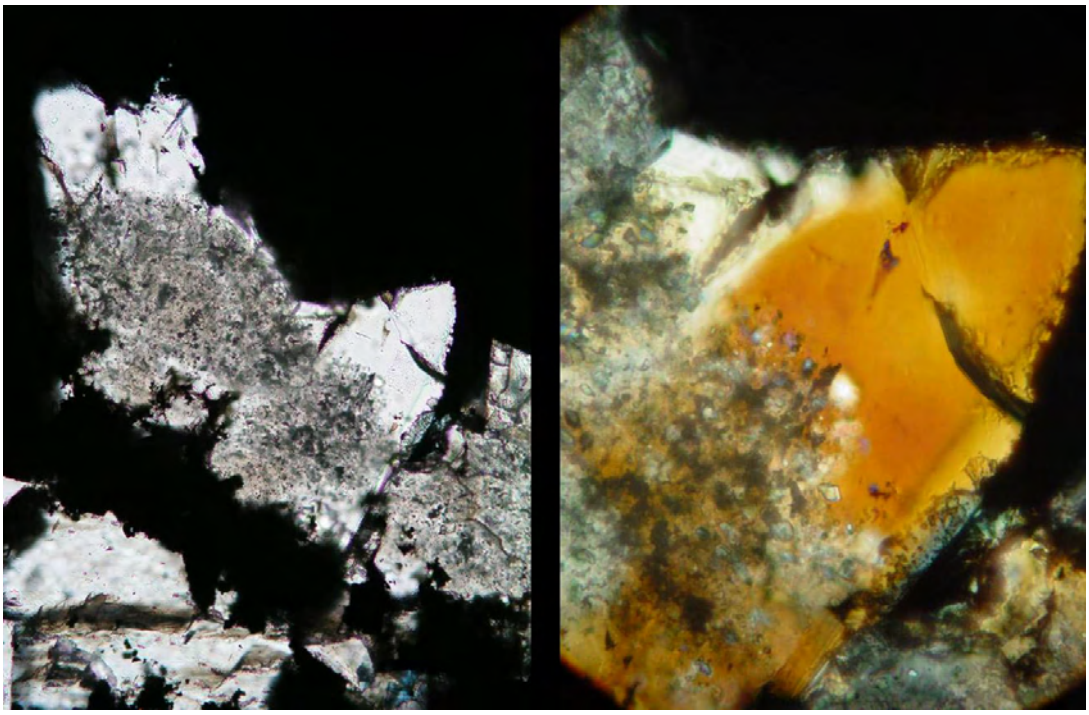

Figure 39. Quartz encapsulating dolomite from the Lisbon NW USA No. B-63 well at 10,004 feet. Height of images is 1.3 mm (left) and 0.7 mm (right). Right-hand image taken under crossed nicols.

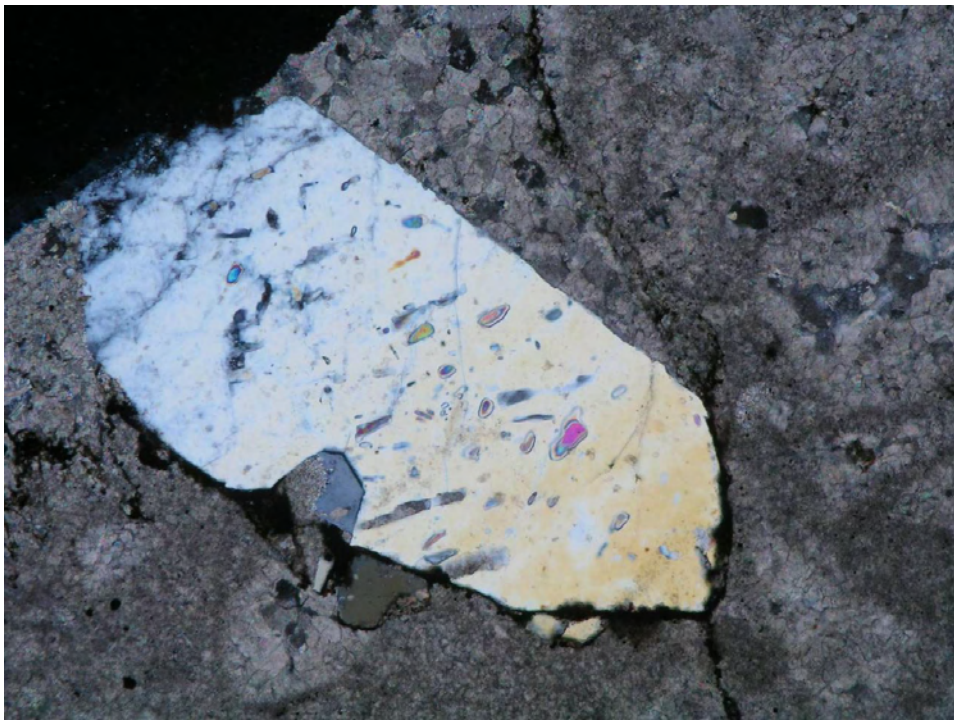

Figure 40. Coarse-grained quartz crystal from the Lisbon No. D-616 well at 8356 feet. Small oriented grains of anhydrite are encapsulated in the quartz. Width of image is 1.3 mm.

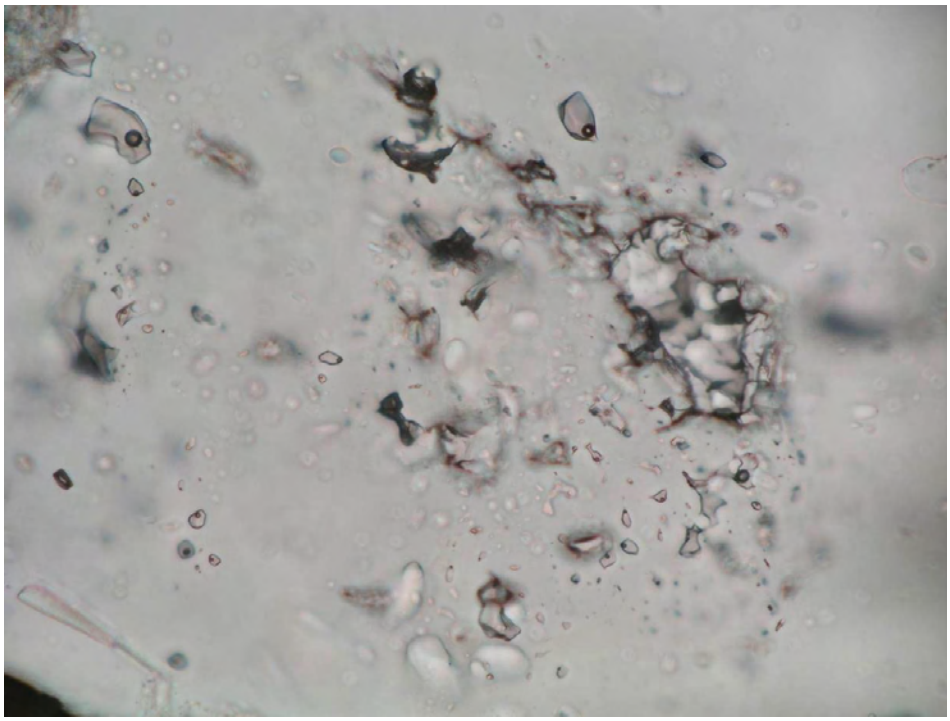

Figure 41. Two-phase, liquid-rich inclusions defining a growth zone in the interior of a quartz crystal from the Lisbon No. D-616 well at 8356 feet. The large, irregular cavity on the right may have been initially filled with anhydrite. Width of image is 0.3 mm.

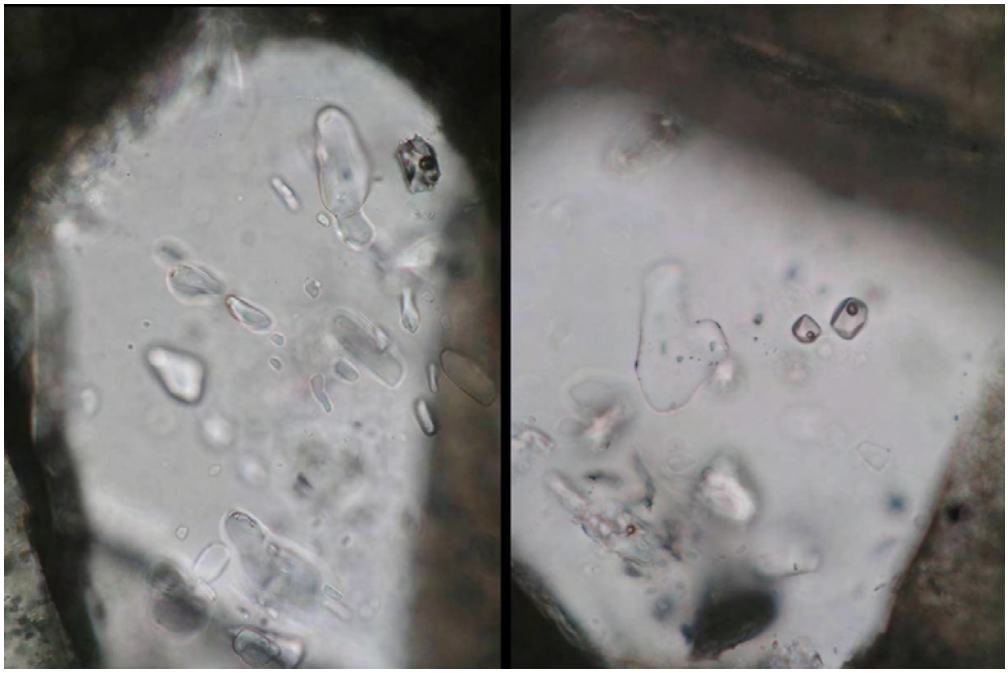

Figure 42. Primary liquid-rich inclusions in quartz from the Lisbon No. D-616 well at 8356 feet. Height of image is 0.3 mm. Irregular shaped inclusions are anhydrite.

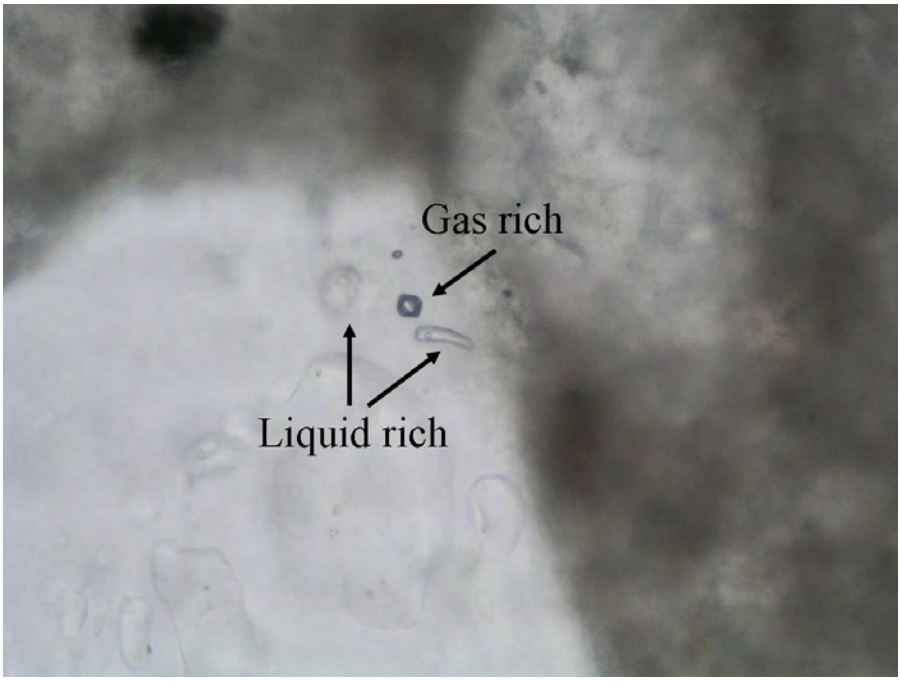

Figure 43. Coexisting primary liquid- and gas-rich inclusions in quartz from the Lisbon No. D-616 well at 8356 feet. Width of image is 0.3 mm.

Homogenization and ice-melting temperatures of quartz-hosted inclusions were measured (figure 44). Primary inclusions yielded homogenization temperatures ranging from 118 to 133°C (244-271ºF) and ice-melting temperatures of -20.5 to -22.8°C (-4.9 to -9ºF). Secondary inclusions yielded lower homogenization temperatures but a much broader range of ice-melting temperatures that overlapped those of the primary inclusions.

The presence of coexisting gas- and liquid-rich inclusions is particularly significant because this suggests that the homogenization temperatures closely approximate the true trapping temperatures (see discussion in Goldstein and Reynolds, 1994). The quartz-hosted inclusions provide the best measure of the maximum burial temperature and depth of any of the minerals studied.

Fluid Inclusions in Late Calcite

Late calcite from depths of 9936 feet, 9991 feet, and 10,005 feet (3028 m, 3045 m, and 3049 m) in Lisbon NW USA No. B- 63 well was studied. The calcite encapsulates dolomite (figure 45) and fills vugs. The relationships between dolomite, quartz, and calcite are shown in figure 46. These textural relationships imply that the calcite also postdates quartz. As shown in figure 45, dissolution of dolomite occurred prior to calcite deposition.

Secondary aqueous and oil inclusions occur in the late calcite. All of the aqueous inclusions display variable liquid to vapor ratios indicative of necking. Ice-melting temperatures of the aqueous inclusions are shown in figure 47; see figure 48 for comparison of ice-melting temperatures of fluid inclusions in calcite vs quartz. The majority of the inclusions from depths of 9939 feet and 10,005 feet (3029 m and 3049 m) yielded comparatively high ice-melting temperatures ranging from -5.5 to about -12°C (22.1-~10 °F), corresponding to salinities of 8.6 to 16 weight percent NaCl equivalent. Inclusions from a depth of 9991.8 feet (3045 m) had higher salinities, up to 18 weight percent NaCl equivalent. These relationships suggest that at least two distinct groups of fluids interacted with the rocks from the Lisbon NW USA No. B-63 well.

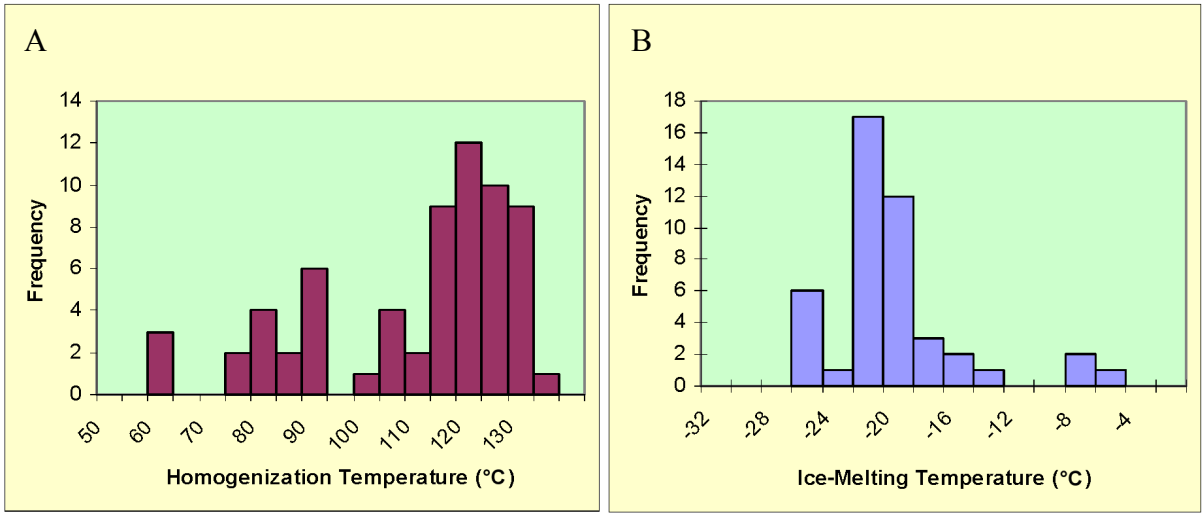

Figure 44. Homogenization (A) and ice-melting (B) temperatures of quartz-hosted aqueous inclusions from the Lisbon No. D-616 well at 8356 feet.

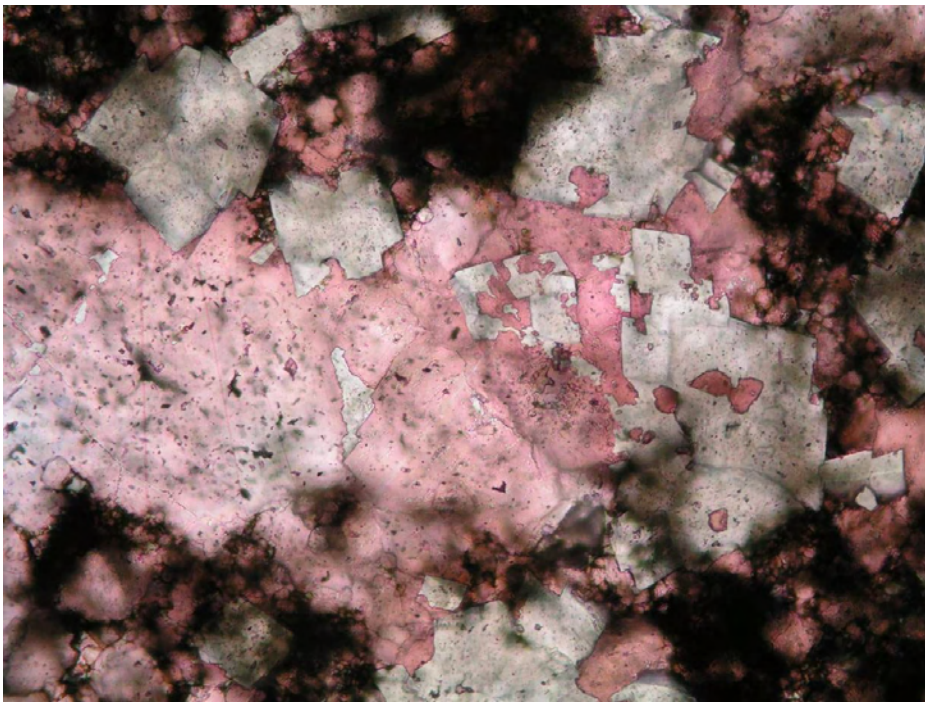

Figure 45. Corroded and dissolved dolomite (white) encapsulated in calcite (pink) from in the Lisbon No. D-616 at 8372 feet. Width of image is 1.3 mm.

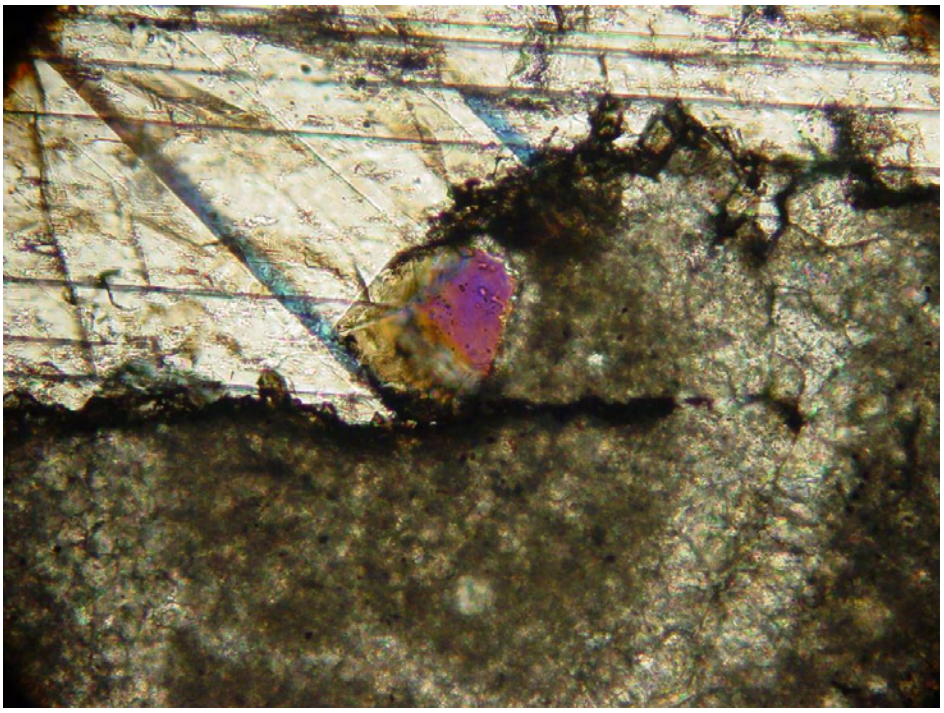

Figure 46. Coarse-grained calcite (upper half of image) that appears to postdate quartz (purple crystal in center) and dolomite (lower half of image). Lisbon NW USA No. B-63 well at 10,004 feet. Width of image is 0.7 mm.

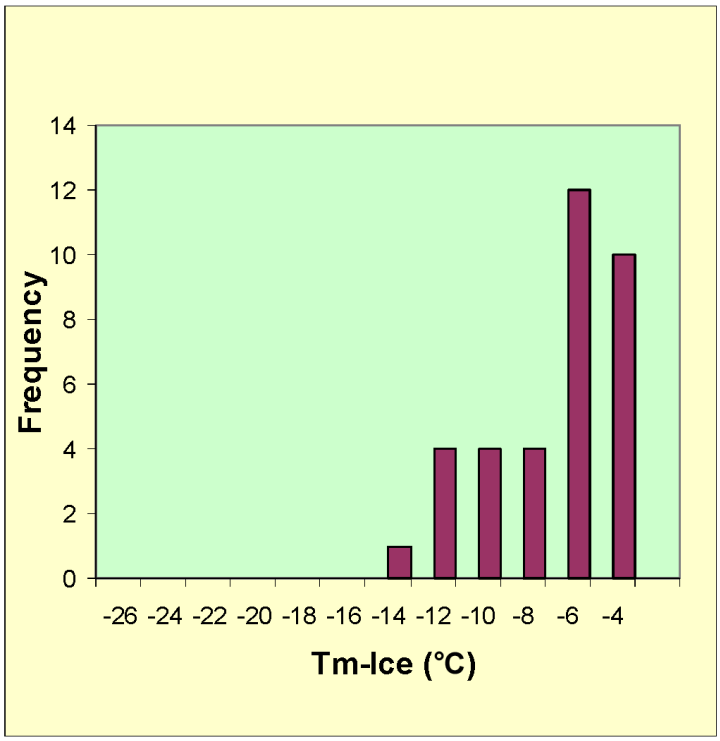

Figure 47. Ice-melting temperatures of late, calcite-hosted fluid inclusions from the Lisbon NW USA No. B-63 well.

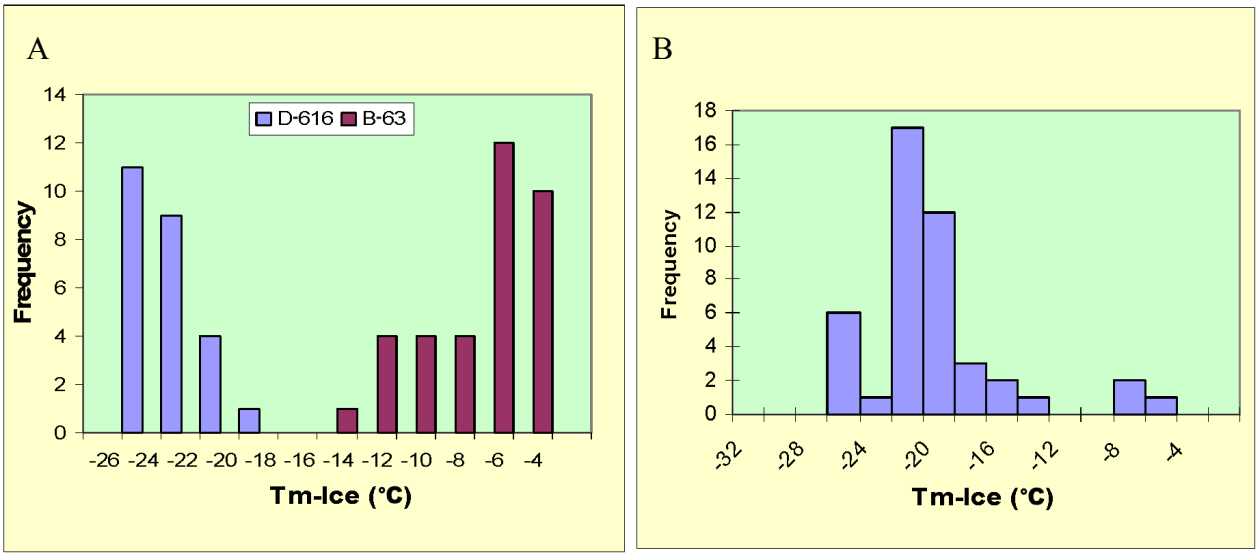

Figure 48. Comparison of ice-melting temperatures of fluid inclusions in calcite (A) and quartz (B) from the Lisbon No. D-616 well.

Late Oil Inclusions

The youngest significant diagenetic event recorded in the rocks is represented by the presence of the bitumen observed in numerous thin sections (see Chidsey and others, 2005). Secondary inclusions trapped in late calcite from a depth of 9936 feet (3028 m) in the Lisbon NW USA No. B-63 well provide unequivocal evidence for a mobile oil phase that postdates calcite deposition. The oil inclusions shown in figure 49 display variable liquid to vapor ratios caused by necking. The oil is fluorescent with an estimated API gravity of 35 to 45°, based on its color. Similar appearing secondary oil inclusions were observed in calcite from a depth of 8372 feet (2552 m) in the Lisbon No. D-616 well (figure 50), although it is not possible to uniquely assign an age to these inclusions. These inclusions yielded consistent homogenization temperatures ranging from 39 to 43°C (102-109°F) (figure 51). For comparison, homogenization temperatures of primary oil inclusions are also shown in figure 51; see figure 52 for comparison of homogenization temperatures of oil inclusions in calcite vs saddle dolomite.

TECHNOLOGY TRANSFER

The UGS is the Principal Investigator and prime contractor for the Leadville Limestone project, described in this report. All maps, cross sections, lab analyses, reports, databases, and other deliverables produced for the project will be published in interactive, menu-driven digital (Web-based and compact disc) and hard-copy formats by the UGS for presentation to the petroleum industry. Syntheses and highlights will be submitted to refereed journals, as appropriate, such as the *American Association of Petroleum Geologists (AAPG) Bulletin* and *Journal of Petroleum Technology*, and to trade publications such as the *Oil and Gas Journal*. This information will also be released through the UGS periodical *Survey Notes* and be posted on the UGS Paradox Basin project Web page.

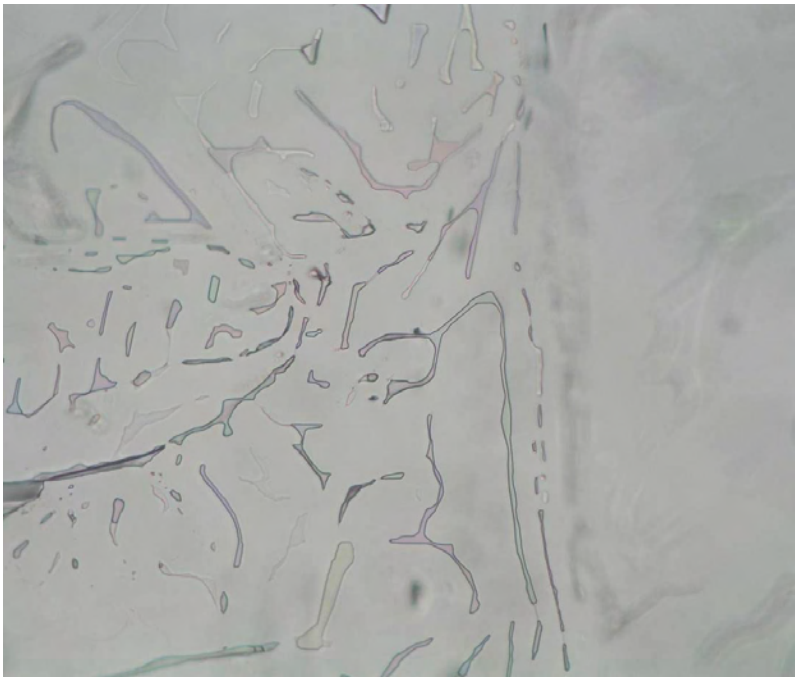

Figure 49. Secondary oil inclusions in late calcite from the Lisbon NW USA No. B-63 well at 9936 feet. The inclusions are necked. The large brown inclusion at bottom center contains only liquid; others contain variable ratios of liquid and gas. Width of image is 0.7 mm.

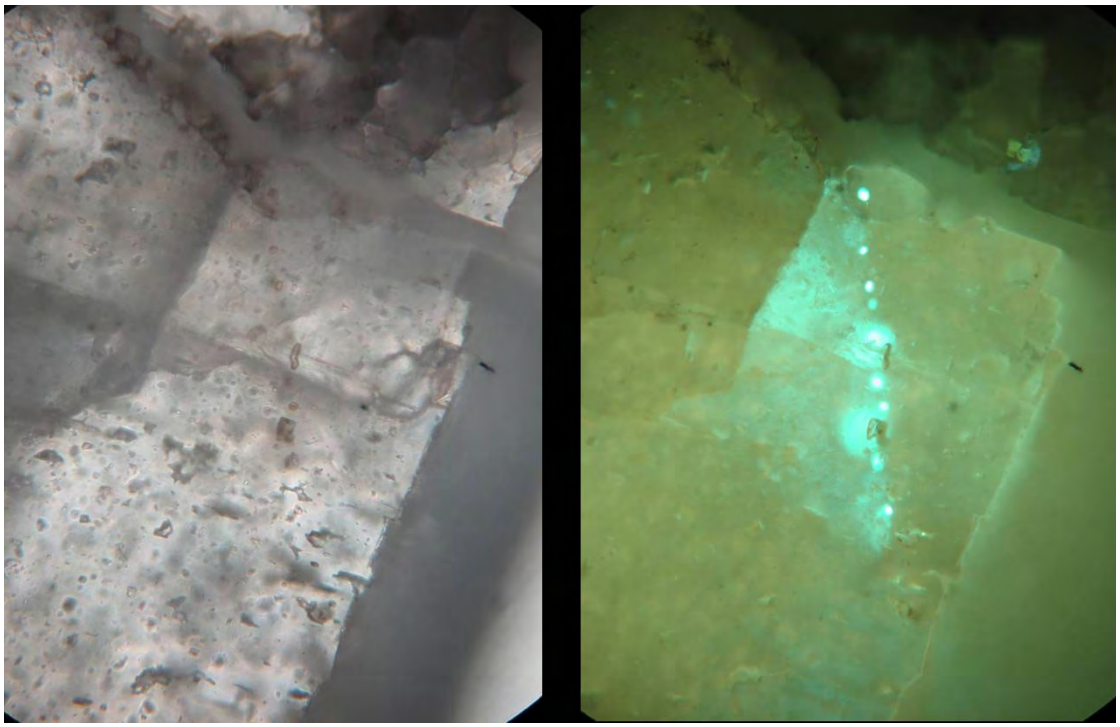

Figure 50. Secondary oil inclusions in calcite from the Lisbon No. D-616 well at 8372 feet. The height of each image is 0.3 mm. Right-hand image was taken under fluorescent light.

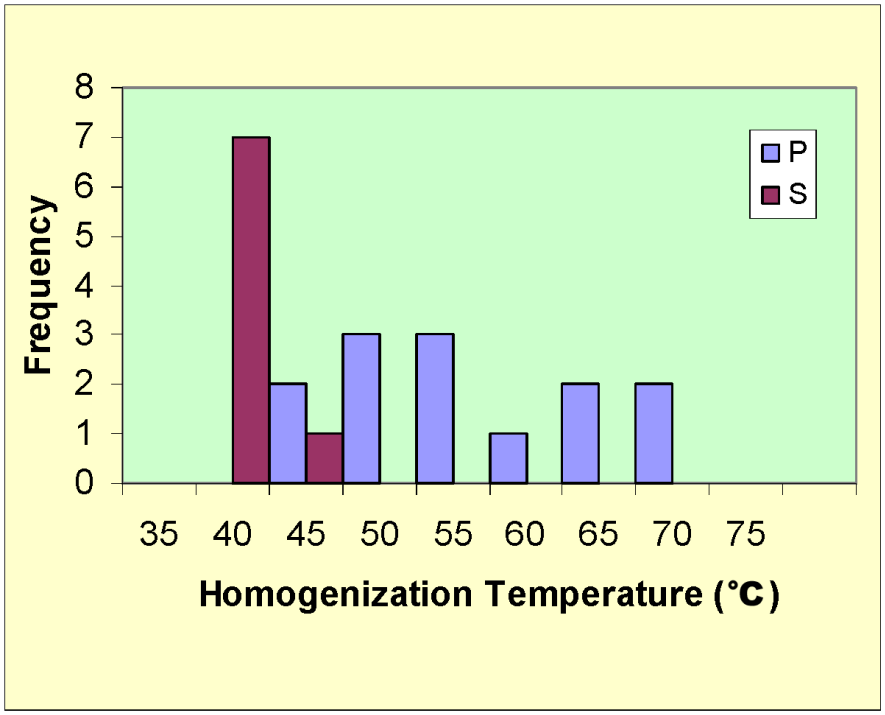

Figure 51. Comparison of homogenization temperatures of primary (P) and secondary (S) oil inclusions in calcite.

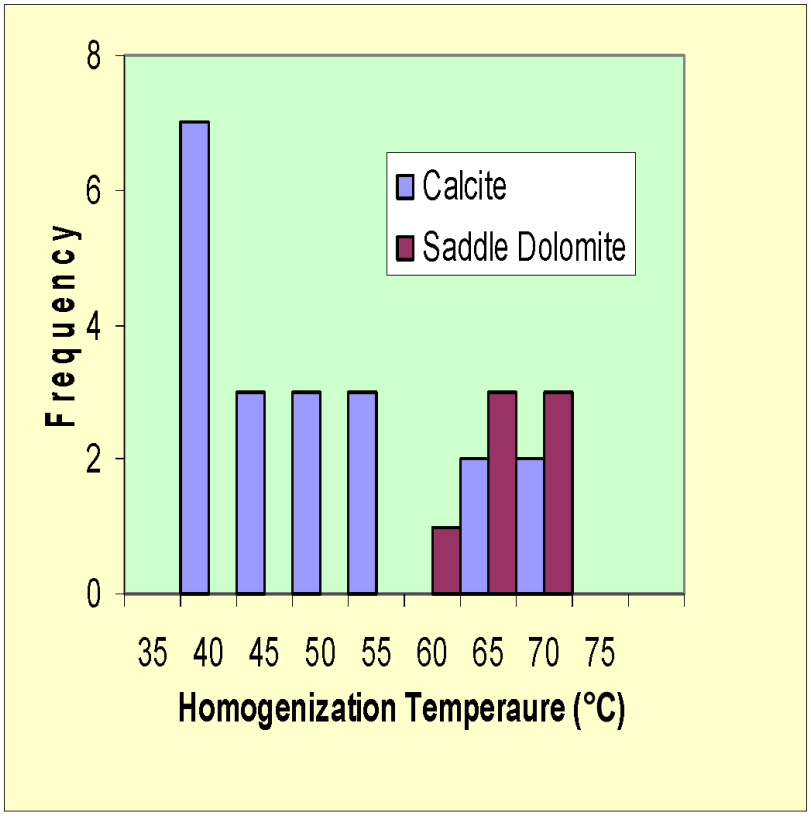

Figure 52. Comparison of homogenization temperatures of oil inclusions in calcite and saddle dolomite. All inclusions are primary except 35 to 40°C inclusions in calcite.

The technology-transfer plan includes the formation of a Technical Advisory Board and a Stake Holders Board. These boards meet annually with the project technical team members. The Technical Advisory Board advises the technical team on the direction of study, reviews technical progress, recommends changes and additions to the study, and provides data. The Technical Advisory Board is composed of Leadville field operators and those who are actively exploring for Leadville hydrocarbons in Utah and Colorado. This board ensures direct communication of the study methods and results to the operators. The Stake Holders Board is composed of groups that have a financial interest in the study area including representatives from the State of Utah (School and Institutional Trust Lands Administration, and Utah Division of Oil, Gas and Mining) and the federal government (Bureau of Land Management). The members of the Technical Advisory and Stake Holders Boards receive all semi-annual technical reports, copies of all publications, and other material resulting from the study. Board members also provide field and reservoir data.

An abstract describing Leadville diagenesis with emphasis on dolomitization was submitted and accepted by the American Association of Petroleum Geologists, for presentation at the 2005 Annual Convention in Calgary, Canada.

Utah Geological Survey *Survey Notes* and Web Site

The UGS publication *Survey Notes* provides non-technical information on contemporary geologic topics, issues, events, and ongoing UGS projects to Utah's geologic community, educators, state and local officials and other decision-makers, and the public. *Survey Notes* is published three times yearly. Single copies are distributed free of charge and reproduction (with recognition of source) is encouraged. The UGS maintains a database that includes those companies or individuals specifically interested in the Leadville project or other DOE-sponsored UGS projects. They receive *Survey Notes* and notification of project publications and workshops.

The UGS maintains a Web site on the Internet, http://geology.utah.gov. The UGS site includes a page under the heading *Oil, Gas, Coal, & CO_2*, which describes the UGS/DOE cooperative studies past and present (PUMPII, Paradox Basin [two projects evaluating the Pennsylvanian Paradox Formation], Ferron Sandstone, Bluebell field, Green River Formation), and has a link to the DOE Web site. Each UGS/DOE cooperative study also has its own separate page on the UGS Web site. The Leadville Limestone project page, http://geology.utah.gov/emp/leadville/index.htm, contains (1) a project location map, (2) a description of the project, (3) a reference list of all publications that are a direct result of the project, (4) poster presentations, and (5) semi-annual technical progress reports.

Presentation

The following presentation was made during the reporting period as part of the technology transfer activities:

> "Dolomitization of the Mississippian Leadville Reservoir at Lisbon Field, Paradox Basin, Utah" by David E. Eby, Thomas C. Chidsey, Jr., John D. Humphrey, and Louis H. Taylor, Rocky Mountain Association of Geologists Hydrothermal Dolomite Symposium and Core Workshop, November 15, 2004, Colorado School of Mines,

Golden, Colorado. The presentation included a technical talk, poster, and core display of the general petroleum geology of the Leadville Limestone, and facies, petrography, and diagenesis, especially dolomite, of the Lisbon case-study field in Utah.

Project Publications

Eby, D.E., Chidsey, T.C., Jr., Humphrey, J.D., and Taylor, L.H., 2004, Dolomitization of the Mississippian Leadville reservoir at Lisbon field, Paradox Basin, Utah [abs.]: Rocky Mountain Association of Geologists Hydrothermal Dolomite Symposium and Core Workshop Program, p. 31-32.

Chidsey, T.C., Jr., 2004, The Mississippian Leadville Limestone exploration play, Utah and Colorado: Rocky Mountain Association of Geologists, The Outcrop, v. 53, no. 10, p. 1 and 6.

Chidsey, T.C., Jr., Morgan, C.D., McClure, Kevin, Bon, R.L., and Eby, D.E., 2005, The Mississippian Leadville Limestone exploration play, Utah and Colorado: exploration techniques and studies for independents – semi-annual technical progress report for the period April 1 to September 31, 2004: U.S. Department of Energy, DOE/BC15424-2, 42 p.

SUMMARY, CONCLUSIONS, AND RECOMMENDATIONS

The Mississippian Leadville Limestone is a shallow, open-marine, carbonate-shelf deposit. The Leadville has produced over 53 million barrels (8.4 million m^3) of oil from six fields in the Paradox fold and fault belt of the Paradox Basin, Utah and Colorado. Most Leadville oil and gas production is from basement-involved structural traps. All of these fields are currently operated by small, independent producers. This environmentally sensitive, 7500-square-mile (19,400 km^2) area is relatively unexplored. Only independent producers continue to hunt for Leadville oil targets in the region.

Lisbon field accounts for most of the Leadville oil production in the Paradox Basin. Its reservoir characteristics, particularly diagenetic overprinting and history, and Leadville facies can be applied regionally to other fields and exploration trends in the basin. Lisbon was selected as the case-study field for the Leadville Limestone project. The following sections summarize the scanning electron microscopy, epifluorescence, cathodoluminescence, and fluid inclusion studies of samples from Lisbon field, and provides conclusions and recommendations for independents exploring for Leadville targets.

Scanning Electron Microscopy

- Scanning electron microscopy demonstrates how Leadville reservoir quality at Lisbon is greatly enhanced by dolomitization and dissolution of shallow water limestone. There are two basic types of dolomite: (1) very fine, early dolomite, and (2) coarse, late dolomite. Early dolomitization preserves depositional fabrics and has limited porosity development, except for limited dissolution of fossils, and has very low permeabilities. Late

dolomitization has two morphologies: rhombic dolomites and saddle dolomites. Most reservoir rocks within Lisbon field appear to be associated with the second, late type of dolomitization and associated leaching events.

- Pyrobitumen coats most intercrystalline dolomite as well as dissolution pores associated with the second type of dolomite. Fractures enhance the permeability in several intervals. Minor euhedral quartz is present in several samples. Anhydrite and sulfide mineral(s) are present in moderate abundance.

- The general diagenetic sequence for these samples, based on SEM analysis, is (1) dolomitization, (2) dissolution, (3) dolomite cementation, (4) fracturing, (5) quartz cementation, (6) calcite cementation, (7) clay precipitation, (8) anhydrite cementation, (9) pyrobitumen emplacement, and (10) sulfide precipitation.

Epifluorescence

- Epifluorescence petrography makes it possible to clearly identify grain types and shapes, within both limestone and dolomite reservoir intervals in Leadville thin sections from cores examined in this study. In particular, identification of peloids, skeletal grain types, and coated grains are easy to see in rocks where these grains have been poorly preserved, partially leached, or completely dolomitized.

- Depositional textures that are frequently occult or poorly preserved can often be clearly distinguished using blue-light EF microscopy. In many limestones and finely crystalline dolomites of the Leadville reservoir at Lisbon field, the differences between muddy and calcarenitic fabrics can only be clearly appreciated with fluorescence lighting.

- Epifluorescence petrography clearly and rapidly images pore spaces that cannot otherwise be seen in standard viewing under transmitted polarized lighting. In addition, the cross-sectional size and shape of pores are easy to determine.

- Much of the Leadville porosity is very heterogeneous and poorly connected as viewed under EF. In particular, intercrystalline porosity within some of the reservoir in Lisbon field can be resolved much more clearly than with transmitted polarized lighting. The EF examination helps in seeing the origin of most types of porosity. Transmitted polarized lighting does not image intercrystalline porosity in carbonate samples very well, even though blue-dyed epoxy can be impregnated into even very small pores. In addition, opaque bitumen linings prevent light from passing through some of the pores to the observer. Without the aid of the EF view, the amount of visible open pore space would be underestimated in the plane-light image.

- Where dolomitization has occurred, EF petrography often shows the crystal size, shape, and zonation far better than transmitted plane or polarized lighting. This information is often very useful when considering the origin and timing of dolomitization as well as evaluating the quality of the pore system within the dolomite.

- Permeability differences within these dolomite and limestone samples are also easy to image because of the differential oil saturations between the tighter areas and the more permeable lithologies. Low-permeability carbonates from this study area show bright yellow fluorescence due to trapped live oil that is retained within tighter parts of the reservoir system. More permeable rocks show red fluorescence due to the epoxy fluorescence where oil has almost completely drained from the better quality portions of the reservoir.

Cathodoluminescence

- Cathodoluminescence imaging of samples nicely complements the types of information derived from EF of carbonate thin sections. Cathodoluminescence also displays original depositional textures and the outlines of original carbonate grains and distinctly images pore spaces. This information is often very useful when considering the origin and timing of dolomitization as well as evaluating the quality of the pore system within the dolomite.

- Cathodoluminescence shows a wide range of crystal size and growth habits within the dull red luminescing, matrix-replacing dolomite. The vast majority of the dolomite within areas of fabric-selective dolomitization is a deep or intense red color. Between many of the grains, there is a lighter red luminescence where early cements have been dolomitized. Some of the coarser dolomite crystals appear to have an overgrowth of brighter red luminescent material.

- The amount of open porosity under CL is considerably greater than that visible under plane-light microscopy. Between other grains, there are interparticle pores that are still open. In a few areas, these early pores have been solution-enlarged and lined with a later generation of coarse, rhombic dolomite.

- Examination of saddle dolomites in the Leadville can provide more information about these late, elevated temperate (often hydrothermal) mineral phases. For instance, saddle dolomites show nice growth banding. These saddle dolomites display dull, red luminescence in their core areas and slightly bright, orange-red luminescence toward their rim areas. In addition, CL makes it possible to see the growth bands in these coarse dolomite crystals due to slight luminescent differences between each growth zone.

- Cathodoluminescence imaging shows that the contact between the transported material related to karstification and the limestone country rock can be sharp, irregular, and corroded.

Fluid Inclusions

- The fluid inclusion and mineral relationships suggest the following sequence of events: (1) dolomite precipitation, (2) anhydrite deposition, (3) anhydrite dissolution and quartz precipitation, (4) dolomite dissolution and late calcite precipitation, (5) trapping of a mobile oil phase, and (6) formation of bitumen.

- Aqueous fluid inclusions in early calcite, which typically forms coarse-grained crystals, display a range of liquid to vapor ratios suggesting they have necked. Primary oil inclusions studied in one calcite crystal from the Lisbon No. D-616 well, however, display consistent liquid to vapor ratios. These oil inclusions yielded homogenization temperatures ranging from 48 to 70°C (118-158°F). These temperatures represent the minimum temperature of oil formation, not of calcite deposition. The oil was generated in place by maturation of organic material. Both the oil inclusions and the common presence of two-phase, necked aqueous inclusions imply trapping at elevated temperatures. It is suggested trapping occurred when the original calcite recrystallized during burial.

- Fluid inclusions in dolomite have reequilibrated (stretched, necked, refilled) since trapping. The common presence of single-phase aqueous inclusions suggests that the fine-grained dolomite and cores of saddle dolomite were deposited at temperatures less than about 50°C (<~122 °F).

- Coarse-grained quartz crystals containing solid inclusions of anhydrite are found at a depth of 8356 feet in the Lisbon No. D-616 well. Homogenization temperatures of primary inclusions range from 120 to 130°C (~248-266°F). The presence of gas-rich inclusions in the quartz suggests these temperatures are close to the true trapping temperatures and possibly maximum burial temperatures.

- The low ice-melting temperatures of quartz and calcite-hosted inclusions from the Lisbon No. D-616 well, suggest chemically complex Ca-Mg-bearing brines associated with evaporite deposits were responsible for mineral deposition. Calcite from the Lisbon NW USA No. B-63 well trapped fluids with lower salinities (figure 48).

- Oil trapped in early calcite as primary inclusions, as secondary inclusions in calcite of undetermined age, and as "primary" inclusions in recrystallized portions of saddle dolomite fluoresces with a bluish green color, suggesting an API gravity of 35 to 40 °. Homogenization temperatures of primary inclusions in early calcite and saddle dolomite are similar and range from 48 to 70°C (118-158 °F) (figure 52). The oil inclusions trapped in the white, recyrstallized and inclusion-poor saddle dolomite indicate the temperature was at least 70°C (158 °F) during oil deposition and recrystallization. Oil trapped in the saddle dolomite must represent oil that was mobile at this time.

- Oil deposited in healed fractures within late, pore-filling calcite has similar fluorescence as the primary inclusions but lower homogenization temperatures of about 40°C (~104 °F). The lower temperatures of the secondary oil inclusions allow the possibility that the temperatures were decreasing, perhaps due to unroofing, prior to bitumen formation.

- It is possible live oil was preserved in the calcite and dolomite, but not in the main fractures, which now contain bitumen because the oil was not degassed.

ACKNOWLEDGMENTS

Funding for this research was provided as part of the Advanced and Key Oilfield Technologies for Independents (Area 2 – Exploration) Program of the U.S. Department of Energy, National Petroleum Technology Office, Tulsa, Oklahoma, contract number DE-FC26-03NT15424. The Contracting Officer's Representative is Virginia Weyland. Support was also provided by Eby Petrography & Consulting, Inc., Littleton, Colorado, and the Utah Geological Survey.

Core and petrophysical data were provided by Tom Brown, Inc. (now Encana Corp.). James Parker of the Utah Geological Survey (UGS) drafted figures and Cheryl Gustin, UGS, formatted the manuscript. This report was reviewed by David Tabet and Michael Hylland of the UGS.

REFERENCES

Allan, J.R., and Wiggins, W.D., 1993, Dolomite reservoirs - geochemical techniques for evaluating origin and distribution: American Association of Petroleum Geologists, Continuing Education Course Note Series 36, 129 p.

Barker, C.E., and Kopp, O.C., editors, 1991, Luminescence microscopy - quantitative and qualitative aspects: Society for Sedimentary Geology (SEPM) Short Course 25 Notes, p. 1-7.

Bodnar, R.J., 1993, Revised equation and table for determining the freezing-point depression of H_2O-NaCl solutions: Geochimica Cosmochimica Acta, v. 57, p. 683-684.

Budd, D.A., Hammes, U., and Ward, W.B., 2000, Cathodoluminescence in calcite cements - new insights on Pb and Zn sensitizing, Mn activation, and Fe quenching at low trace-element concentrations: Journal of Sedimentary Petrology, v. 70, p. 217-226.

Burruss, R.C., 1981, Hydrocarbon fluid inclusions in studies of sedimentary diagenesis, *in* Hollister, L.S., and Crawford, M.L., editors, Fluid inclusions - applications in petrology: Mineralogical Association of Canada Short Course Notes, v. 6, p. 138-156.

---1991, Practical aspects of fluorescent microscopy of petroleum fluid inclusions, *in* Barker, C. E., and Kopp, O.C., editors, Luminescence microscopy - quantitative and qualitative aspects: Society for Sedimentary Geology (SEPM) Short Course 25 Notes, p. 1-7.

Burruss, R.C., Cercone, K.R., and Harris, P.M., 1986, Timing of hydrocarbon migration: evidenced from fluid inclusions in calcite cements, tectonics and burial history, *in* Schneidermann, Nahum, and Harris, P.M., editors, Carbonate cements: Society for Sedimentary Geology (SEPM) Special Publication 36, p. 277-289.

Cander, H.S., Kauffman, J., Daniels, L.D., and Meyers, W.J., 1988, Regional dolomitization in the Burlington-Keokuk Formation (Mississippian), Illinois and Missouri - constraints

from cathodoluminescent zonal stratigraphy, *in* Shukla, V., and Baker, P.A., editors, Sedimentology and geochemistry of dolostones: Society for Sedimentary Geology (SEPM) Special Publication No. 43, p. 129-144.

Cather, M.E., Morrow, N.R., Brower, K.R., and Buckley, J.S., 1989a, Uses of epi-fluorescent microscopy in evaluation of Mesaverde tight gas sands [abs.]: American Association of Petroleum Geologists Bulletin, v. 73, p. 1150-1151.

Cather, M.E., Morrow, N.R., and Klich, I., 1989b, Applications of fluorescent dye staining techniques to reservoir studies of tight gas sands, Measverde Group, southwestern Colorado [abs.]: American Association of Petroleum Geologists Bulletin, v. 73, p. 342.

Cercone, K.R., and Pedone, V.A., 1987, Fluorescence (photoluminescence) of carbonate rocks - instrumental and analytical sources of observational error: Journal of Sedimentary Petrology, v. 57, p. 780-782.

Chidsey, T.C., Jr., Morgan, C.D., McClure, Kevin, Bon, R.L., and Eby, D.E., 2005, The Mississippian Leadville Limestone exploration play, Utah and Colorado: exploration techniques and studies for independents – semi-annual technical progress report for the period April 1 to September 31, 2004: U.S. Department of Energy, DOE/BC15424-2, 42 p.

Coniglio, M., Zheng, Q., and Carter, T.R., 2003, Dolomitization and recrystallization of Middle Silurian reefs and platformal carbonates of the Guelph Formation, Michigan Basin, southwestern Ontario: Bulletin of Canadian Petroleum Geology, v. 51, p. 177-199.

Choquette, P.W., and Pray, L.C., 1970, Geologic nomenclature and classification of porosity in sedimentary carbonates: American association of Petroleum Geologists Bulletin, v. 54, no. 2, p. 207-250.

Clark, C.R., 1978, Lisbon, San Juan County, Utah, *in* Fassett, J.E., editor, Oil and gas fields of the Four Corners area: Four Corners Geological Society, v. II, p. 662-665.

Dansereau, P., and Bourque, P.A., 2001, The Neigette breccia - remnant of the West Point reef tract in the Matapedia Valley area, and witness to Late Silurian synsedimentary faulting, Gaspe Belt, Northern Appalachians, Quebec: Bulletin of Canadian Petroleum Geology, v. 49, p. 327-345.

Doelling, H.H., 2000, Geology of Arches National Park, Grand County, Utah, *in* Sprinkel, D. A., Chidsey, T.C., Jr., and Anderson, P.B., editors, Geology of Utah's parks and monuments: Utah Geological Association Publication 28, p. 11-36.

Dorobek, S.L., Read, J.F., Niemann, J.M., Pong, T.C., and Haralick, R.M., 1987, Image analysis of cathodoluminescence-zoned calcite cements: Journal of Sedimentary Petrology, v. 57, p. 766-770.

Dravis, J.J., 1988, Deep-burial microporosity in Upper Jurassic Haynesville oolitic grainstones, East Texas: Sedimentary Geology, v. 63, p. 325-341.

---1991, Carbonate petrography – update on new techniques and applications: Journal of Sedimentary Petrology, v. 61, p. 626-628.

---1992, Burial dissolution in limestones and dolomites – criteria for recognition and discussion of controls: a case study approach (Pt. 1: Upper Jurassic Haynesville limestones, East Texas; Pt. 2: Devonian Upper Elk Point dolomites, western Canada): American Association of Petroleum Geologists Bulletin/Canadian Society of Petroleum Geologists Short Course Notes, Subsurface dissolution porosity in carbonates.

Dravis, J.J., and Yurewicz, D.A., 1985, Enhanced carbonate petrography using fluorescence microscopy: Journal of Sedimentary Petrology, v. 55, p. 795-804.

Dunham, R.J., 1962, Classification of carbonate rocks according to depositional texture, *in* Ham, W.E., editor, Classification of carbonate rocks: American Association of Petroleum Geologists Memoir 1, p. 108-121.

Eby, D.E., and Hager, R.C., 1986, Fluorescence petrology of San Andres dolomites – H.O. Mahoney lease, Wasson field, Yoakum County, Texas: Permian Basin Section, Society for Sedimentary Geology (SEPM) Publication 86-26, p. 37-38.

Embry, A.R., and Klovan, J.E., 1971, A Late Devonian reef tract on northeastern Banks Island, Northwest Territories: Canadian Petroleum Geologists Bulletin, v. 19, p. 730-781.

Fairchild, I.J., 1983, Chemical studies of cathodoluminescence of natural dolomites and calcites: Sedimentology, v. 30, p. 572-583.

Filippelli, G.M., and DeLaney, M.L., 1992, Quantifying cathodoluminescent intensity with an on-line camera and exposure meter: Journal of Sedimentary Petrology, v. 62, p. 724-725.

Folk, R.L., 1987, Detection of organic matter in thin sections of carbonate rocks using a white card: Sedimentary Geology, v. 54, p. 193-200.

Frank, J.R., Carpenter, A.B., and Oglesby, T.W., 1982, Cathodoluminescence and composition of calcite cement in Taum Sauk Limestone (Upper Cambrian), southeast Missouri: Journal of Sedimentary Petrology, v. 52, p. 631-638.

Frank, T.D., Lohmann, K.C., and Meyers, W.J., 1996, Chemostratigraphic significance of cathodoluminescence zoning in syntaxial cement - Mississippian Lake Valley Formation, New Mexico: Sedimentary Geology, v. 105, p. 29-50.

Gardner, K.L., 1980, Impregnation technique using colored epoxy to define porosity in petrographic thin sections: Canadian Journal of Earth Sciences, v. 17, p. 1104-1107.

Gies, R.M., 1987, An improved method for viewing micropore systems in rocks with the polarizing microscope: Society of Petroleum Engineers Formation Evaluation, v. 2, p. 209-214.

Goldstein, R.H., 1988, Cement stratigraphy of Pennsylvanian Holder Formation, Sacramento Mountains, New Mexico: American Association of Petroleum Geologists Bulletin, v. 72, p. 425-438.

---1991, Practical aspects of cement stratigraphy with illustrations from Pennsylvanian limestone and sandstone, New Mexico and Kansas, *in* Barker, C.E., and Kopp, O.C., editors, Luminescence microscopy - quantitative and qualitative aspects: Society for Sedimentary Geology (SEPM) Short Course 25 Notes, p. 123-131.

Goldstein, R.H., and Reynolds, T.J., 1994, Systematics of fluid inclusions in diagenetic minerals: Society for Sedimentary Geology (SEPM) Short Course 31, 199 p.

Gregg, J.M., and Karakus, M., 1991, A technique for successive cathodoluminescence and reflected light microscopy: Journal of Sedimentary Petrology, v. 61, p. 613-635.

Guihaumou, N., Szydlowskii, N., and Padier, B., 1990, Characterization of hydrocarbon fluid inclusions by infra-red and fluorescence microspectrometry: Mineralogical Magazine, v. 54, p. 311-324.

Harry, D.L., and Mickus, K.L., 1998, Gravity constraints on lithospheric flexure and the structure of the late Paleozoic Ouachita orogen in Arkansas and Oklahoma, south-central North America: Tectonics, v. 17, no. 2, p. 187-202.

Hemming, N.G., Meyers, W.J., and Grams, J.C., 1989, Cathodoluminescence in diagenetic calcites - the roles of Fe and Mn as deduced from electron probe and spectrophotometric measurements: Journal of Sedimentary Petrology, v. 59, p. 404-411.

Hintze, L.F., 1993, Geologic history of Utah: Brigham Young University Geology Studies Special Publication 7, 202 p.

Kirby, K.C., and Tinker, S.W., 1992, The Keg River/Winnipegosis petroleum system in northeast Alberta [abs.]: American Association of Petroleum Geologists Annual Convention, Official Program with Abstracts, v. 1, p. A66.

Kluth, C.F., 1986, Plate tectonics of the Ancestral Rocky Mountains, *in* Peterson, J.A., editor, Paleotectonics and sedimentation in the Rocky Mountain region, United States: American Association of Petroleum Geologists Memoir 41, p. 353-369.

Kluth, C.F., and Coney, P.J., 1981, Plate tectonics of the Ancestral Rocky Mountains: Geology, v. 9, p. 10-15.

LaFlamme, A.K., 1992, Replacement dolomitization in the Upper Devonian Leduc and Swan Hills Formations, Caroline area, Alberta, Canada [abs.]: American Association of

Petroleum Geologists Annual Convention, Official Program with Abstracts, v. 1, p. A70.

LaVoie, D., Chi G., and Fowler, M.G., 2001, The Lower Devonian Upper Gaspe Limestones in eastern Gaspe - carbonate diagenesis and reservoir potential: Bulletin of Canadian Petroleum Geology, v. 49, p. 346-365.

LaVoie, D., and Morin, C., 2004, Hydrothermal dolomitization in the Lower Silurian Sayabee Formation in northern Gaspe – Matapedia (Quebec) - constraint on timing of porosity and regional significance for hydrothermal reservoirs: Bulletin of Canadian Petroleum Geology, v. 52, p. 256-269.

Machel, H.G., 2000, Application of cathodoluminescence to carbonate diagenesis, *in* Pagel, M., Barbin, V., Blanc, P., and Ohnenstetter, D., editors, Cathodoluminescence in geosciences: New York, Springer, p. 271-301.

Machel, H.G., and Burton, E.A., 1991, Factors governing cathodoluminescence in calcite and dolomites and their implications for studies of carbonate diagenesis, *in* Barker, C.E., and Kopp, O.C., editors, Luminescence microscopy - quantitative and qualitative aspects: Society for Sedimentary Geology (SEPM) Short Course 25 Notes, p. 37-57.

Marshall, D.J., 1988, Cathodoluminescence of geological materials: Winchester, Massachusetts, Allen and Unwin, 128 p.

---1991, Combined cathodoluminescence and energy dispersive spectroscopy, *in* Barker, C.E., and Kopp, O.C., editors, Luminescence microscopy - quantitative and qualitative aspects: Society for Sedimentary Geology (SEPM) Short Course 25 Notes, p. 27-36.

Meyers, W.J., 1974, Carbonate cement stratigraphy of the Lake Valley Formation (Mississippian), Sacramento Mountains, New Mexico: Journal of Sedimentary Petrology, v. 44, p. 837-861.

---1978, Carbonate cements: their regional distribution and interpretation in Mississippian limestones of southwestern New Mexico: Sedimentology, v. 25, p. 371-400.

---1991, Cement stratigraphy - an overview, *in* Barker, C.E., and Kopp, O.C., editors, Luminescence microscopy - quantitative and qualitative aspects: Society for Sedimentary Geology (SEPM) Short Course 25 Notes, p. 133-148.

Miller, J., 1988, Cathodoluminescence microscopy, *in* Tucker, M., editor, Techniques in sedimentology: Oxford, Blackwell Publications, p. 174-190.

Parker, J.W., and Roberts, J.W., 1963, Devonian and Mississippian stratigraphy of the central part of the Colorado Plateau: Four Corners Geological Society, 4th Field Conference Guidebook, p. 31-60.

Petroleum Information, 1984, Paradox Basin–unravelling the mystery: Petroleum Frontiers, v. 1, no. 4, p. 22.

Radke, B.M., and Mathis, R.L., 1980, On the formation and occurrence of saddle dolomite: Journal of Sedimentary Petrology, v. 50, p. 1149-1168.

Rost, F.W.D., 1992, Fluorescence microscopy, v. 1: New York, Cambridge University Press, 253 p.

Scholle, P.A., and Ulmer-Scholle, D.S., 2003, A color guide to the petrography of carbonate rocks: American Association of Petroleum Geologists Bulletin Memoir 77, p. 427-440.

Sipple, R.F., and Glover, E.D., 1965, Structures in carbonate rocks made visible by luminescence petrography: Science, v. 150, p. 1283-1287.

Soeder, D.J., 1990, Applications of fluorescent microscopy to study of pores in tight rocks: American Association of Petroleum Geologists Bulletin, v. 74, p. 30-40.

Smith, K.T., and Prather, O.E., 1981, Lisbon field – lessons in exploration, *in* Wiegand, D.L., editor, Geology of the Paradox Basin: Rocky Mountain Association of Geologists Guidebook, p. 55-59.

Smouse, DeForrest, 1993, Lisbon, *in* Hill, B.G., and Bereskin, S.R., editors, Oil and gas fields of Utah: Utah Geological Association Publication 22, non-paginated.

Stevenson, G.M., and Baars, D.L., 1987, The Paradox—a pull-apart basin of Pennsylvanian age, *in* Campbell, J.A., editor, Geology of Cataract Canyon and vicinity: Four Corners Geological Society, 10th Field Conference, p. 31-55.

Teichmuller, M., and Wolf, M., 1977, Application of fluorescence microscopy in coal petrology and oil exploration: Journal of Microscopy, v. 109, p. 49-73.

Utah Division of Oil, Gas and Mining, 2005, Oil and gas production report, March: non-paginated.

van Gijzel, P., 1967, Palynology and fluorescence microscopy: Reviews of Paleobotany and Palynology, v. 1, p. 49-79.

Walker, G., and Burley, S., 1991, Luminescence petrography and spectroscopic studies of diagenetic minerals, *in* Barker, C.E., and Kopp, O.C., editors, Luminescence microscopy - quantitative and qualitative aspects: Society for Sedimentary Geology (SEPM) Short Course 25 Notes, p. 83-96.

Yanatieva, O.K., 1946, Polythermal solubilities in the systems CaCl2-MgCl2-H2O and $CaCl_2$-NaCl-H_2O: Zhurnal Prikladnox Khimii, v. 19, p. 709-722.

Yanguas, J.E., and Dravis, J.J., 1985, Blue fluorescent dye technique for recognition of microporosity in sedimentary rocks: Journal of Sedimentary Petrology, v. 55, p. 600-602.